THE MESSENGER

EL MENSAJERO

No. 74 – December 1993

TELESCOPES AND INSTRUMENTATION

News from Council

The following is Section 1 (the section relevant for the VLT Project) of the resolution issued by Council during its meeting of December 2, 1993:

In its October 4 and 5, 1993 meeting Council expressed its approval of the revised VLT/VLTI project as referred in June 1993 Cou-483 for content, schedule and staff. Financial difficulties discussed in the Finance Committee meeting of November 8 and 9, 1993 and recent expression of concern in a diplomatic note from the French Government have led to reconsideration of this plan.

Following the presentation and discussion of different alternatives for cost reduction, Council adopts further modifications to the VLT programme plan. This includes the postponement of the implementation of VLTI, VISA, Coudé Train and associated adaptive optics for all telescopes. In consultation with the Scientific Technical Committee a solution will be sought to introduce adaptive optics at the Nasmyth foci at the earliest possible time.

Furthermore, the Executive will endeavour to reintroduce full Coudé and interferometric capabilities at the earliest possible date. This will include provisions for continuing technological research and development programmes devoted to this end.

VLT News from the VLT Division

M. TARENGHI, ESO

The status of VLT activities is shifting more and more from the design to the construction phase. Major progress was achieved in the following areas:

Mechanical Structure

The detailed design of the structure is reaching completion. The calculated lowest locked rotor eigenfrequency is 8.1 Hz around the elevation axis and about 10 Hz around the azimuth axis. To obtain this and to optimize the manufacturing, the mass has increased with respect to the original design. The maximum total moving mass is 450 tons which include 320 tons of structural steel.

A demonstration test of the encoder was carried out successfully. This encoder uses two laser interferometers and a number of flat mirrors fixed on the structure. Each mirror can cover a range of about 4 degrees and the two heads permit the transition from one mirror to another without the loss of information.

Enclosures

The design and construction of the enclosures were contracted to the SEBIS Consortium in Italy. The final design is near to completion (January 1994).

Wind tunnel tests have been performed for the assessment of wind loads on a single enclosure. Additional tests will be performed in November 1993 to study the interference between the enclosures.

Mirrors and M1 Unit

The first primary mirror blank has been delivered to REOSC and the pads for the axial supports have been glued on the back. The manufacturing of other blanks by Schott proceeds as planned. Two parallel contracts were issued for the design of the mirror cell. The Preliminary Design Review will take place at the beginning of next year.

M2 Unit

The call for tenders has been issued and the tenders are expected in mid-December. The requirements include a fast guiding mode (field stabilization) and a chopping mode for frequencies up to 5 Hz and amplitude of up to 1 arcminute.

Coating Plant

The technical specifications and statement of work for the Call for Tenders have been completed. The specifications are based on a sputtering process. The start of the contract is expected to be May 1994.

Washing Unit and Cleanroom

The specifications and statement of work for the call for tenders is being prepared. The contract for the washing unit will include the pilot washing unit (for the 3.6-metre mirrors) for La Silla. Cleanroom specifications have been prepared. The cleanroom will comprise both the coating and washing unit for the 8-m mirrors.

Cassegrain and Nasmyth Adapters

The conceptual design has been completed and the call for tenders will be sent out early in 1994 after analysis of the results of a preliminary enquiry. A call for tenders is running for the procurement of CCD cameras for autoguiding and wavefront sensing applications.

Coudé Station

The concept is based on a large turntable on which all the coudé station equipment is fixed. It is used to compensate the field rotation for coudé instruments and to position the collimating units to be used for the different types of beam combinations. The contract for the construction of turntables has been issued.

Adaptive Optics

An optimization study has permitted the finalization of the essential parameters necessary for the establishment of specifications.

Handling Aspects

A new concept for the M1 handling tool has been developed. The principle is a hydraulic whiffle tree. The geometry is identical to that of the REOSC tool. The M1 handling tool will include the lifting system and will form a self-standing unit in the Mirror Maintenance Building.

VLTI System Level

A number of studies at system level are currently being carried out or have been completed. These studies are important for assessing the overall performance of the VLTI as well as for the specification of VLTI subsystems, such as the delay lines. Studies include:

- Control model of delay line/fringe sensor
- Structural deformation of unit telescopes under wind loads
- Study of acoustic noise inside UT enclosures
- Study of thermal environment in VLTI facilities
- Measurements of ground transfer functions on Paranal

Auxiliary Telescopes

Calls for tenders for the design, manufacture, test in Europe, transport to and erection in Chile of three auxiliary telescopes and equipment for 11 stations were sent to industry in July 1993.

Beam Combiner System

An in-house design study of the beam combiner is nearing completion. The main objective of the study is a conceptual design which allows the assessment of the interface to the civil engineering infrastructure and understanding of the tradeoffs between various concepts for the homothetic mapping.

Instrumentation

The VLT Medium Resolution Spectrometer/Imager (ISAAC) reached the Final Design Review (FDR). The CONICA (High Resolution Near Infrared Camera) and FORS (Focal Reducer Spectrograph) are approaching the FDR stage. The UV-Visual Echelle Spectrograph (UVES) completed the Preliminary Design Review in October. The Multi-Fiber Area Spectrograph (FUEGOS) is being studied by a consortium composed of the Observatoire de Meudon, the Observatoire de Genève, the Observatoire de Toulouse and the Osservatorio di Bologna. The Phase A study ended in October and is being reviewed by ESO technical staff. The Mid-Infrared Image Spectrometer is being studied by the Service d'Astrophysique CEA/DAPNIA and is making progress in Phase A.

First Light from the NTT Interferometer

T.R. BEDDING, O. VON DER LÜHE and A.A. ZIJLSTRA, ESO
A. ECKART and L.E. TACCONI-GARMAN, MPE Garching, Germany

It is not obvious that placing a mask over a telescope and blocking most of the light will improve its imaging performance. Yet several groups have done just this in an effort to overcome the limits of atmospheric seeing and achieve the best angular resolution from large telescopes such as the 4.2-m WHT, the 3.9-m AAT, the Hale 5-m and the Mayall 4-m at Kitt Peak. Aperture masking has mainly been used for bright sources having reasonably simple structure. Fortunately, there are some very interesting objects that satisfy these criteria: cool giant stars, whose large angular diameters (up to ~0.05″) make them ideal targets for big telescopes. Aperture masking has so far allowed detection of convective hot spots on the red supergiant α Ori and asymmetries in the atmosphere of Mira (e.g., Wilson et al. 1992; Haniff et al. 1992).

This article describes aperture-masking observations of cool giants with the 3.5-m NTT in the near infrared (1.5 μm). We chose the infrared because, although the angular resolution is somewhat poorer than at visible wavelengths, the stars are much brighter and the atmospheric seeing is more favourable.

Before describing our observations, we give a brief introduction to the techniques involved.

Optical/IR Interferometry

To produce images that have high angular resolution one must overcome the seeing. This means compensating for perturbations in the wavefront of the light that result from its passage through the atmosphere. These perturbations arise because the refractive index of the atmosphere is continually fluctuating, primarily due to turbulent mixing of regions of air with differing temperatures. The incoming wavefront can be thought of as being made up of a large number of patches, each having a diameter of r_0, where the wavefront is approximately flat across each patch. The quantity r_0 determines the seeing: at a wavelength λ, the seeing disk has a FWHM of about $1.2\,\lambda/r_0$ (e.g., r_0 = 15 cm at 550 nm for 1″ seeing).

Adaptive optics seeks to compensate for wavefront perturbations in real time using a small deformable mirror. Provided the mirror has enough actuators (one for every r_0-sized patch on the pupil), it is possible to place most of the light in a diffraction-limited core. Of course, one also requires sufficient photons per r_0-patch to measure the wavefront and calculate the correction.[1]

It is possible to achieve high angular resolution passively (i.e. without adaptive optics), provided one has a fast detector. This involves recording the distorted image in a succession of short exposures, each of which "freezes" the seeing, and processing them off-line. This is the basis of speckle interferometry. Each short-exposure image contains high-resolution information which can be extracted via a Fourier transform and calibrated using similar observations of a nearby unresolved star.

Aperture masking is identical to speckle interferometry, except that one places a mask over the telescope pupil. The mask may consist of a small number of holes arranged in a non-redundant pattern (i.e., so that all baseline vectors are distinct). Alternatively, it may be partially redundant, such as an annulus or a slit. The pros and cons of aperture masking have been discussed elsewhere (Haniff & Buscher 1992; Buscher & Haniff 1993; Haniff 1993) and here we simply try to summarize the main arguments.

[1] *Adaptive* optics is not the same as *active* optics. The latter involves adjusting the primary mirror to correct for telescope flexure, etc., and the corrections are necessarily made on a much slower timescale. This type of correction produces excellent long-exposure images, but cannot be used for real-time seeing compensation.

Why Use an Aperture Mask?

Each r_0-sized patch on the pupil has an unknown phase error, corresponding to the unknown thickness of atmosphere above it. Each *pair* of patches forms an interferometer that measures a particular spatial frequency on the sky. With an un-masked pupil there are many different pairs measuring a given spatial frequency. Each one contributes a different phase error, so that many fringe patterns with the same spatial frequency are superimposed on the detector with different position offsets. The resultant fringe power will be the sum of these randomly-phased contributions. The problem is that the wavefront errors are different in every short-exposure image, so the final fringe power, being the sum of a random walk, will also fluctuate. This introduces so-called atmospheric noise in the power spectrum. A non-redundant aperture mask, in which no baseline is sampled more than once, eliminates atmospheric noise. This is particularly important in the infrared, where the large numbers of photons mean that atmospheric noise usually dominates over photon noise.

Another advantage of non-redundant aperture masking is that it improves the accuracy with which one can correct for variations in atmospheric seeing, something which is often the limiting factor in high-resolution imaging. This is because a pupil composed of subapertures each having size $\lesssim r_0$ is quite insensitive to changes in the actual value r_0. Of course, a mask also reduces the light level and restricts observations to bright objects. But for those objects, there is an additional advantage if the light being discarded does not carry useful information. This last point becomes clear if one imagines observing an object which is only barely resolved by the full telescope aperture. In this case, the "useful" light comes from the outer parts of the pupil and the remainder only serves to add noise to the signal we are interested in. By using a mask, one can effectively increase the resolving power of the telescope by giving more emphasis to high spatial frequencies.

A big drawback of using a non-redundant mask with a small number of holes is the poor coverage of spatial frequencies. A good compromise in the photon-rich infrared regime is an annular mask. This has full spatial frequency coverage while being minimally redundant: roughly speaking, each baseline is measured twice. Furthermore, a thin annulus largely retains the other advantages mentioned above, namely accurate calibration and enhanced resolution. However, an annular mask is not a good choice in the visible regime, where photon noise generally dominates over atmospheric noise. Here, Buscher & Haniff (1993) advocate the use of a long slit.

Figure 1: *To change between masks, the NTT was tilted to 15° from the horizontal and the mirror cover (grey) was partially closed. Here, Oskar von der Lühe (left) and Tim Bedding (right) stand on the telescope structure and show off the 7-hole mask. The black circle behind their heads is the annular mask attached to the M3 baffle. Andreas Eckart is standing at floor level.*

We do not wish to give the impression that masking a telescope is always the best strategy. In some situations, however, there are powerful arguments for doing so and these issues are discussed more fully in the references. To summarize, an aperture mask with non-redundant holes provides more accurately calibrated measurements at the full diffraction limit, but at the expense of lower sensitivity and poorer spatial-frequency coverage. As noted above, an annular mask should be a good compromise in the infrared, but this method has so far only been tested on binary stars (Haniff et al. 1989).

Masking the NTT

Our observations were made on the NTT in August 1993, using the SHARP infrared camera (Eckart et al. 1991). In order to sample the images fully at the diffraction limit at the J band, it was necessary to magnify the image scale. We did this by placing a focal expander just in front of the dewar window. This device, which we named COSHARP, consisted of a pair of lenses mounted in an aluminium tube. COSHARP performed perfectly and we wish the same success to its more expensive space-based cousin.

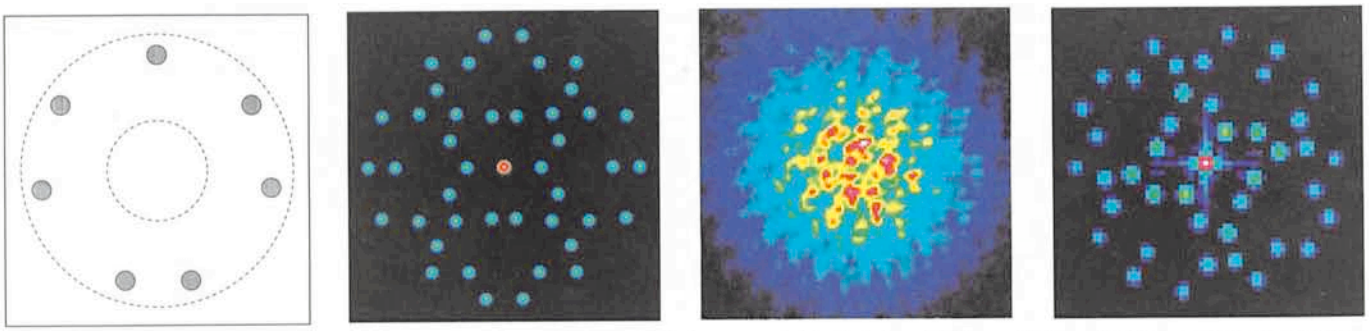

Figure 2: *(a) The 7-hole non-redundant mask, with the pupil of the NTT shown as dashed circles. (b) Theoretical spatial-frequency coverage. The central red dot is the origin and the other points (in symmetrical pairs) show the 21 different baselines.*
(c) Typical 0.1-s exposure of a bright star. The envelope corresponds to the airy disk of a single hole and fringes from the interferometric array are clearly visible. The image is 2.9″ across.
(d) The average power spectrum of 200 interferograms like the one in (c). Since the telescope has an alt-azimuth mount, the orientation of the pattern varies with the rotation angle of the mask with respect to the sky.

We observed several red giants and Mira variables using both an annular mask and a 7-hole non-redundant mask. Placing a full-sized mask over the primary mirror of a large telescope is rather difficult, especially if you want to change between different masks during the night. The solution adopted by most observers is to place the mask inside the instrument at an image of the telescope pupil. Re-imaging the pupil to a diameter of ~20 mm with a lens allows one to use a correspondingly smaller mask, which is very convenient but requires extra optics to be inserted in the system. With SHARP on the NTT, this was not practicable.

The NTT is a compact alt-azimuth telescope in a small enclosure, making it quite easy to access the telescope structure. This allowed us to place the masks on the baffle in front of Mirror 3, at which point the converging f/11 beam has a diameter of 45 cm. The masks were made from 5 mm thick black PVC and, by bolting a mounting ring to the M3 baffle, we were able to attach and remove them very easily. To reach the M3 baffle, we drove the telescope to its lowest elevation (15°), partly closed the primary mirror cover and climbed onto the telescope structure. The whole process of changing the mask took two people about 5 minutes (see Figure 1).

The mirror cover of the NTT opens like a pair of sliding doors, which makes it useful as a secure handhold. We note in passing that this mirror cover can easily be used to create a *slit* mask, simply by opening the cover to the desired width. As mentioned above, a slit mask can be used for interferometry at visible wavelengths.

The design of the 7-hole mask is shown in Figure 2(a). When projected on the entrance pupil of the NTT, the holes have a diameter of 25 cm and lie on a circle of diameter 3.05 m. We did not use the full diameter of the pupil (3.5 m) in order to avoid vignetting that would arise from the mask not being exactly at the pupil plane. Figure 2(b) shows the two-dimensional spatial frequency coverage. The arrangement of the holes is based on a design by Cornwell (1988), except that we moved the lower pair of holes closer together to make the radially-averaged coverage of spatial frequencies more uniform. Figures 2(c) and (d) show data from a bright star. The signal in the power spectrum is attenuated relative to the theoretical pattern (2b), mainly due to seeing decorrelation during each 0.1-s exposure. This exposure time, which was set by the detector system, is a little long and we plan to install a fast shutter for future observations.

The annular mask (Figure 3) has an effective outer diameter of 3.3 m and a width of 20 cm. The transfer function (Figure 3b) gives strong emphasis to high spatial frequencies. In the mid-frequency range the transfer function is a factor of ~7 below that of the unmasked telescope. However, in the presence of seeing, the signal from the unmasked telescope is strongly attenuated, while that from the annular mask (Figure 3d) is less severely affected.

Results and Future Prospects

Despite poor weather, we obtained good observations of several southern red giants and Miras that we would expect to have large angular diameters.

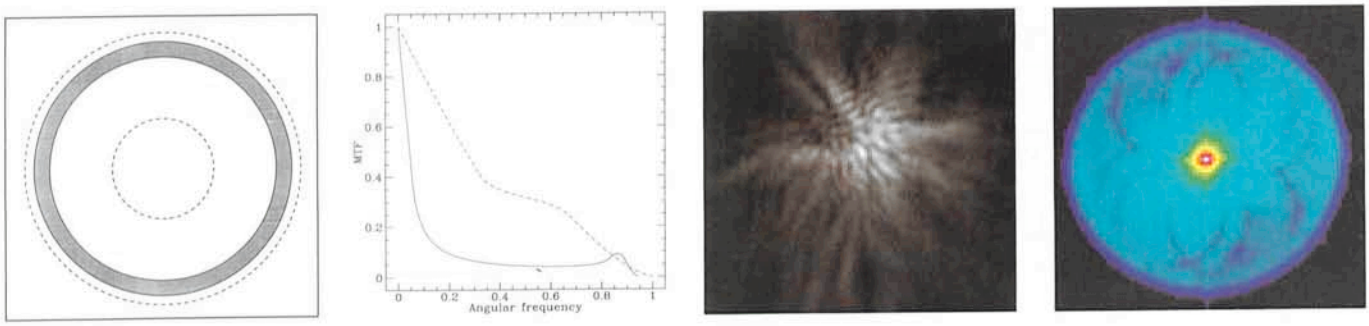

Figure 3: *(a) The annular mask, with the pupil of the NTT shown as dashed circles.*
(b) Radial cuts through the NTT modulation transfer function in the absence of seeing effects. The solid curve is for the annular mask and the dashed curve is without a mask (but including the telescope's central obstruction). An angular frequency of 1 corresponds to the diffraction limit of the full 3.5-m aperture.
(c) Typical 0.1-s exposure of a bright star, showing many small speckles. The image is 2.9″ across.
(d) The average power spectrum of 500 interferograms like the one in (c). The origin of the spatial frequency domain is at the centre, where the signal is strongest. The arc-like features are due to the telescope spiders and also to a deposit on M3 courtesy of the bird life on La Silla.

Preliminary analysis of the data indicates that these stars are resolved and that they probably rival Betelgeuse and Mira in angular size. If this turns out to be the case, we will be able to look for evidence of asymmetries and surface features on these stars.

The number of stars that can be resolved by 4-m-class telescopes is small, but the results so far have proved very interesting. The new generation of 8–10-m telescopes will give a big improvement in angular resolution, and masking observations similar to those we have described should allow detailed study of stars with large angular diameters. At the moment, however, there are always practical difficulties with aperture masking. We therefore hope that future instruments will be designed to contain a reimaged pupil at which masks can be easily inserted.

We thank Reiner Hofmann for making COSHARP, Gerardo Ihle and the staff in the La Silla workshop for making the masks, and telescope operator Francisco Labraña for excellent support during the observations.

References

Buscher, D.F., & Haniff, C.A., 1993, *J. Opt. Soc. Am. A.* **10**, 1882.

Cornwell, T.J., 1988, *IEEE Trans. Antennas and Propagation* **36**, 1165.

Eckart, A., Hofmann, R., Duhoux, P., Genzel, R., & Drapatz, S., 1991, *The Messenger* **65**, 1.

Haniff, C.A., & Buscher, D.F., 1992, *J. Opt. Soc. Am. A.* **9**, 203.

Haniff, C.A., Buscher, D.F., Christou, J.C., & Ridgway, S.T., 1989, *MNRAS* **241**, 51P.

Haniff, C.A., Ghez, A.M., Gorham, P.W., Kulkarni, S.R., Matthews, K., & Neugebauer, G., 1992, *AJ* **103**, 1662.

Haniff, C.A., 1993, Speckle v non-redundant masking. In: Robertson, J.G., & Tango, W.J. (eds.), *Proc. IAU Symp. 158, Very High Angular Resolution Imaging*, Sydney, Australia, January 1993, in press.

Wilson, R.W., Baldwin, J.E., Buscher, D.F., & Warner, P.J., 1992, *MNRAS* **257**, 369.

Optical Gyro Encoder Tested on the NTT

H. DAHLMANN, B. HUBER, W. SCHRÖDER, L. SCHÜSSELE, H. ZECH, Fachhochschule Offenburg and Steinbeis Transfer Zentrum Physikalische Sensorik, Offenburg, Germany

M. RAVENSBERGEN, European Southern Observatory

The prototype of the optical gyro encoder (see [1] and [2]) has been successfully tested on the NTT telescope in the period of 5 to 10 September 1993. Day time tests until 20 September proved the repeatability of the measurements. The tests confirmed the specifications of the encoder and qualified this type of angular encoder for the use in an optical telescope.

The optical gyro encoder (OGE) consists of two gyros:

1. A ring laser gyro. This gyro consists of a triangular or square light path with mirrors in the corners. Laser light from an ionizing laser source (e.g. HeNe) is emitted in the 2 directions of the light path and the resulting interference pattern is measured.
   The light path is made in a glass block with a thermal expansion coefficient of zero. It has therefore a very stable scale factor but the resolution is not sufficient.
2. A fiber optic gyro. This gyro consists of a polarization maintaining fiber, which is wound on a coil. A light source emits light in the two directions of the coil, and the interference pattern is measured. Compared with a ring laser gyro with the same enclosed area for the light path, the sensitivity multiplies with the number of turns. This results in an excellent resolution and low noise. On the other hand, the scale factor is not sufficient because of imperfections in the optical elements and thermal effects.

In principle, the OGE integrates the signal of the ring laser gyro and compensates it for misalignments and earth rotation in order to get the angles in telescope coordinates. The ring laser gyro data are also used to stabilize the fiber optic gyro. The data collection was however done for the two gyros individually and the data were evaluated off-line in order to find the best integration time constant.

The OGE data were transformed into altitude/azimuth coordinates according to its system equations and calibration data. This was compared with the readings of the altitude and azimuth encoders of the NTT.

The OGE was first mounted on the

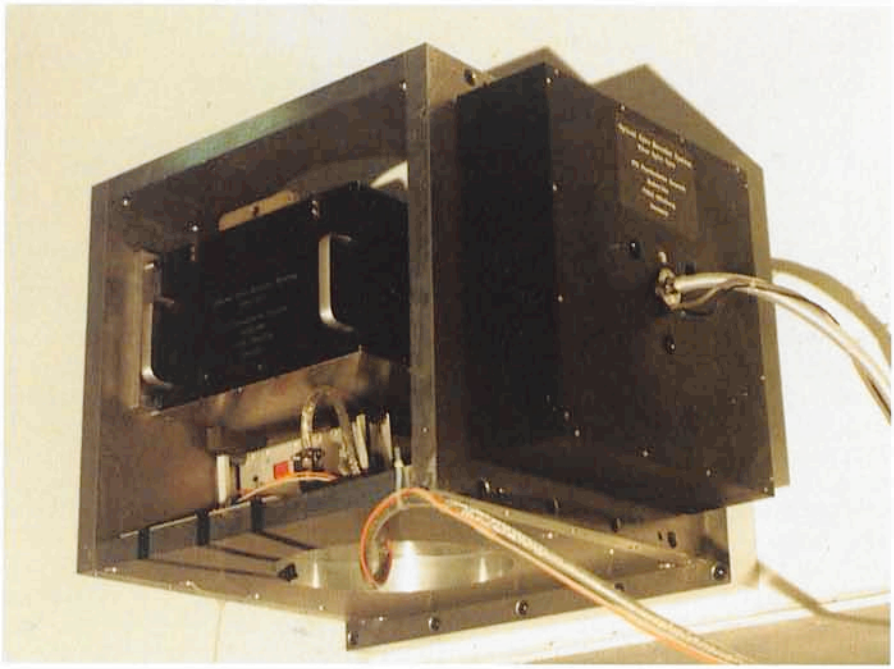

The optical gyro encoder mounted on the NTT centre piece (altitude axis). The ring laser with its front-end electronics is mounted in the box, while the fiber gyro is mounted on the right-hand plate. Dimensions of the mounting box are about 45 × 45 × 45 cm. The axis of the optical gyro encoder is from left to right on this picture.

azimuth box to measure azimuth rotation and was later fixed to the centrepiece in order to measure altitude rotation.

The OGE measures in respect to inertial space, while the NTT encoders measure in respect to altitude/azimuth coordinates of the earth frame. Because of this basic difference in operation, several special effects were detected:

1. Stressing of the azimuth bearing support ring. When the telescope starts to move from a stand-still position, the telescope is already moving before the NTT encoder measures a rotation. This is due to the friction in the radial bearing of the azimuth axis, which is also the mounting location of the NTT encoder.
2. Sag of structural parts of the centerpiece of the NTT according to the altitude position.
3. Minor nonlinearities of the NTT encoders in the sub arcsec range.
4. Details of the control loop behaviour.

The preliminary evaluation of the test data gave the following characteristics:

Pointing accuracy: Azimuth axis: < 0.7 arcsec rms
Altitude axis: < 1 arcsec rms

Tracking accuracy: < 0.1 arcsec rms over a time of 30 seconds

Resolution: $< 3\times10^{-4}$ arcsec at a read-out rate of 10 Hz

Bandwidth: up to 120 Hz (adjustable by software)

No temperature compensation had to be applied.

In gyro terms the data are as follows:

Bias stability: $< 2\times10^{-3}$ degrees/hour

Scale factor stability: < 1 ppm

Random walk coefficient: $< 5\times10^{-4}$ degrees/$\sqrt{\text{hour}}$.

The high resolution and bandwidth make the OGE an excellent device for telescope tracking. Having fiber optic gyros mounted on the telescope tube, the rotation rate has to be zero during tracking for alt-azimuth mounted telescopes as well as for equatorial mounted telescopes. However, the intrinsic integration principle and drift require the use of an initialization reference and an autoguider.

The installation of an OGE is easy because it does not need to be mounted in the telescope axis and there are no tight mechanical tolerances to be respected.

On an equatorial mounted telescope, the application is even easier because no coordinate transformation is needed: If one OGE is mounted on the alpha and another one on the delta axis, they see an inertial rate of zero during tracking. This also means that, in this case, the tracking performance is not dependent on a pointing model: the OGEs drive the motors in such a way that the inertial rate becomes zero.

The test campaign proved that this device is also quite useful for calibrating existing encoders and for analysing existing telescope control loops and structures.

Acknowledgement

The authors would like to thank:

- the personnel of ESO in Chile for their support in the preparation and the execution of the test,
- B. Gilli from ESO Garching for the preparation of the software on the NTT,
- the co-workers at the Fachhochschule Offenburg and the STZ Physikalische Sensorik for their excellent development work and
- the Ministry for Research and Technology of Baden-Württemberg.

References

[1] F. Merkle and M. Ravensbergen: *The Messenger* No. **65**, Sept. 1991.

[2] W. Schröder et al. (1991): Proc. SPIE 1585.

Infrared Astronomy with Arrays: the Next Generation

A. MOORWOOD and G. FINGER, ESO

The title is that of a conference held at UCLA in July 1993 at which approximately 250 participants experienced a feast of 73 papers and 120 posters covering both recent astrophysical results and future prospects for the next generation of infrared array instruments on large ground-based telescopes and in space. Although it was a very exciting meeting both scientifically and technically with many highlights, the purpose of this article is not to review the conference (to be published as a book by Kluwer and edited by Ian McLean) but to draw attention to developments in the field of infrared array detectors reported there which are of great interest for both planned and future VLT instruments. Partly because the conference was in California, the infrared detector manufacturers were represented in force to present their products and solicit feedback from users on the performance of current arrays and their future requirements in a special "meet the industry" evening session. Such sessions have become a regular feature of specialist infrared conferences, and this one really demonstrated the extensive cooperation which has developed between astronomers and industry during the last few years and the remarkable progress made in the development/optimization of arrays for infrared astronomy.

Based on the quantity and quality of the scientific results presented, the standard in the near infrared (1–2.5 μm) region has clearly been set during the last few years by the 256×256 Hg:Cd:Te NICMOS3 array developed for the HST instrument with whose name it has become synonymous (and whose home was visited by many of the participants on an oversubscribed tour organized by the Rockwell International Science Center). This is the array installed in IRAC2 at the 2.2-m telescope on La Silla and currently baselined for the short wavelength channels of the ISAAC (see *The Messenger*, 70, 10) and CONICA (*The Messenger*, 67, 17) instruments for the ESO VLT. With its relatively short long wavelength cut-off this array yields extremely low dark current (~0.1 e/s) and read noise (~20 e) at comfortable operating temperatures ~70K. Results at the conference, however, revealed the strong competition it now faces from the new SBRC 256×256 InSb array, successor to their famous 58×62 device, which is sensitive out to 5 μm and has been baselined for the long wavelength channels of ISAAC and CONICA. Somewhat unexpectedly, the first tests of these arrays have shown that they can also compete with the Hg:Cd:Te arrays with regard to dark current and noise, albeit at less comfortable temperatures (~30K) and with much more stringent requirements on the instrumental background due to their longer cut-off wavelength. They also yield quantum efficiencies >0.8 which are higher than the Hg:Cd:Te

arrays at the short wavelengths and do not appear to suffer from the persistence and "glow" problems of these arrays under extremely low background conditions. Among the first instruments equipped with such an array is the Caltech infrared camera for the Keck telescope which has already achieved a 1σ K′ (2.1 μm) limit of 22 mag./sq. arcsec in 20s of integration time. Unfortunately, the well capacities of the first devices are rather low (~$2 \cdot 10^5$e) for ground-based L (3.8 μm) and M (4.8 μm) broadband imaging. At ESO, however, we are currently preparing to test an engineering array of this type and expect delivery early next year of a science grade array with higher well capacity if current experiments with higher doping at SBRC are successful. Cincinnati Electronics also presented their new 256×256 InSb array which yields higher well capacities of ~10^6e at the expense of higher dark current and read noise and could be of great interest for long-wavelength imaging. The big news, however, was that both Rockwell and SBRC have now started development of 1024×1024 arrays, i.e. jumping the previously anticipated next step in format. Both plan to utilize four quadrant readout chips so that 512×512 arrays should also be available if required and offer a fallback if yield of the full arrays proves to be a major problem. Both companies appear to be more concerned, in fact, by yield (and hence cost) than technical performance aspects although Rockwell plan a concerted attack on the persistence problem and hope also to increase quantum efficiency and reduce the read noise of the new devices to ~5e. The prospect now, therefore, is not only of much larger formats but also improved sensitivity and hence a considerable overall performance gain. One of the VLT infrared instruments still in the definition phase at ESO – the cryogenic infrared echelle spectrometer – actually requires arrays of this size for a reasonable echelle format and will clearly profit from any improvement in noise performance as such an instrument should be detector limited over much of its wavelength range. Technically, it is also not too late to plan for the use of these larger format arrays in ISAAC and CONICA. Although the present 256×256 arrays were baselined even before these arrays became commercially available, the optical designs of both instruments were specified to accommodate 512×512 arrays in anticipation of future developments. An expansion to 1024×1024 now appears possible without major optomechanical changes if and when they become available.

Considerable progress was also reported on the development of longer wavelength arrays which cover the 10 and 20 μm atmospheric windows and are of interest for the VLT mid-infrared imager/spectrometer for which ESO has contracted a Phase A study to a consortium of institutes led by the Service d'Astrophysique, Saclay (see *The Messenger*, 73, 8). Performance of the high well capacity (~10^7e) 64×64 Ga:Si photoconductor array developed by LETI/LIR in France for ground-based use in the 10 μm window was demonstrated to good effect by an image of the β Pic disk obtained by P.O. Lagage using TIMMI at the ESO 3.6-m and voted one of the conference scientific highlights by Mark Morris in his closing summary. The follow-on development of this device to a format of 128×192 pixels being managed by INSU and with ESO participation was also presented. A novel feature of this array, appreciated by many participants, is the possibility of switching between high and low values of the charge capacity in order to optimize its performance under different background conditions (e.g. imaging and spectroscopy). Both SBRC and Rockwell have also developed low-noise, high-capacity (10^7e), As:Si IBC/BIB (Impurity Blocked Conduction/Blocked Impurity Band) arrays with formats up to 256×256 which are sensitive throughout the 10 and 20 μm windows although it has yet to be established that such devices can be exported outside the United States. Rockwell also reported progress with As:Si solid-state photomultipliers which have high q.e.'s (~0.7) and are capable of counting single photons with a response time of 50ns. Although the present formats are small (10×10), these devices may be of interest in the future for very low background (e.g. high-resolution spectroscopy) applications and the measurement of fast transient phenomena.

This is obviously an exciting and probably exceptional period in the history of infrared array development. If, as expected, the detectors highlighted here materialize within the next few years, infrared astronomers will have evolved from using noisy single detectors to almost "perfect" arrays of one million pixels within a period of little more than a decade. Coupled with the new instrumental opportunities created and the larger telescopes now under development, they will clearly open the way for the next big step in our exploration of the infrared universe.

Current CCD Projects at ESO and Their Relation to the VLT Instruments

O. IWERT, ESO

1. Introduction

The following is a brief description of CCD detectors foreseen to be used with VLT instruments currently under study or design and of the contracts under way to procure them.

In the actual sequence of work, the requirements on the detectors to be used are set in the instrument design phase and this is the starting point for the procurement activities. In this presentation, it is more convenient to describe the various developments now under way and then state their relevance to the different VLT instruments.

Different strategies of procurement are necessary because large CCD detectors for application in advanced astronomical instrumentation are not available as off-the-shelves products. Moreover it is not possible to define a standard CCD device, because the requirements change from instrument to instrument depending on its scientific aim. One can differentiate between the following types of CCDs:

- Well-specified "catalogue products" where a design and manufacturing process already exist and the device is to a basic extent tested at the manufacturer. For large sizes, however, the manufacturing itself still implies a number of risks (e.g. in thinning) thus making the delivery unforeseeable.

- Devices on a best-effort contract with detailed specifications but without manufacturer's guarantee to meet them and mostly without any manufacturer's involvement in device testing and characterization.
- Unique prototypes to test new developments which, when successful, can lead to the definition of new catalogue products.

It will be impossible to describe and compare all parameters of the various CCDs here, so that this article is focusing on the physical device format, pixel size, buttability, number of outputs, thick or thin version, the latter being the fundamental requirement to reach high quantum efficiency over the spectral range from UV to NI. The performance in read-out noise, well capacity, uniformity, etc. is equally important but would require a detailed discussion which is outside the scope of this article. The relevance of these parameters change also very much depending on the specific, astronomical application they are intended for.

2. 2048^2, 15-μm Pixel Size CCDs from Thomson TCS

Based on scientific requirements for current and future instruments, all main parameters of a CCD were set up in a baseline specification in November 1991 to look for a supplier being able to accept certain risks in the development of a thinned product of the required size.

After a formal call for tender procedure, Thomson TCS, Grenoble, was selected in June 1992 for the development of this product. The intention was to establish a specified product being characterized almost completely by the manufacturer himself, thus providing a "standard" product with guaranteed performance.

The specifications were developed in co-operation of ESO and TCS as a trade-off between scientific requirements and technical solutions – risks the manufacturer could accept in terms of predictability, yield and accuracy. The result is the product Thomson THX 7397 M, which – assuming the development is successful – is intended to be offered also to other customers.

It features a 2048^2 detector with 15-μm pixel size, 3-side buttable, two outputs and will be thinned with subsequent surface treatment not requiring UV flooding for optimal operation. The specifications are summarized in Table 1.

A number of mechanical/electrical samples and an engineering grade are to be delivered until January 1994 followed by the final delivery until May 1994 of five devices fully meeting all specifications.

Table 1: *Summarized Specification for the main parameters of the thinned Thomson 2048^2, 15-μm Pixelsize devices*

PARAMETER	GUARANTEED PERFORMANCE
*CHIP TOPOLOGY	
Operation mode	Frame transfer, single field
Readout mode	– At least two identical on-chip output amplifiers on one chip side offering the possibility of simultaneous readout to reduce the overall readout time – The entire charge pattern of the light sensitive area may be read through either one of those output amplifiers or simultaneously through all of them, if so required
*GEOMETRICAL CHARACTERISTICS	
Pixel size	15 micron square format 100 % aperture
Pixel number	2048 × 2048
*MECHANICAL CHARACTERISTICS	
Flatness of light sensitive area	15 micron peak to peak
Package and Chip design	Three-side buttable
Dead surface gap	Less than 400 micron between sensitive areas (mounted in TMS package) of the specified CCDs
*ELECTRICAL PERFORMANCE	
Readout noise in slow scan operation	Less than $4e^-$ (target): $10e^-$ (upper limit) at Data rate 50 KHz with C.D.S. measurement performed at −40 °C
Full well capability	More than $100000e^-$ measured at −80 °C (Design goal $130000e^-$)
Charge transfer efficiency per clock cycle	Better than 0.99995 measured at −80 °C (Design goal 0.99999)
Dark Current (D.C.)	Less than 0.1 e-/min/pixel at −80 °C Measurement performed at +20 °C: D.C. (−80 °C) = 3.10^{-6} × D.C. (+20 °C)
Additional Features	Binning facility for 2 × 2 pixels with full signal (design goal) Nominal operating mode is MPP Either Inverted or Non-inverted mode operation is possible
*OPTICAL PERFORMANCE	
Quantum efficiency	> 20 % at 350 nm (design goal: 30 %) > 45 % at 450 nm (design goal: 50 %) > 60 % at 600 nm > 25 % at 900 nm (design goal: 30 %) All QE values measured at −80 °C
Uniformity of QE across light sensitive area	Within 30 % peak to peak over the whole light sensitive area Typical value of High Frequency Photo Response Non Uniformity: ± 3 % Measurement at −80 °C
Cosmic Ray Sensitivity	< 3 events/(cm^2 * minute) at a CCD temperature of −80 °C
Defects	Not more than 10 bad columns Less than 500 hot or dark pixels

Figure 1 shows a first frontside illuminated (thick) sample shown in the course of the CCD workshop 4/5 October in Garching. Looking at the photograph you might notice the rather unconventional package construction of the CCD, attempting to implement mechanical requirements for mosaicking right from the design start with minimal mechanical adjustment needs.

The final use of these detectors is foreseen at the echelle spectrographs (UVES) under construction for the Nasmyth foci of the VLT. One of the instrument configurations under study is based on the use of a 3 × 1 mosaic. If the manufacturing is successful, these devices could also be used to upgrade La Silla instrumentation and be implemented in second-generation VLT instruments. A mosaic of 2 × 2 devices of this type can also be considered as a

backup solution for the Focal Reducer spectrographs for the VLT (FORS1 and FORS2).

3. 2048^2, 24-μm Pixel Size CCDs from SITE

The CCD department of Tektronix was sold in November 1993 to SITE (= Scientific Imaging Technologies), a wholly owned subsidiary of CBA Int. Three "catalogue" devices TK2048EB featuring 2048^2 format, 24-μm pixel size, non buttable, 2 (4) outputs, thinned, not requiring UV flooding are on order. The possibility to apply a special UV coating to even improve the quantum efficiency of the thinned CCD mainly between 300–350 nm is still investigated but, as a drawback, would require UV flooding. As this is a "catalogue" product, the devices are characterized partly by SITE.

The final use is foreseen at the red camera of EMMI at the NTT and the Focal Reducers at the VLT (FORS1 and 2).

The delivery of these devices is crucial, since EMMI red has been waiting for it for a number of years, thus operating presently at only 50 % of the foreseen efficiency. Envisaged delivery dates are January 1994, January 1995 and July 1995 but may change so that here the establishment of a reasonable backup solution is necessary.

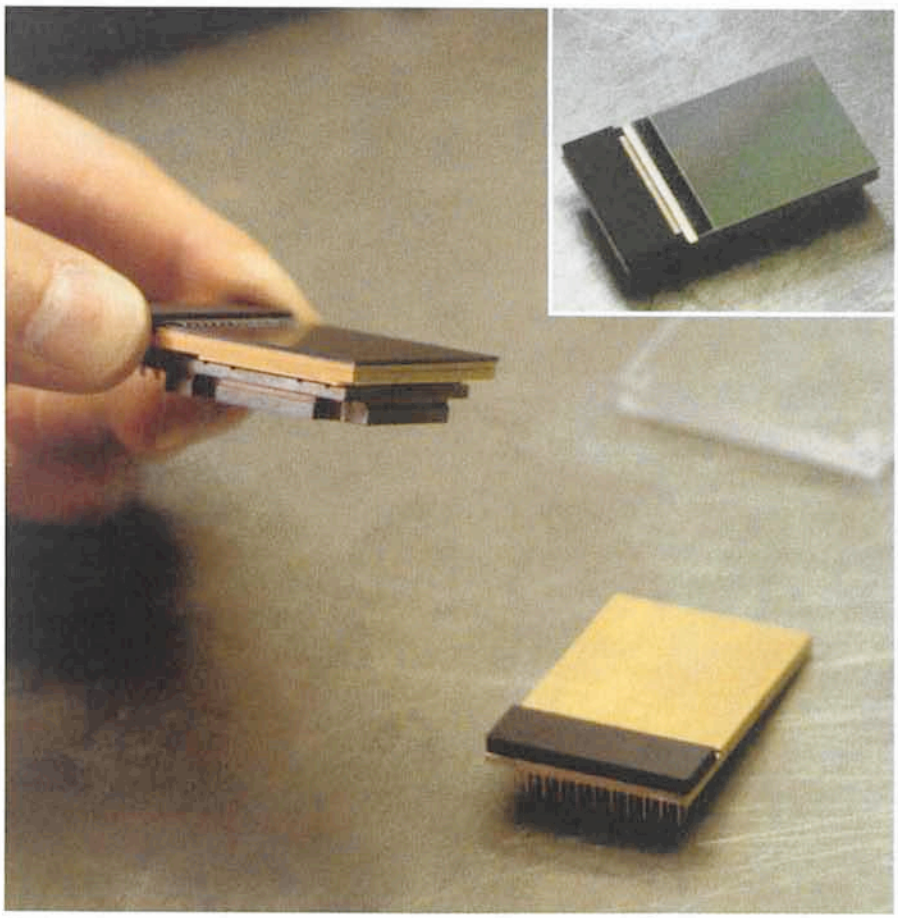

Figure 1: *The first-front side sample of the described Thomson 2048^2 CCD during inspection at ESO (left), together with a "package sample", i.e. the support without the chip (lower right). A view of the sample almost face-on is shown in the insert.*

4. 2048^2 Format, 15-μm Pixel Size and 2048^2 Format, 24-μm Pixel Size CCDs from LORAL South

In order to establish a backup solution for devices of 2K format with 15-μm pixel size, a foundry run of an existing design was ordered in June 1993 at LORAL. The design of this device was done by John Geary, Harvard Smithsonian Inst., and has the following main characteristics: 2048^2 detector with 15-μm pixel size, 3-side buttable, two outputs. Devices produced by LORAL are thick devices and can at LORAL only be enhanced with lumigen coating (not requiring UV flooding). As a consequence, the quantum efficiency in the blue is poor and could be improved by means of thinning and surface treatment. In this case the foundry approach basically delivers only the processed wafers of which by preliminary tests a selection of the CCDs must be done for frontside (thick) packaging, lumigen coating or for later thinning as described in the next paragraph. No device characterization or packaging solution for buttability is offered by the manufacturer, so that the customer has to find his specific solution. Delivery of the raw wafers is foreseen at the beginning of 1994.

Figure 2 shows another custom design of a special CCD under way at LORAL for ESO since April 1993. It features the following characteristics: 2048^2, 24-μm pixel size, 4 outputs, non buttable together with the following tracker CCDs on the same chip: 2 guiding CCDs of format 180×200 active imaging zone, 24-μm pixel size, 1 output and 2 guiding CCDs of format 180×400 active imaging zone, 24-μm pixel size, 1 output. Here the design was partly done by LORAL and partly at ESO in-house in a very flexible co-operation. Again the devices are thick and solutions for packaging, testing, enhancement, etc. have to be provided by the customer. These CCDs are intended to be mounted in the two direct CCD cameras which are foreseen as testing devices for the optical quality and the operation of the VLT Unit Telescopes. The field covered by the scientific CCD corresponds to approximately 1.5×1.5 arcmin. Besides the standard readout, the CCD will be used in 2×2 or 4×4 binned mode (pixel size 0.08 and 0.16 arcsec respectively).

Other possible uses of the devices are to serve as a backup solution for the CCDs of the FORS instruments (single use of the scientific CCD) and to be used for tests of the improvements in image quality by rapid guiding with one of the four small frame-transfer CCDs accommodated at the four corners on the same die (i.e. wafer substrate) as the scientific CCD (Figure 2). Delivery of the raw wafers is envisaged for March 1994.

5. CCD Thinning at Steward Observatory, University of Arizona

The group led by Mike Lesser at the Steward Observatory has been working extensively on the actual thinning process and surface treatment for about 10 years and demonstrated very promising results in 1992 with the thinning of Loral South CCDs. Although being capable of reaching high quantum efficiency, the devices do presently require UV flooding as the surface treatment is not a permanent solution in terms of the energy conditions for surface charge. At that time ESO placed a contract to thin and optimize four LORAL devices of 2K format, 15-μm pixel size, 2-side buttable design, and first results are expected until the end of 1993.

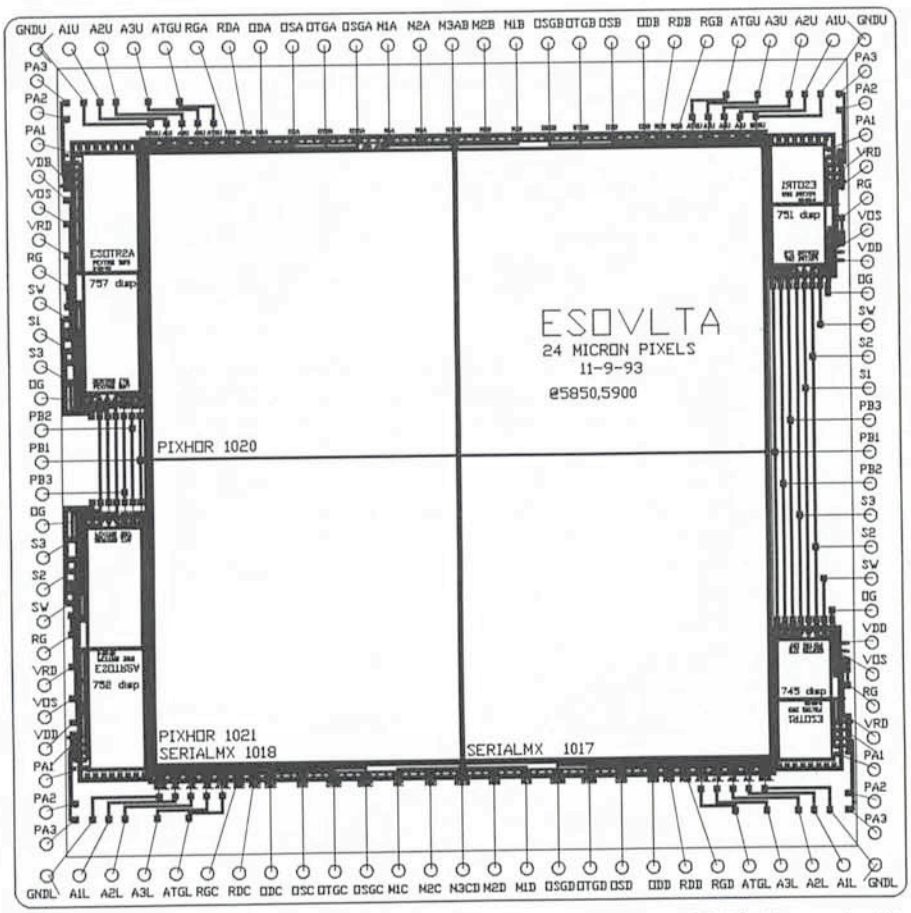

Figure 2: *Sketch of the CCD design foreseen for the VLT test camera: a 2048², 24-μm scientific CCD, surrounded by four tracker CCDs, of two different sizes.*

Currently, a follow-up contract for thinning and optimization of six 2048², 3-side buttable LORAL South CCDs (described in the previous paragraph) is in preparation. It foresees the delivery of the final thinned CCDs, requiring UV flooding, in June 1994. A packaging construction with similar mechanical interface as for the Thomson CCDs of identical format (described above) is under study in order to simplify potential exchanges of the two.

As a consequence, these devices represent an alternative to the Thomson CCDs and could be used in all applications for which these are planned.

6. Concluding Remarks

The more recent main CCD procurement activities for the VLT have been described here in a summarized form. The assessment of the probability of a given development to be completed successfully has to be updated on a weekly basis depending on the technical results obtained by the manufacturers in the various phases of their processing. Another source of worry is the fact that the CCD field has – especially in 1993 – undergone dramatic changes concerning the future of major suppliers, with recurring announcements of closures of manufacturing lines and of change of property.

The limitation on ESO manpower and budget considerations necessarily limit the number of parallel developments we can carry out, but the floating situation forces us, as well as any other group working in this field, to systematically explore alternative routes of procurement in industry and in research laboratories. These might become the single alternative solution of the future.

In many observing modes of the VLT, the photons collected by the 8-m mirrors end up on the few square cm of the CCD detectors and the success or failure of the best scientific programme of European astronomy can depend on the final performance of these devices. While sometimes one feels the weight of this responsibility, this is what ultimately makes the work in this field so exciting and any result towards better detectors so much rewarding.

The Limits of Faint-Object Polarimetry

R. FOSBURY[1] (ST-ECF), A. CIMATTI (ESO/Florence, Italy)
S. DI SEREGO ALIGHIERI (Arcetri, Italy)

Introduction

A common problem in observational astrophysics is the investigation of complex geometrical structures which are below the resolution capabilities of telescopes. In some cases, small-scale structures can be inferred from the global morphology, e.g., the beautiful "ionization cones" seen in some of the nearby Seyfert galaxies (Figure 1), but a geometry-sensitive tool is needed in order to make real progress with the inference of the fundamental physical processes.

The study of rapid time variability has been valuable for the determination of physical scale sizes and, in some cases, the discovery of bulk relativistic effects as an explanation of apparent superluminal motion. It is polarimetry, however, which is capable of giving us the most detailed information about "directionality". This is, of course, a well-established technique in astronomy with many applications in many wavebands. Polarimetric studies cover a wide range of astrophysical subjects. In particular, it is important for solar system objects, in many fields of stellar astrophysics (star-forming regions, young stars, binary systems, variable stars, pulsars, etc.) and in all extragalactic sources, from normal galaxies (magnetic fields, ISM) to active galaxies and QSOs (synchrotron emission, ISM, scattering, geometry). It is not our intention to review here either the applications or the physical processes and observing techniques. Rather it is to concentrate on a particular aspect of the subject which has yielded a rich harvest of new results on faint sources with the current generation of 4-m-class telescopes and promises even more from the yet-larger photon collectors which are just starting to become available. This is the study of the surroundings of active galactic nuclei (AGN) which show many indications of a predominantly axial symmetry determined by the properties of the fundamental source of luminosity.

Following the discovery of the "alignment effect" in high-redshift radio galaxies (HzRG) by McCarthy et al. (1987) and by Chambers, Miley & van Breugel (1987), there has been considerable interest in trying to disentangle those components in the galaxies which can tell the story of their stellar evolutionary history from those which are the result of the presence of a powerful AGN. These objects show a roundish, red component and an irregular blue structure which is aligned – but not necessarily coincident – with the extended double radio source (Rigler et al. 1992, Dunlop & Peacock 1993). Attempts to explain the elongated blue component have centred on two mechanisms. One proposes that the particle jets which drive the extended radio source somehow trigger the formation of stars as they traverse the galaxy ISM (Rees 1989, De Young 1989). This young stellar population shines brightly in the UV and, rather like the track of a particle in a bubble-chamber, traces the radio axis before dynamical effects in the galaxy smear the structure. The second derives from the hypothesis that powerful radio galaxies and radio quasars are one and the same type of object and differ in appearance only by the inclination of the radio axis with respect to our line-of-sight. This unification scheme clearly implies the presence of a quasar nucleus in the HzRG which, as proposed by Tadhunter et al. (1988), will have profound effects on the ISM and will be impossible to hide – especially in the ultraviolet where the galaxy host may be relatively faint.

Optical observations of the HzRG with $z \geq 1$ sample the rest-frame UV and so it is not surprising that they show significant morphological differences from their (extremely rare) low redshift counterparts which are observed in the optical. One important question we have to answer, whatever the correct explanation of the alignment phenomenon, is whether these differences are *entirely* due to the different wavebands of the observations or whether we see evolutionary effects *in addition*. Our polarization observations have been directed towards testing the hypothesis that the blue, aligned structures result from the scattering of the nuclear quasar combined with locally generated line fluorescence excited by the EUV continuum. Clearly, the scattering will produce a linear polarization signature with a precisely defined geometry having the electric vector perpendicular to the direction of the illuminating source in the nucleus. This is a strong hypothesis since, with the appropriate observations, it is readily refutable.

Techniques

The determination of polarization demands the measurement of intensity ratios. For faint extragalactic sources, the fluxes from which the ratios are formed are measured in the presence of a strong, and generally polarized, sky background. Even small variations in this background would make sequential measurements of different polarization directions prone to severe systematic errors. The techniques in common use, therefore, make flux measurements in orthogonal polarization directions *simultaneously*. The method that we use with EFOSC1 (see *The Messenger*, September 1989, No. 57) for both imaging and spectro-polarimetry employs a Wollaston prism in the parallel beam and an aperture mask in the focal plane of the telescope. The mask ensures that the sky from one polarization is not superimposed on the object in the other (Figure 2).

We have used this method to measure polarizations in radio galaxies with redshifts as high as 2.63 and fainter than an R magnitude of 22. Our experience has been that, for these faint objects, the accuracy of the measurement is relatively free from systematic effects while the precision is entirely limited by counting statistics with CCD detectors. Instrumental polarization – which is $<1\%$ for imaging and $<5\%$ for spectropolarimetry – is straightforward to measure and correct for by looking at field stars and polarimetric standards. The critical part of the analysis is, fairly obviously, the extraction of the object flux – including faint extensions – from the background. Optimum methods for doing this, using high s/n sums of all the individual observations to define a weighting scheme, are being developed.

[1] Affiliated to the Astrophysics Division, Space Science Department, European Space Agency.

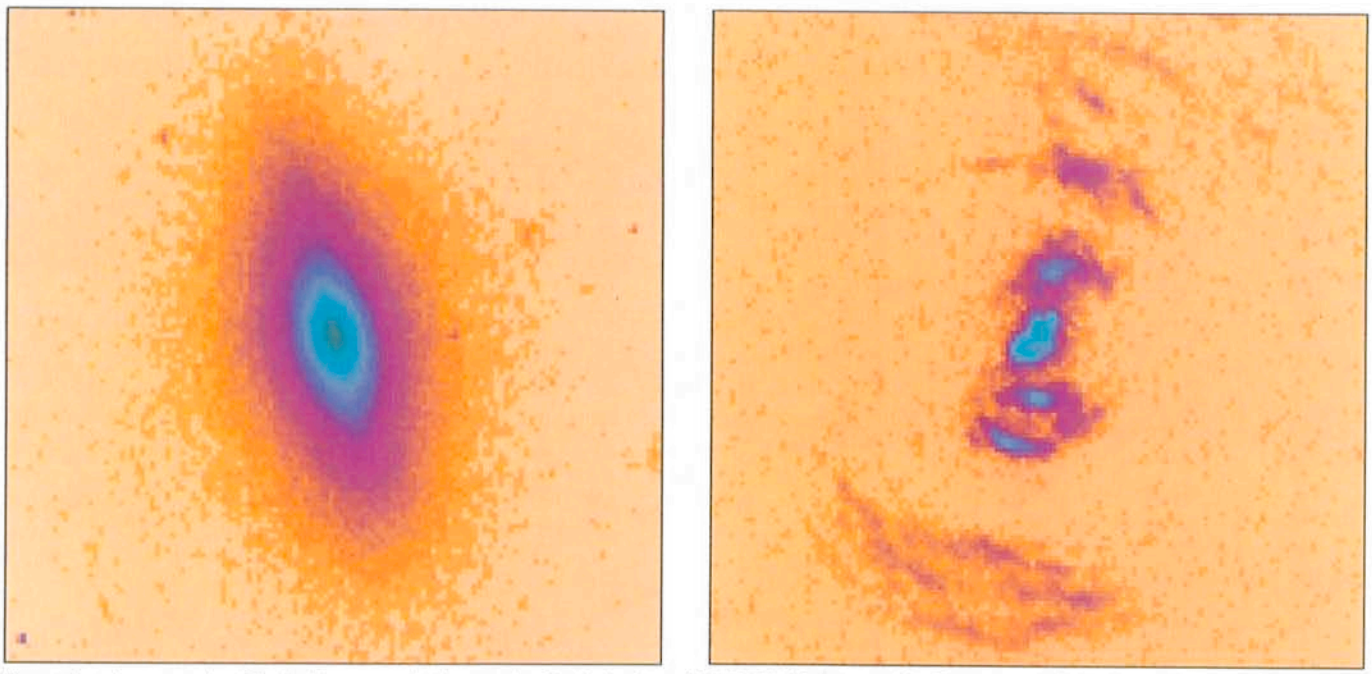

Figure 1 a: *An example of ionization cones in the nearby Seyfert galaxy NGC5252 (Courtesy of Z. Tsvetanov & C. Tadhunter). The two images – with the same scale and orientation – show at the left line-free continuum (starlight) and at the right [OIII]l5007 line emission (excited by the AGN).*

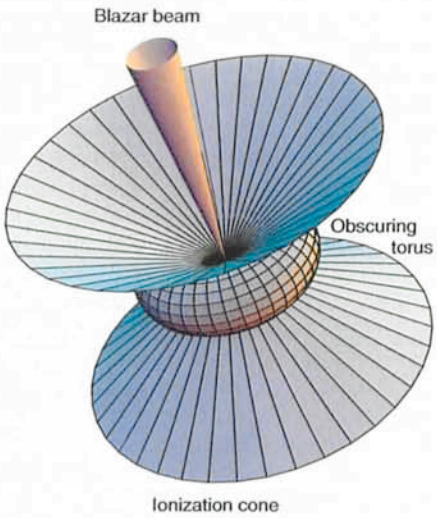

Figure 1 b: *A cartoon of the origin of the ionization cone phenomenon by shadowing close to the AGN. In addition is shown the blazar beam which is thought to be produced by Doppler boosting in regions associated with the formation of the radio jet in radio galaxies. The radio-quiet Seyferts show no evidence of a blazar component.*

Given our experience with the 3.6-m telescope, it is straightforward to extrapolate to the capability of an 8-m VLT element. The new, large telescopes are going to give enormous gains in this type of measurement and will allow detailed polarization mapping and high-resolution spectropolarimetry where now we struggle to do broad-band "aperture" polarimetry and coarse-resolution spectral measurements. The ability to reach galaxies at redshifts greater than one and to separate stellar and nuclear components will have profound implications for our understanding of massive galaxy formation.

In recognition of the fact that the VLT will give very important gains for polarization measurements, most of the planned instruments will have polarimetric capabilities which are briefly reviewed here.

FORS, an imager/spectrograph designed to work at the Cassegrain focus

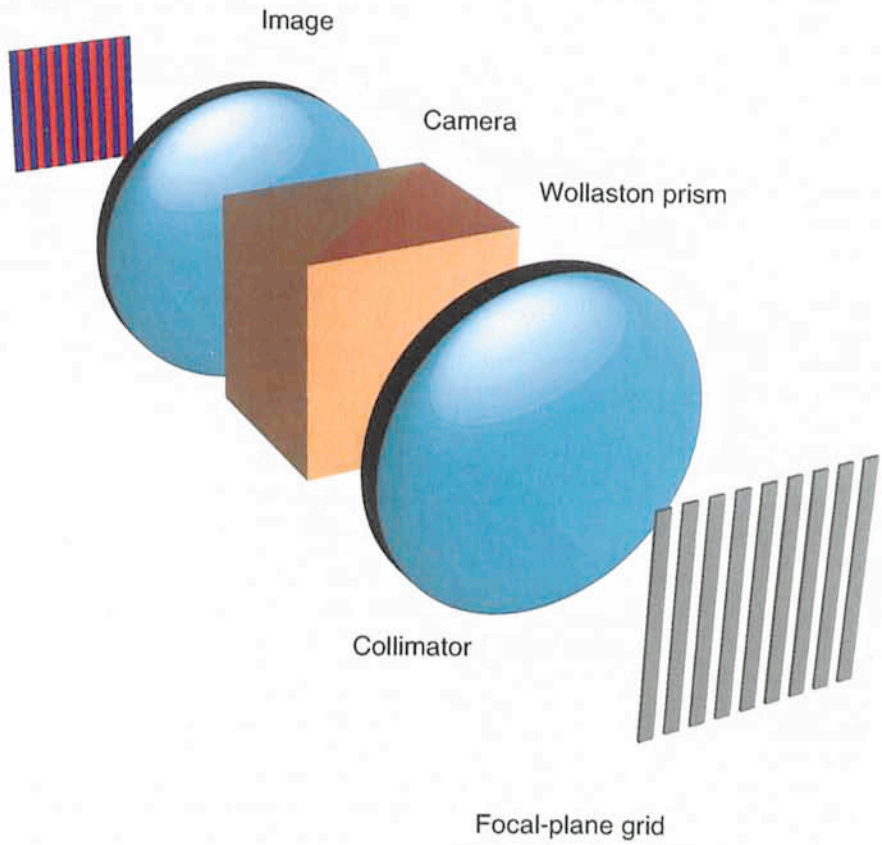

Figure 2: *A schematic view of an imaging polarimeter using a Wollaston prism to split the polarized beams and a focal-plane mask to avoid overlapping images at the detector. At ESO, this facility is available with EFOSC and can be converted for spectropolarimetry by adding a grism in the parallel beam. An achromatic half-wave plate has been obtained and will shortly be added to the instrument so that the plane of polarization can be rotated with respect to the mask. This is especially important for spectropolarimetry.*

between 330 and 1,100 nm with spectroscopic resolution up to 2000, will have both imaging- and spectropolarimetry modes. These are provided by rotatable retarders and a Wollaston prism to be used in combination with filters or grisms and focal plane masks or slitlets. It is anticipated that the degree of linear polarization will be measured with an accuracy of 1 % in one hour down to U, B, V and R magnitudes of 22–23 in imaging and down to V = 17.3 in spectroscopy with 2.5 Å resolution.

ISAAC, the IR imager/spectrograph for the Nasmyth focus will work between 1 and 5 μm with spectroscopic resolutions in the range 300–10,000. It will do imaging polarimetry using a fixed analyser in one of the filter wheels, to be used in combination with filters and with rotation of the whole instrument.

Similarly, imaging polarimetry will be possible with CONICA, the high spatial resolution, near-IR (1–5 μm) camera. This is designed to work at the coudé focus in combination with adaptive optics but the effects of the coudé optical train on polarization measurements have yet to be carefully assessed.

UVES is an echelle spectrograph for the Nasmyth with a spectroscopic resolution of 40,000. The possibility of doing spectropolarimetry with a polarization analyser in the pre-slit optical train has been investigated, but is not in the present plan because of possible difficulties with the polarization induced by M3, the image slicer, the image derotator and the spectrograph. Nevertheless these problems are not insoluble and polarimetry with UVES would be useful, e.g., to study the line polarization structure in AGN.

The present design of the 10–20 μm Cassegrain imager/spectrograph anticipates that both imaging- and spectropolarimetry will be possible with a rotatable retarder and fixed analyser.

Simulation and Error Estimates

The state of polarized light is described by the four Stokes parameters, *I, Q, U* and *V*. These can be normalized to unit intensity for the light source and it is then the second two components of the vector, *q* and *u* from which the state of linear polarization is derived. In a practical polarimeter, *q* and *u* are represented by appropriate intensity ratios in orthogonal polarizations. When poisson noise from the object and the sky is the only source of error, the distribution functions of *q* and *u* are straightforward to calculate and only become non-normal at very low signal/noise ratios (Clarke et al. 1983). The quantities of direct astrophysical interest, the degree of polarization *p* and the orientation of the electric vector ϑ, are derived from *q* and *u* as their quadratic sum and the arctangent of their ratio respectively. The distribution functions of *p* and ϑ are no longer normal and that of *p* becomes skewed as $p \rightarrow 0$ (Figure 3). These distribution functions have to be calculated, either analytically or by Monte-Carlo simultation, before proper confidence limits can be attached to measurements (Simmons & Stewart 1985, Clarke & Stewart 1986). Because of its skewed distribution, measurements of *p* close to zero are biased and this has to be removed using the calculated distribution function (Wardle & Kronberg 1974).

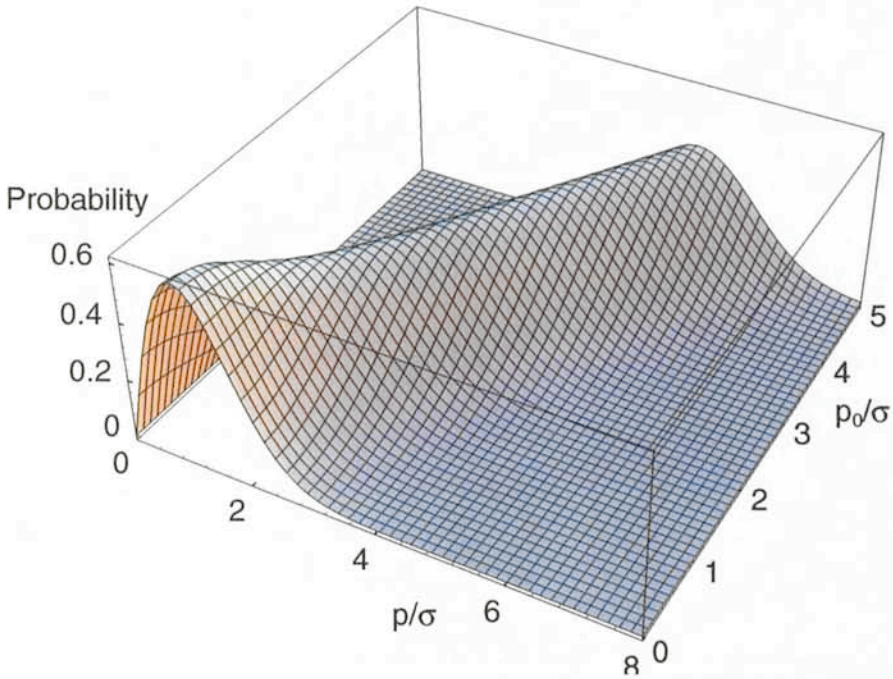

Figure 3: *A three-dimensional plot of the analytic distribution function (a Rice distribution) for the linear polarization measured in the presence of poisson noise. The* x*-axis shows the measured polarization (normalized to the observational* σ*), while the* y *(depth)-axis shows the similarly normalized true (input) polarization. The distribution becomes highly skewed as* $p/\sigma \rightarrow 0$ *and so the resulting measurement bias must be removed.*

While the analytic functions can be used to reduce observations, we have found it convenient to build a stochastic model of the polarimeter which can be readily adjusted to match a particular observational setup and set of measurement angles. In addition to calculating the distribution functions for the quantities of interest, the simulation can be used to optimize the use of a given amount of observing time amongst a sequence of exposures at different orientations of the polarizing prism. Our version is implemented in the Interactive Data Language (IDL) and runs on a Sun workstation. A typical run of 30,000 trials for a set of four angles takes just a few minutes on a Sparc 10. The sample output shown in Figure 4 represents a set of imaging observations of the z=2.63 galaxy MRC2025-218 (Cimatti et al. 1993b). In this case, *q* and *u* are the amplitudes of the sine and cosine terms in a sinusoidal fit to a set of intensity ratios at different orientation angles of the instrument. The bias in the measurement of *p* is obtained by comparing the value input to the simulation with that derived from fitting the peak of the *p*-distribution. These observations used a total observing time of 270 min on the 2.2-m and 3.6-m telescopes and are close to the limit of what can be achieved with these instruments. The same precision could be reached in less than an hour with the same type of instrumentation on an 8-m telescope.

Scientific Highlights

The first detection of polarization in HzRG with $z > 1$ was in 3C 386 and 3C277.2 (di Serego Alighieri et al. 1989) and this was followed by a polarization map of 3C368 made by the Durham group (Scarrott, Rolph & Tadhunter 1990). There are now measurements of some forty objects with z>0.1 (Cimatti et al. 1993a) and a remarkably well-defined trend is emerging. The degree of linear polarization is strongly correlated with the rest wavelength of the observed radiation (Figure 5). For a given filter, this manifests itself as a correlation with redshift but it appears that the wavelength dominates any evolutionary effects (Cimatti et al. 1993a). For those objects observed at a rest wavelength below 4000 Å, the polariza-

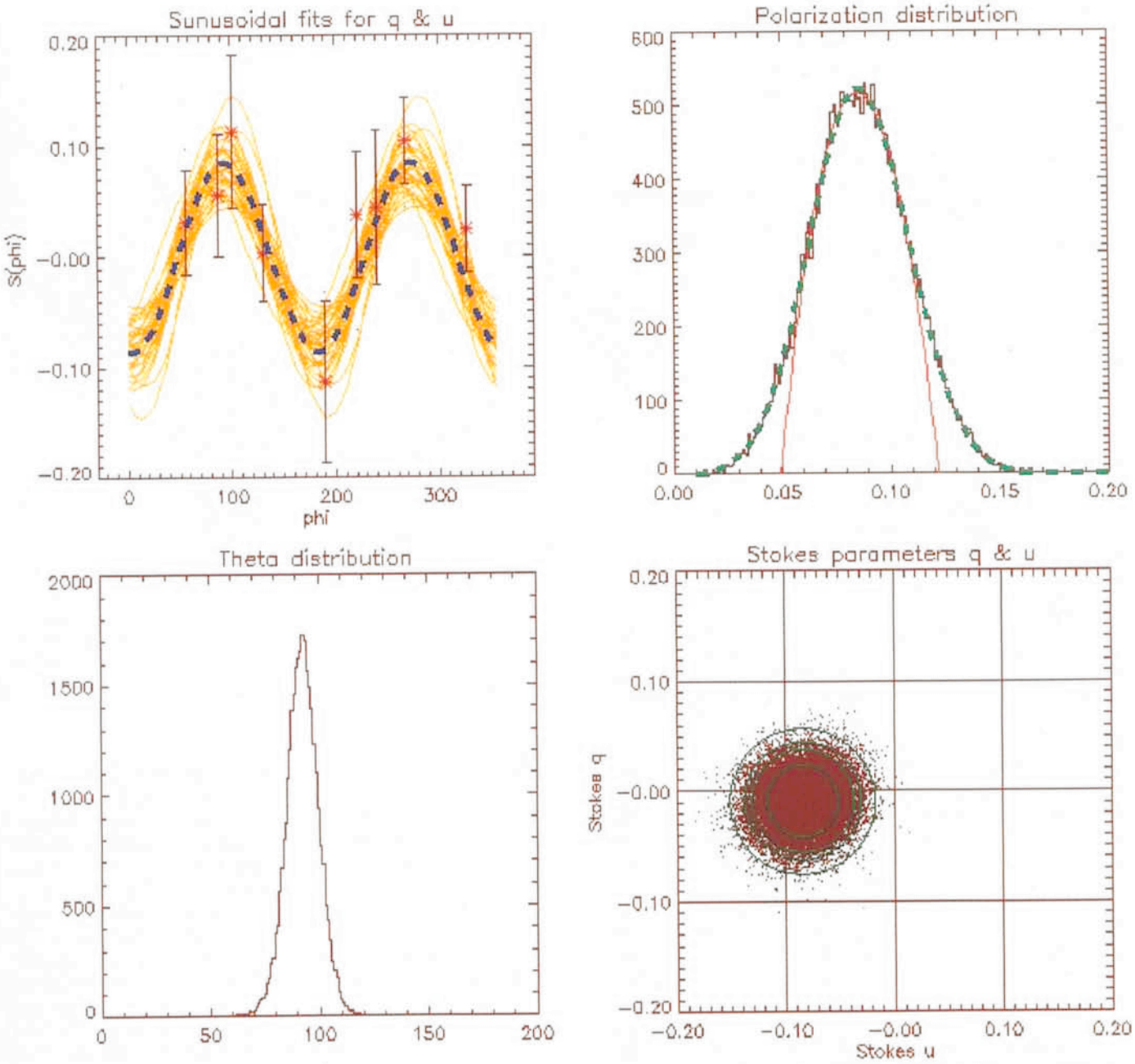

Figure 4: *A representation of our stochastic model of imaging polarimetry. This shows the measured data for the high redshift radio galaxy MRC2025-218 (z=2.63) from the ESO 2.2 and 3.6-m telescopes. In clockwise order, the four frames show: (1) The measured data points with their 1s error bars (red stars) and the fitted sinusoid (blue dashes). The yellow curves represent every thousandth fit to 30,000 simulated data sets with poisson noise added to sky and object counts. (2) The polarization distribution resulting from the simulations. The gaussian (green) and paraboloidal (red – fitted to the peak only) fits are used for finding the most probable polarization. This measurement corresponds to a* p/s *of 3.8 and so the distribution function differs only slightly from a normal curve. (3) The distribution function for the position angle of the E-vector. (4) The distribution of simulated points in the* q, u*-plane. The circles represent 67 %, 90 % and 95 % confidence limits.*

tion is generally higher – ranging up to 20% – than the objects observed at longer wavelengths and has an E-vector which is, in all measured cases, perpendicular to the radio axis within the measurement error.

Spectropolarimetry (di Serego Alighieri, Cimatti & Fosbury 1993 and in preparation) shows this polarization drop longward of 4000Å very clearly in two individual objects. This is interpreted as the increasing dominance of unpolarized starlight above the H&K-break from an old stellar population (Figure 6).

Attempts to model the spectral energy distributions and polarizations of these HzRG using a combination of starlight and scattered quasar light are hampered by the paucity of spectropolarimetric – or line-free imaging polarimetric – data. They do, however, indicate that it is possible to reproduce these two types of measurement simultaneously using an old stellar population and scattering by dust. Electron scattering cannot, however, be ruled out and remains a possibility especially close to the nucleus and, possibly, for sources in rich clusters.

Taken with other tests of the radio-loud unification scheme, the polarimetry provides very strong evidence that the HzRG indeed harbour obscured quasar nuclei. Many details, however, remain to be investigated. For example, it is not known how much the blazar beam – thought to be present in all radio-loud quasars – contributes to the scattered radiation. This will have a bearing on the relative strength of any scattered broad-line radiation. There is also evidence that the non-stellar continuum radiation from AGN may be as extended or even more extended than the BLR (Binette,

Fosbury & Parker 1993, Antonucci 1993) which will also have an effect on the ratio of line to continuum radiation in polarized light.

Conclusions

Both imaging and spectropolarimetry are now playing an important role in the understanding of the AGN phenomenon. We have discussed here only the polarization produced by scattering. Intrinsically polarized emission mechanisms like synchrotron radiation are also, of course, the subject of intensive study in these objects. The nearby Seyfert galaxies can now be studied in great detail using polarimetric techniques, and we fully expect to be able to emulate such investigations at cosmologically interesting distances when we have access to the bigger telescopes. The extension of the measurements into the infrared will also be interesting, especially for resolving the electron vs. dust scattering question.

Finally, we stress that the use of spectropolarimetry to identify and remove the AGN contribution to the luminosity of very distant radio galaxies can allow deductions to be made about their stellar evolutionary histories with much greater confidence than pure spectroscopy. The epoch of galaxy formation is one of the outstanding questions in cosmology today.

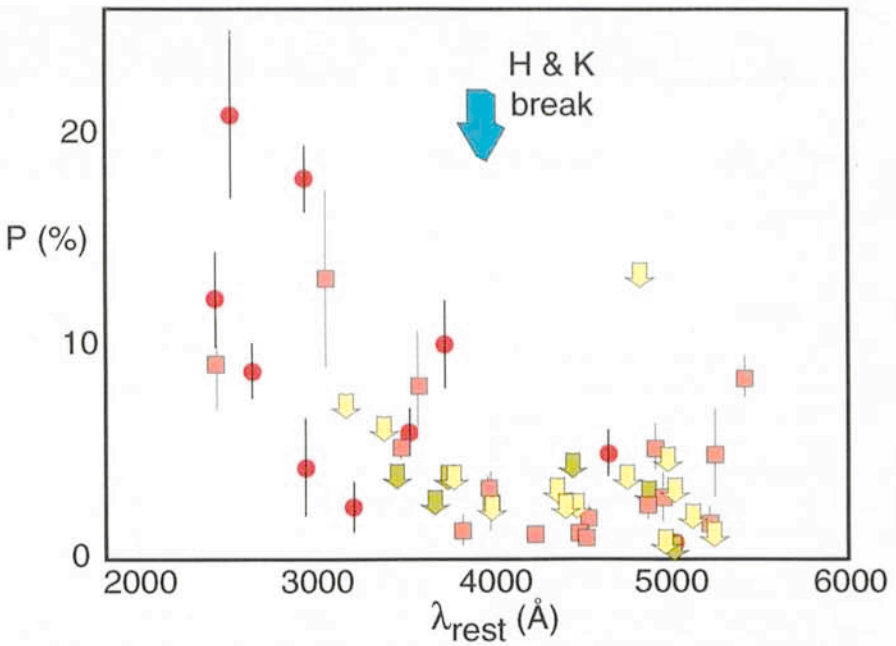

Figure 5: *Linear polarization measurements for radio galaxies with z>0.1 collected by Cimatti et al. (1993a). The arrows represent upper limits and the different symbols are from different observers. The fractional polarization is plotted against the wavelength of the filter passband in the rest-frame of the galaxy. All the detected polarizations to the left of the H&K break have E-vectors perpendicular to the radio axis.*

References

Antonucci, R., 1993. In: IAU Symposium #159. "Active galactic nuclei across the electromagnetic spectrum", Geneva, 1993.

Binette, L., Fosbury, R.A.E. & Parker, D., 1993. *PASP*, **105**, 1150.

Chambers, K.C., Miley, G.K., & van Breugel, W. 1987, *Nature*, **329**, 604.

Cimatti, A., di Serego Alighieri, S., Field, G.M., G.M. & Fosbury, R.A.E., 1993b, *ApJ*, in press.

Cimatti, A., di Serego Alighieri, S., Fosbury, R.A.E., Salvati, M., & Taylor, D. 1993a, *MNRAS*, **264**, 421.

Clarke, D. & Stewart, B.G., 1986. *Vistas in Astron.* **29**, 27.

Clarke, D., Stewart, B.G., Schwarz, H. E. & Brooks, A., 1983. *A&A*, **126**, 260.

De Young, D.S. 1989. *ApJ*, **342**, L59.

di Serego Alighieri, S., Fosbury, R.A.E., Quinn, P.J. & Tadhunter C.N., 1989. *Nature*, **341**, 307.

di Serego Alighieri, S., Cimatti, A., Fosbury, R.A.E., 1993, in *Active Galactic Nuclei across the Electromagnetic Spectrum*, Courvoisier et al. eds., in press.

Dunlop J.S., Peacock J.A., 1993, *MNRAS*, in press.

McCarthy P.J., van Breugel W., Spinrad H. & Djorgowski S., 1987. *Ap J*, **321**, L29.

Rees, M., 1989. *MNRAS*, **239**, 1p.

Rigler, M.A., Lilly, S.J., Stockton, A., Hammer, F. & Le Févre, O., 1992, *Ap J*, **385**, 61.

Scarrott, S.M., Rolph, C.D. & Tadhunter, C.N., 1990. *MNRAS*, **24**, 5p.

Simmons, J.F.L. & Stewart, B.G., 1985, *A&A*, **142**, 100.

Tadhunter, C.N., Fosbury, R.A.E., di Serego Alighieri, S., 1988. In: "BL Lac Objects", Maraschi, L., Maccacaro, T. & Ulrich, M-H., eds. Springer-Verlag, Berlin, p. 79.

Wardle, J.F.C. & Kronberg, P.P., 1974. *Ap J*, **194**, 249.

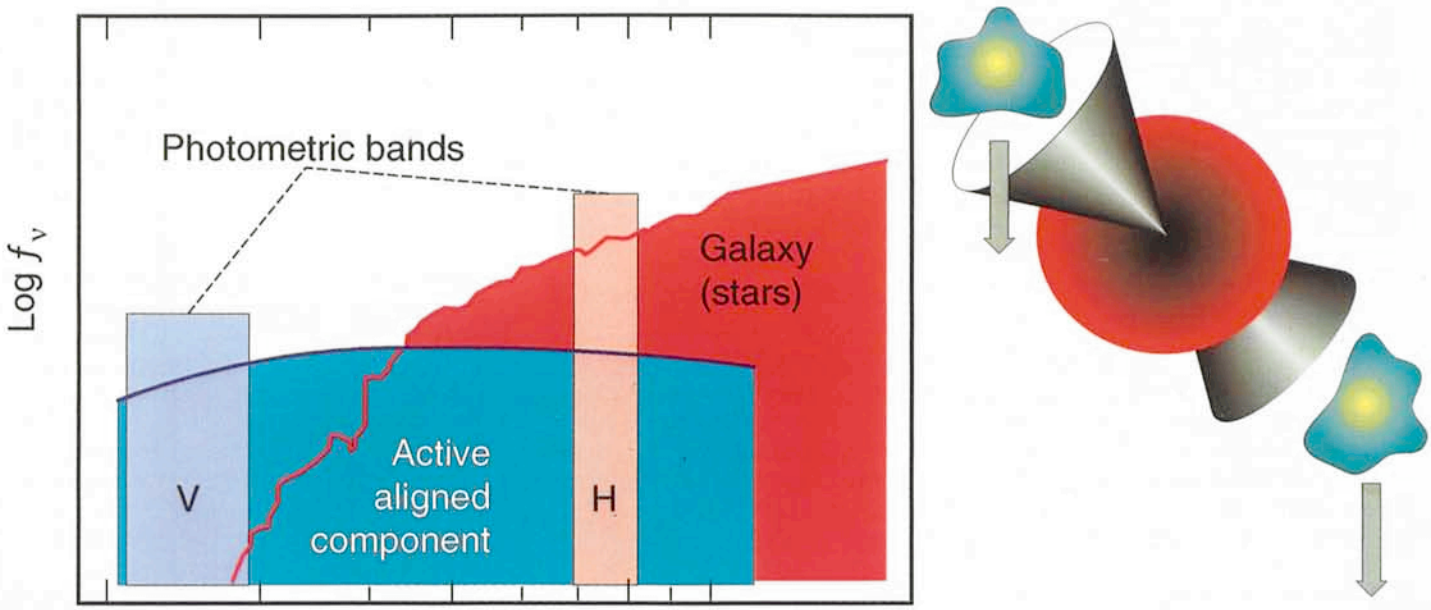

Figure 6: *A cartoon of the spectral energy distribution of a HzRG adapted from Rigler et al. (1992). This shows the two spectral components which will alternatively dominate the measured flux above and below the H&K break in the restframe of the galaxy. We identify the blue component with the alignment effect which results from fluorescence and scattering processes powered by the AGN.*

CCD Astrometry. No, Really – It is Interesting!

C. G. TINNEY, ESO

Introduction

In recent years, the field of astrometry – usually considered a stuffy backwater by most astronomers – has been revitalized by the introduction of CCDs into general astronomical use. Not only have these devices made photographic plates outdated for most astrometric purposes, but they have significantly advanced the precision with which astrometry can be done. In the process they are turning astrometry from a field dominated by large, long-term measurement programmes and endless reductions of celestial co-ordinates, into a vital and fundamental contributor to current research programmes. In this article, I'd like to show what CCDs can (and can't) be used for, why they are so much better than photographic plates, how easy it is to do astrometry with them, and to look at where progress in this field can be expected to go.

What CCD Astrometry Can't Do

Of course, no device is perfect, and there are some astrometric applications for which CCDs have not proved successful. Perhaps the most serious unsolved problem is that of dynamic range. Whereas photographic plates can be successfully used for astrometry when the cores of images are saturated, no technique has yet been devised which allows saturated CCD images to be centroided with the same precision as unsaturated images. This is a major problem for the astrometry of distant and bright objects, like Galactic giants, supergiants and AGB stars – these include, of course, the distance-indicator objects everyone would like to obtain parallaxes for; Cepheids and RR Lyrae stars.

The difficulty is that these stars are intrinsically very bright, and rather rare. So, within a given CCD field-of-view the number density of stars suitable for use as reference objects is very small – to obtain sufficient counts on the intrinsically fainter background stars requires saturating the programme object. Photographic programmes deal with this by the deposition of uniform Nichrome attenuation spots onto filters mounted against the plates, allowing selective dimming of the programme star. However, astrometric results with the precisions attained by CCD programmes have yet to be obtained with any magnitude compensation system and a CCD. This means that while CCD astrometric programmes can obtain parallaxes to more distant stars than photographic programmes, they can only do so for relatively faint ($V \gtrsim 15$) magnitudes.

The second difficulty with CCDs is the limited size in which they are currently available. Photographic plates can be purchased (at least for the immediate future) in sizes up to $\approx$ 400 mm on a side. The largest CCDs currently available are more like 50 mm in size. This means that CCDs cannot be used for applications requiring wide-angle (i.e. $\gtrsim$ 20–30′) astrometry. However, this may not be as serious a problem as it seems. Studies of the astrometric effects of the atmosphere have shown that the residuals produced in astrometric solutions increase with the FOV used and decrease with exposure time (Han 1989, Monet & Monet 1989). This means that for useful exposure times ($\sim$ 1000s), solutions for reference frames in fields of $\approx$ 20′ never get much better than $\approx$ 10 mas[1] – and this uncertainty scales roughly as both the one third power of field size and inversely with the square root of the exposure time. This means that for large fields of view ($\sim$ 1°), the limiting precision is set by the atmosphere, not the detector, and the use of CCDs may produce no gain. It also implies that taking short exposures in order to avoid the saturation problems described above significantly degrades astrometric performance.

What CCD Astrometry Can Do

So, those are the minuses – you can't measure very bright stars, and you can't measure very large angles. However, those are exactly the classes of object for which HIPPARCOS will be producing superior astrometric data in the next few years in any case. It is in measuring faint objects – objects which HIPPARCOS can't reach – that ground-based CCD astrometry really finds its niche.

Perhaps the biggest advantage which CCDs provide for astrometry is that since CCD data are inherently digital, they can be easily evaluated as observations are being carried out. In particular, this means that the observer can examine test images, and place the programme object back in exactly the same location on the telescope's focal plane as the last epoch's observations. The immediate result of this is to allow CCD astrometry to be almost purely differential – except for applications requiring the highest of precision, the telescope's field distortion becomes irrelevant.

Second, CCDs have much higher quantum efficiencies than photographic plates – allowing the observation of objects $\sim$ 3 magnitudes fainter for a given telescope and observing conditions. In particular, they are more sensitive in the red. This latter point is especially important because the astrometric effects of the atmosphere become less severe when observations are made at red wavelengths.

And lastly, because the matrix of pixels in modern CCDs are so regular, and charge-transfer efficiencies are so good, the precision of centroiding becomes almost photon-counting limited – the more photons you collect the better your position comes. This allows images to be centroided to hundredths of an image size. Photographic plates, on the other hand, have an irregular matrix of grains, and they also must be digitized with a measuring machine, with all the mechanical uncertainties that those machines introduce. It should be noted, though, that centroiding to this precision requires that all the objects have the same point-spread-function, that is they must be unresolved. (This has important implications for the astrometry of the very distant objects. If extragalactic reference objects are required, they must be QSOs – galaxies will not do.)

Taken together, these advantages allow astronomers to acquire astrometry at the several mas-level in a very straightforward manner, using the common-user CCD instruments now available at most telescopes. Moreover, they allow more dedicated astrometric programmes to push precisions below the mas-level. The pioneers in this field have

[1] "mas" is used as an abbreviation for milliarcsecond throughout.

been the US Naval Observatory's Flagstaff station, which has been carrying out a CCD parallax programme since 1983 (see Monet et al. 1992). This programme has been so phenomenally successful, that it has led to the termination of the observatory's long-running photographic programme. Its success has also led to the initiation of smaller astrometric programmes at other observatories – most notably, Mt. Stromlo (Ianna 1992), Cerro Tololo (Ruiz et al. 1991) and Palomar (Tinney 1993a).

These programmes, however, have been significantly different from most previous astrometric programmes. To some extent, astrometric programmes have traditionally been carried out on dedicated, small aperture telescopes and have targetted large numbers of stars. They have tended to be run as a "service" to the astronomical community, rather than with a specific and immediate scientific goal in mind. The ease of doing astrometry with CCDs, however, has changed that. The smaller programmes listed above have all been scientifically motivated, and targeted at particular classes of objects of interest to the astronomers concerned. In short, they are no different from any other type of astronomical project.

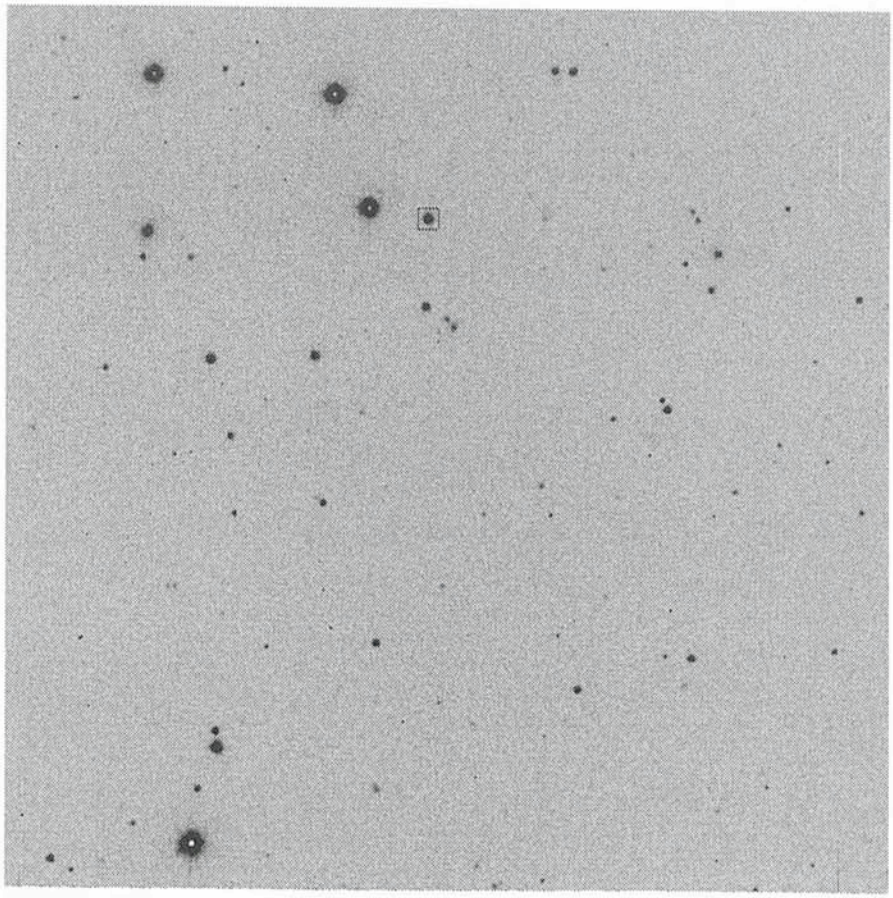

Figure 1: *A typical CCD frame of the recently discovered VLM star TVLM513-46546 (north is up, west to the left. The object is marked with a box).*

"Do-It-Yourself" Parallaxes

The Palomar Parallax programme was motivated by the need for more parallaxes for the very faintest of main sequence stars. A photometric survey for these stars (Tinney 1993b, Tinney, Reid & Mould 1993), had indicated a need for more Very Low Mass (VLM, $M \lesssim 0.2M_{\odot}$) stars with measured distances, in order to define the colour-magnitude relations essential for photometric selection of these stars. The USNO's results encouraged us to try and obtain these parallaxes for ourselves, rather than rely on their heavily overburdened programme.

Observations were carried out at five epochs per year (roughly evenly spaced throughout the year so as to provide good sampling of our VLM survey fields), with the Palomar 60″ (1.5-m) telescope. The CCD used was a Tektronix 1024×1024 thick, front-side illuminated device. When mounted at the Cassegrain focus of the 60″ the CCD's 24μm pixels gave a scale of 0.372″/pix. The field-of-view then was ≈ 6′ – this was found to be sufficiently large to provide a good background reference frame of stars for our programme objects, which were situated at b ~ 40° – 60°. All observations were carried out through a Gunn i filter ($\lambda_{eff} \approx 790$nm, $\Delta\lambda \approx 100$nm). The choice of this filter was motivated by several factors; first, the target stars were all extremely red, making observations at as long a wavelength as possible desirable; second, the effects of atmospheric differential colour refraction are minimized by observing in the red; and third, as the CCD used was frontside illuminated, observing at a red wavelength reduces the sub-pixel effects of observing through the CCDs frontside gate structure.

Multiple images (3–4) of each programme object were obtained at high parallax factors several times a year. Some effort was made to place objects at roughly the same location on the CCD at each epoch. All the data were flattened with dome flats. The stellar images were centroided using DAOPHOT – we found that each observation could be centroided to about 1/200th of an image size. That is, for a star of I = 16.5, a single 300s exposure in 1.″0 seeing gives a position good to ≈ 5 mas. (Observations were not carried out in seeing worse than 2.″5 – it was found to be not worth the time spent reducing the data). All our observations were mapped onto a common coordinate system using a reference frame of background stars – since our programme objects are intrinsically very faint, an average background star of similar magnitude is more than 100 times further away, making corrections from relative to absolute parallax very small. A sample CCD frame for one of our programme objects (TVLM513-46546) is shown in Figure 1. Figure 2 shows its preliminary astrometric solution as derived in Tinney (1993a). Over the 2 years for which data have been reduced to date we typically obtain parallaxes with 2–3 mas uncertainties. Over the total 3 years which our programme will run (observations will terminate in November 1993) we expect to obtain parallaxes with uncertainties of 1–2 mas. For the one object we have measured in common with the USNO (VB10), agreement was found within our estimated 1-σ uncertainties (Monet et al. 1992).

The greatest problem to surmount in carrying out a parallax programme for these stars, is dealing with the effects of differential colour refraction (DCR) – put simply, the reference stars have a shorter effective wavelength through the Gunn i filter than the much redder programme stars. This results in the programme stars suffering less atmospheric refraction than the reference stars. However, so long as observations are made reasonably close to the meridian, this effect can be substantially corrected. We do this by observing each object as it rises and sets on a single night. The motion introduced by DCR can then be measured and calibrated out on subsequent nights. We found

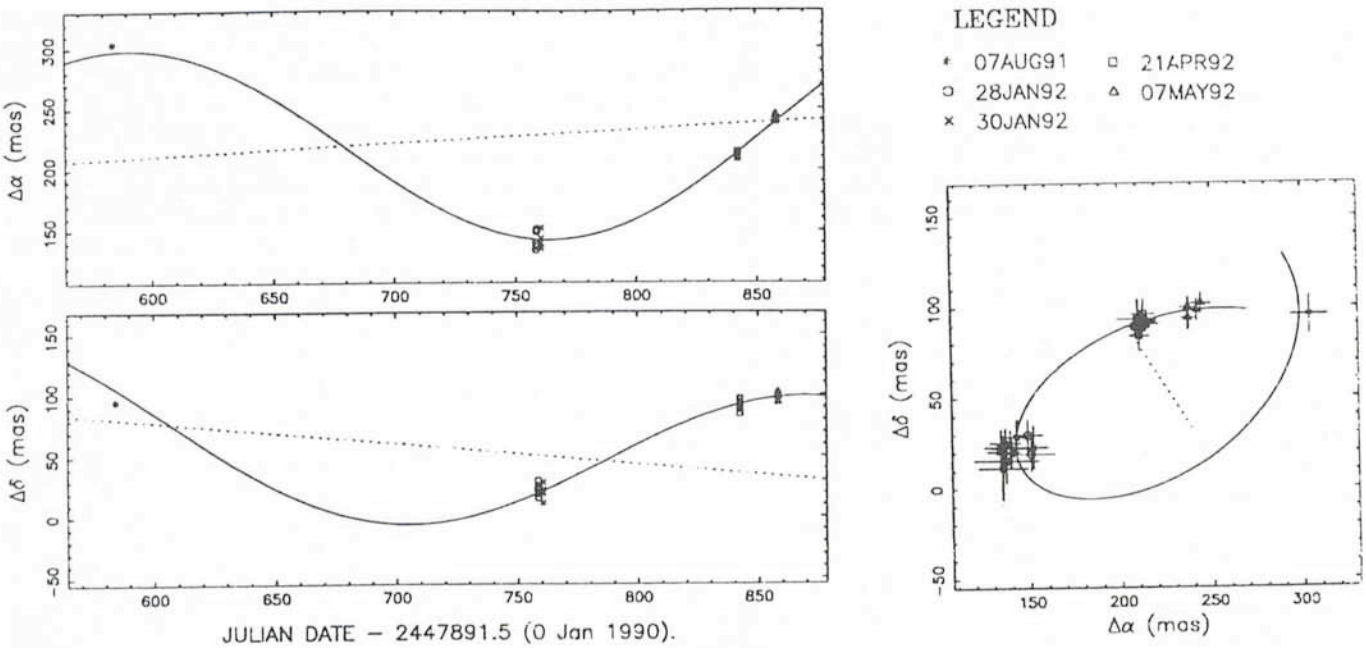

Figure 2: *The preliminary astrometric solution for this object (Tinney 1993a).*

that our use of a Gunn i filter gave us a significant reduction (a factor of about 4) in the amount of DCR observed, compared with that seen at the USNO, where a much wider filter ($\lambda_{eff} \approx 690$ nm, $\Delta\lambda \approx 300$ nm) is in use. This means that while we need to take longer exposures, we have considerably more flexibility in scheduling, since we can observe ≈ 4 times further from the meridian for a given DCR effect. For a non-dedicated facility this flexibility is important. In any case, longer exposures allow differential seeing effects over the field of view to be averaged out and therefore increases astrometric precision.

Figure 3 shows how this small programme has been able to make a significant contribution to the specific problem it was designed to address. The first panel shows the colour-magnitude diagram as it existed when our VLM survey was begun, the second shows it as of earlier this year. Almost half of the VLM stars ($M_{Bol} > 13$) which now have parallaxes come from the Palomar programme. It is also worth noting that by carrying out our own parallax observations, this improvement could be obtained quite quickly – the total time between the identification of TVLM513-46546 as a VLM candidate and the measurement of its absolute magnitude (it is the second faintest VLM star known) was only 18 months.

Pushing Back the Envelope

If "common-user" astrometric programmes can obtain results at the several mas level over only a few years, what are the prospects for specialized programmes to achieve higher precisions? Currently, the barrier preventing sub-mas astrometry is the atmosphere – both due to differential colour refraction, and due to differential seeing effects. The obvious solution is to carry out astrometry from space with a CCD camera, something the corrected HST may be able to do. But in the nearer term, what can be done from the ground? It turns out that there are a number of regions in the "observing phase space" which have yet to be fully explored, and which may produce some exciting new results.

Higher precisions can be achieved by observing reference frames over smaller fields of view, so long as a rich enough field of unresolved objects is available to transfer all the data onto a common coordinate system. Narrow-band filters, longer integration times and larger telescopes should be used to minimize the atmosphere's effects whenever possible. Sites with superior seeing should obviously also be preferred. By taking advantage of all these, it should be possible to push the astrometry of faint objects below the 1-mas barrier.

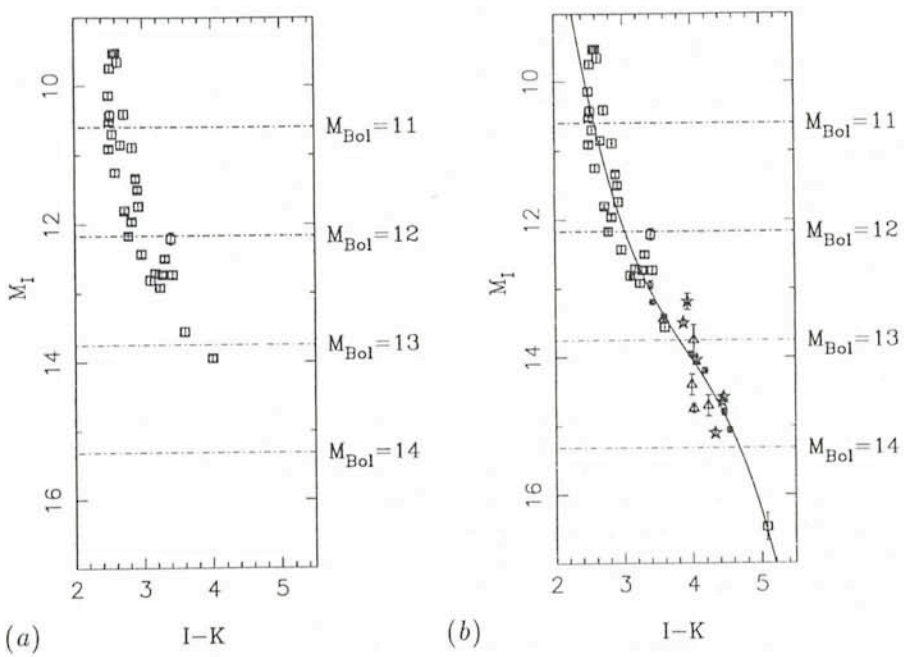

Figure 3: *(a) The M_I/I-K diagram as known circa 1985. (b) The current M_I/I-K diagram, including parallaxes from the Palomar (stars, Tinney 1993a), USNO (squares and circles, Monet et al. 1992) and Mt. Stromlo (triangles, Ianna 1992) programmes.*

Figure 1: *ESO 50-cm telescope with the TV guiding system of FLASH. The total weight of the guiding system is only about 35 kg. It contains the fiber-fed interface, comparison lamps and a conventional SIT low-light-level camera.*

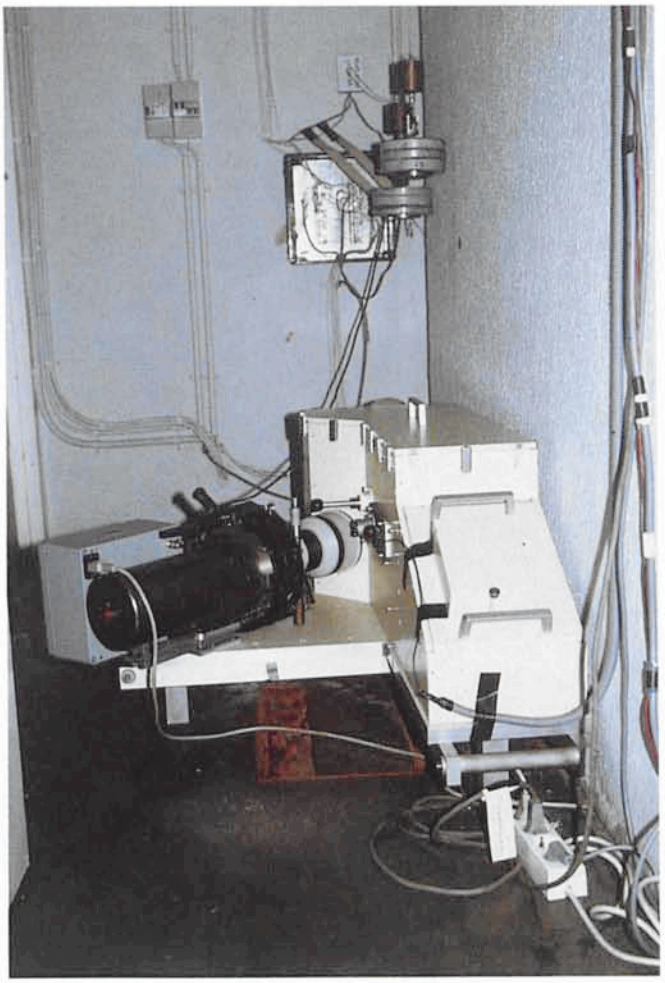

Figure 2: *Our spectrograph with CCD and CCD electronics, in the small cabin at the concrete base of the telescope, the smallest coudé room in the world. In the background some counterweights of the telescope balancing system can be seen.*

plifies the merging of the reduced different echelle orders. One also eliminates flexure problems while housing the instrument in a temperature and humidity controlled room. During observing at the ESO 50-cm telescope the spectrograph was placed in the small cabin at the concrete base of the telescope behind the astronomers office with only two connections to the outside world, one incoming fiber and one outgoing coaxial cable.

With an efficient detector, stars down to a magnitude of 7 are in the reach of the ESO 50-cm telescope. Using an EEV CCD with 1252×770 pixel of 22 μ, we get 2700 Å in one exposure. At standard setup we selected the wavelength range from 4050 to 6780 Å. This setting allows observations of 57 echelle orders simultaneously, with a generous overlap between the orders. With a 100 μ fiber, which corresponds to 2".75 at the ESO 50-cm telescope, the spectral resolution is about 20,000. During observation, up to 100 CCD frames (including ThAr- and flatfield-spectra) can be stored on the hard disk of the CCD control computer. These frames are transferred to magnetic tapes each morning and later copied to DAT-tapes by ESO.

Luminous Blue Variables

Apart from supernovae at outburst LBVs are the most luminous stars in the Universe ($M \approx -9$ to -11). For more recent reviews see Wolf (1992) and Stahl (1993). The LBVs have recently been recognized as keys in connection with the evolution of massive stars. At quiescence they define an inclined instability strip of OB supergiants (Wolf, 1989) close to the Eddington limit. They are characterized by photometric variations of 1 to 2.5 mag in timescales of years and longer. At maximum brightness they are surrounded by cool ($\approx$ 8000 K), dense ($N \approx 10^{11}$ cm^{-3}) slowly expanding ($v \approx 100$ km s^{-1}) envelopes of typically equivalent spectral type A. In addition to the large outbursts, photometric microvariations of 0.1 to 0.2 mag on timescales of 1 to 2 months or more have been found in all those cases observed in more detail (van Genderen, 1989).

During the past decade our group has observed spectra of the established and newly discovered LBVs of the Galaxy and of the Magellanic Clouds more or less regularly each year at La Silla with CASPEC. The exhibited long-term spectral variations shown by the LBVs have been of vital importance for a better understanding of the outburst phenomenon. They have contributed quite considerably to derive the general picture sketched above. On the other hand, with snap shot observations, typically separated by one year, the detailed hydrodynamic processes cannot be studied.

The Campaign

For a better understanding of the atmospheric motions, systematic spectroscopic monitoring over a time span of months with good resolution in wavelength and time is badly needed. We therefore applied for two contiguous observing runs of two months each at

But what can you do with that sort of astrometry? The prospects are enormous – to name just a few: parallaxes of more distant and/or fainter classes of objects like very low-mass white dwarfs, optical counterparts of neutron stars, and brown dwarf candidates; orbits for close (2–10″) binaries; proper motions of globular clusters, and proper motions within globular clusters; and proper motions for the Galaxy's satellite galaxies.

There are also prospects for CCDs to be extended towards the observation of bright stars – those objects too faint for HIPPARCOS and too bright for current CCD techniques, or those objects too distant for HIPPARCOS. The use of anti-blooming techniques, and the development of CCDs with larger full-well capacities, may allow precise astrometry to be done with the brightest stars. An alternative technique, being explored at the USNO, is to carry out observations with a CCD mosaic, bonded onto a single silicon substrate, in which one of the CCDs is configured as a frame transfer CCD, allowing very short (and unsaturated) exposures of a target star, while the surrounding CCDs acquire deep images of the surrounding stars for use as reference objects.

Conclusion

I've tried to show, in the sections above, some of the interesting results currently being obtained with CCD astrometry, some of the exciting prospects for its future, and how straightforward it is to actually do it. Several programmes at La Silla currently use CCDs for astrometric purposes, both for studies of the solar system and nearby stars, and future programmes are planned to expand on their use for these local studies. Within the next year, I hope to carry out test observations with the NTT, to explore its use for high precision astrometry below the 1-mas barrier in studies of the Galaxy's satellites. It is my hope that the activity in this field will encourage more members of the general community to investigate this "rediscovered" astronomical technique – one which shows such astounding promise for the future.

References

Han, I., 1989, *AJ*, **97**, 607.

Ianna, P., 1992, IAU Symposium 156, ed: Mueller.

Monet, D.G., et al. 1992, *AJ*, **103**, 638 (M92).

Monet, D.G., & Monet, A.K.B., 1992, *BAAS*, **24**, 1238.

Ruiz, M.T., et al., 1991, *ApJ*, **367**, L59.

Tinney, C.G., 1993a, *AJ*, **105**, 1169 (T93).

Tinney, C.G., 1993b, *ApJ*, **414**, 279.

Tinney, C.G., Reid, I.N., Mould, J.R., 1993b, *ApJ*, **414**, 254.

High-Resolution Spectroscopy at the ESO 50-cm Telescope: Spectroscopic Monitoring of Galactic Luminous Blue Variables

B. WOLF[1], H. MANDEL[1], O. STAHL[1], A. KAUFER[1], TH. SZEIFERT[1], TH. GÄNG[1], C.A. GUMMERSBACH[1], J. KOVACS[2]

[1]Landessternwarte Heidelberg-Königstuhl, Heidelberg, Germany;
[2]Gothard Astrophysical Observatory, Szombathely, Hungary

Introduction

High-dispersion spectroscopy used to be the domain of big coudé spectrographs attached to large telescopes. At least since the launch of IUE it has become quite obvious that high-resolution spectroscopy can be done with a telescope as small as 45 cm if equipped with an echelle spectrograph. With IUE even extragalactic objects are being investigated. All known Luminous Blue Variables (LBVs) of the Magellanic Clouds, for example, have been repeatedly observed by our group in the high-resolution echelle mode.

For obvious reasons it is also very desirable to use echelle spectrographs connected to small telescopes for ground-based observations. The pressure for observing time is much smaller than for large telescopes and hence long-term programmes have a better chance of being realized if achievable with a small telescope.

Echelle spectrographs, however, are well known to be very sensitive to bending effects. If directly attached to the telescope, e.g. at the Cassegrain focus, the necessary mechanical stability can be reached only at the expense of great weight (e.g. CASPEC of the ESO 3.6-m telescope weighs more than 500 kg). The use of echelle spectrographs for ground-based observations at small telescopes, therefore, used to be very limited. The possibilities for doing this, however, have improved dramatically since the advent of optical fibers for astronomical observations.

With our fiber-linked echelle spectrograph attached to the ESO 50-cm telescope we obtained unprecedented time series of highly resolved spectra of a few galactic LBVs and, as a by-product, of two other hot stars. A short description of the instrumentation and of the campaign and observational results are presented in this report.

Instrumentation

The idea of building a compact, fiber-linked, portable high-resolution echelle spectrograph was conceived in 1984 and looked very promising in filling an instrumentation gap of nearly all smaller telescopes. The spectrograph named FLASH (fiber-linked astronomical spectrograph of Heidelberg) has been designed and constructed at the Landessternwarte Heidelberg (Mandel, 1988) and has subsequently been successfully used for spectroscopic monitoring campaigns at different sites and telescopes.

Our equipment, comprising the spectrograph, a TV guiding system, mechanical interfaces, a computer system with a magnetic tape, monitors and power supplies with a total weight of about 600 kg fits into eight medium-size containers. Two well-trained people are able to install and adjust the system in less than half a day.

In practice, our spectrograph works much like CASPEC with only two significant differences; the rectangular spectrograph slit is replaced by a round fiber with 100 μ core diameter and the spectrograph is not mechanically connected with the telescope. The light scrambling property of the fiber results in a homogeneous illumination of the echelle grating independent of guiding errors and seeing variations which also sim-

the ESO 50-cm telescope in periods 50 and 51 to observe the established galactic LBVs η Car, AG Car and HD 160529 with FLASH. The length of the period was motivated by the timescales mentioned above for photometric microvariations for which in the case of HD 160529 semi-periods of 57 and 101 days have been quoted in the literature (Sterken, 1977 and Sterken et al., 1991). Note that the typically expected dynamical timescales of the extended atmospheres of LBVs of a few hundred solar radii during outburst are also of this order. ESO generously allocated the requested observing time from February through May 1993. Only 15 nights could not be used due to bad weather. The campaign has thus certainly contributed to improved statistics of useful nights in 1993 at this telescope, which is normally used for photometry only.

Fortunately, ESO has provided travel expenses for six observers so that the heavy burden of securing more than one thousand scientific frames could be distributed upon the shoulders of several members of the Wolf pack. At the end of his run of typically three weeks duration, each observer sent the DAT tapes to the Landessternwarte Heidelberg-Königstuhl, where the gathered data were feverishly reduced. It should be noted that the efficient handling of the huge amount of spectroscopic data was only possible due to the already existing far-reaching automatization of the reduction procedure which is a modified version of the ESO-MIDAS echelle reduction package running at the UNIX workstations of the Landessternwarte (cf. Stahl et al., 1993a).

Figure 3: *Control room at astronomers office with CCD-, computer- and TV-guiding-monitor, personal computer, and magnetic tape. With this equipment we are completely independent, using only the naked telescope at each observation site.*

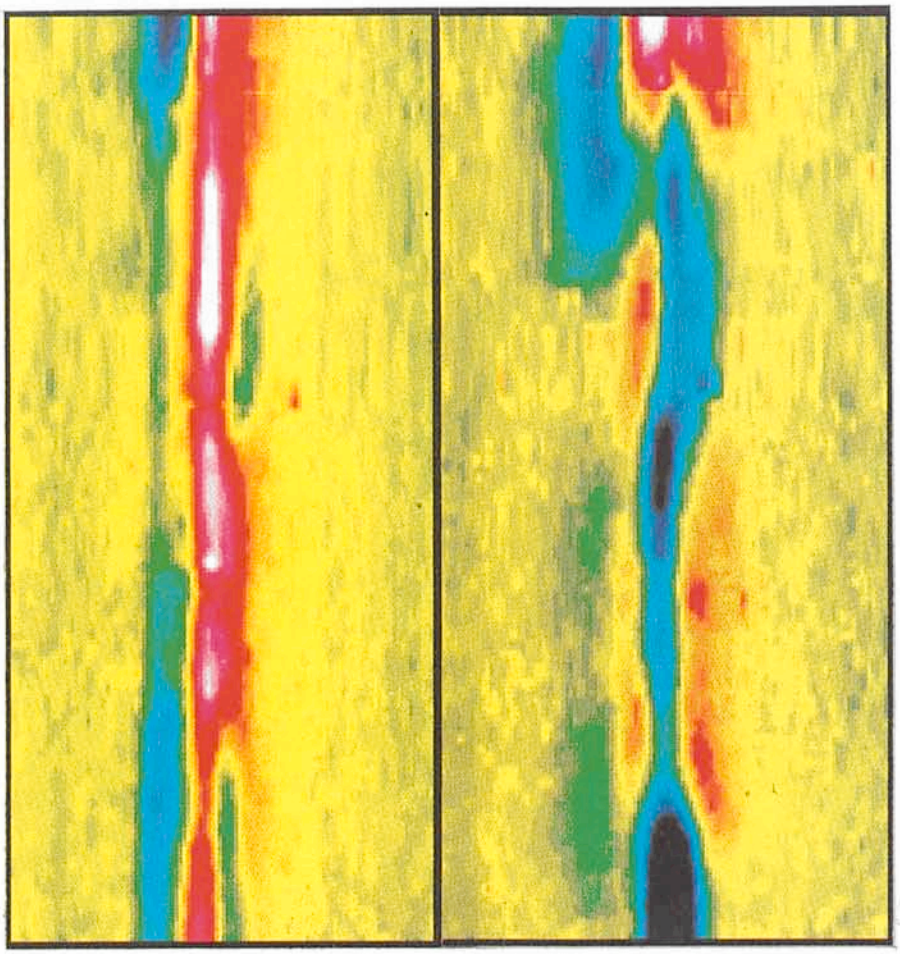

Figure 4: *Line profiles and profile variations of SiII 6347 (left) and HeI 6678 (right) of AG Car. Look up table: black, blue (absorption) – green, yellow (continuum) – red, white (emission). The lines are centred to the systemic velocity (+ 20 km s^{-1}) of AG Car. The complete width of the abscissa is from –300 to +300 km s^{-1} for both lines. The ordinate gives the time from JD2449023 (bottom) to JD2449139 (top).*

Results

A quick inspection of the incoming data has readily shown the considerable line profile variations of the target stars. This is demonstrated in Figure 4 by HeI 6678 (right) and SiII 6347 (left) of AG Car which had a visual magnitude of about 7 during the campaign. A spectrum with a S/N ratio of about 100 in the red spectral range was obtained in about two hours exposure time. In the time span JD2449023 to JD2449139 we could observe AG Car in 91 nights. Figure 4 exhibits the variations of the colour coded intensity distributions of the lines. The lines are centred at the system velocity (+20 km s^{-1}) of AG Car. The total width of the abscissa is 600 km s^{-1} for both lines. The ordinate gives the time interval increasing from bottom to top. The increasing intensity is coded from black, blue (absorption) to green, yellow (continuum), and to red, white (emission). Spline fits through the intensity at each wavelength and resampling in equidistant time steps were used to interpolate for those few nights of not spectroscopic quality and to account for not completely equal time intervals from night to night.

As shown by the Figure, in the beginning HeI 6678 showed a strong absorption line at virtually systemic veloci-

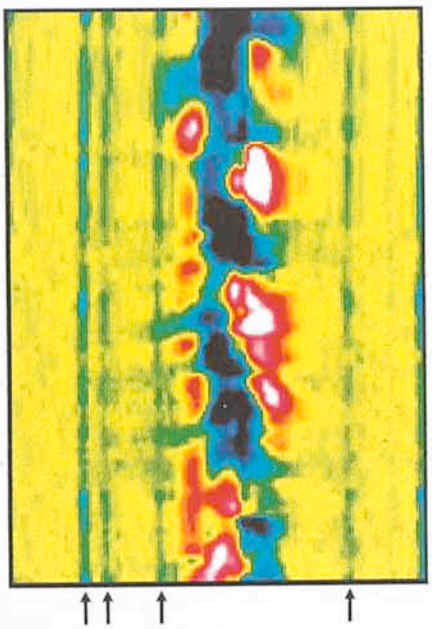

Figure 5: *The dramatic Hα-profile variations of β Ori. Centre of the abscissa is the laboratory wavelength of Hα; the complete width is from –410 to +410 km s^{-1}. Look up table as for Figure 4. The ordinate extends from JD2449023 to JD2449128 (bottom to top). Note the smooth curvature of the terrestric lines (indicated by arrows) due to the reduction of the spectra to heliocentric velocities, which also demonstrates the accuracy of the radial-velocity measurements.*

ty. A few days later an additional faint absorption at a velocity of about 120 km s^{-1} and slightly later a redshifted emission became discernible. This type of profile was followed by an inverse P Cygni-type profile after the third month of our campaign. Finally, during the last month, quite drastic changes occurred from an inverse P Cygni-type profile via a double absorption to a pronounced P Cygni-type profile.

The corresponding profile variations of SiII 6347 are less pronounced. A P Cygni-type profile is prevailing with an expansion velocity of about 100 km s^{-1} which agrees with the wind velocity previously derived for AG Car by Wolf and Stahl (1982). But the intensities both of the emission and absorption components vary quite considerably. Occasional substructures in the emission component are also discernible.

Since our spectrograms cover a large wavelength range, a number of strategic lines formed in different layers can be scrutinized and can be used to probe the time- and depth-dependent velocity fields in the atmospheres of LBVs. The results clearly demonstrate that the campaign has provided a wealth of information, a very good basis for a deeper understanding of the physics of the winds of LBVs and for modelling the hydrodynamic processes connected with the LBV phenomenon.

In addition to the galactic LBVs, we observed the B9Ia supergiant β Ori and the O7V star Θ^1 Ori C. β Ori was always exposed for five minutes at the beginning of each night to check the setup of the equipment and to control the focus of the telescope. In 86 nights (JD2449023-JD2449127) spectra were secured. Quite interestingly, dramatic Hα-profile variations ranging from inverse to normal P Cygni-type profiles via double emission to pure absorption were observed (see Figure 5; look up table like for AG Car). The change from normal to inverse P Cygni-type profiles and vice versa sometimes occurs within a few nights.

Hα emission in B supergiants is often interpreted in terms of steady-state mass loss. The rapid variability of the surface phenomena concluded from the Hα variations of β Ori, however, indicates that a steady-state approach to describe these extended atmospheres and their winds is at least not a complete one. Allowance has to be made for time-dependent hydrodynamic processes.

In addition, it is well known that fiber-fed spectrographs with their light scrambling properties allow for particularly precise radial-velocity measurements. Therefore, the set of data of β Ori represents an invaluable treasure for oscillation analyses and theoretical investigations of pulsational motions. Such a homogeneous set of data over such a long time period and broad spectral range has never been obtained before with modern detectors for any of the hot supergiants.

Again it is evident that for realistic wind models of even "normal" supergiants the impact of long-term spectroscopic monitoring programmes is quite essential.

Our attention has been drawn to Θ^1 Ori C by Manfred Pakull. This famous O7V star of the Trapezium of the Orion nebula is known to be spectroscopically peculiar and variable. Occasional inverse P Cygni-type profiles of the HeII 4686 line had been observed and reported in the literature (Conti, 1972). Therefore, we put this star into the list of our targets. In the period JD2449023 to

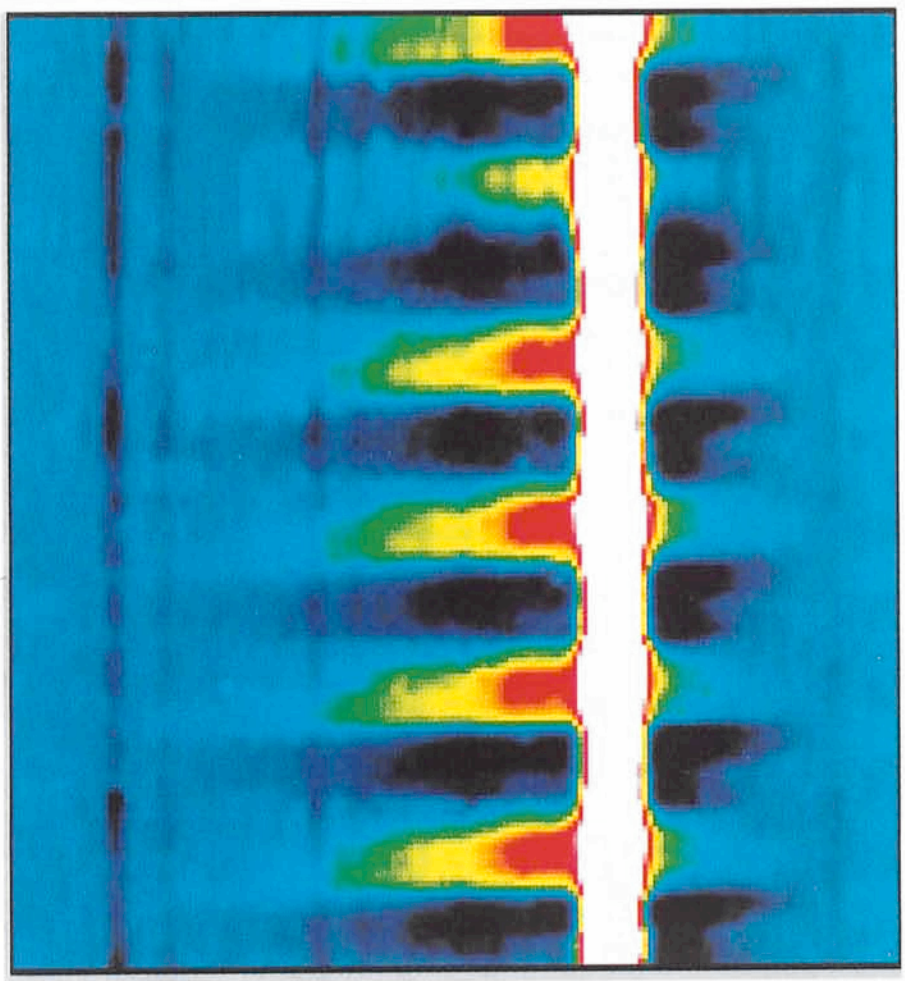

Figure 6: *The spectacularly regular Hα-profile variations with a period of 15.43 ± 0.03 days of Θ^1 Ori C. Look up table: black (absorption – blue (continuum) – green, yellow, red, white (emission). The spectrum extends from the nebular emission (white), to –600 km s^{-1} to the left and to +300 km s^{-1} to the right. The time span on the ordinate is JD2449023 to JD2449112. The curvature of the terrestric lines is again evident.*

JD2449112 we exposed Θ^1 Ori C in 89 nights. The typical exposure time was one hour. As evidenced by Figure 6, the spectrum of Θ^1 Ori C is distinguished by extremely regular variations of Hα, the period being 15.43 ± 0.03 days (see Stahl et al. 1993b). In the Figure, the nebular emission (white) is shifted so that a range of –600 to +300 km s^{-1} around Hα is displayed. Continuum is blue. Blue-shifted stellar emission and absorption alternate very regularly with virtually no difference from cycle to cycle. The apparent deviation during the fifth period is caused by worse sampling due to bad weather. Note that the discernible substructure in the black stripes is due to a second maximum of (redshifted) emission. This same strict periodicity was also found for He II 4686 and other different lines. Θ^1 Ori C is a good example to show the importance of having long time series with regular sampling and good resolution in time. Based on previous snap shot observations, the inverse P Cygni-type emission of He II 4686 "occurred on an irregular fashion" and was therefore ascribed to accretion rather than to something strictly connected to the rotation of Θ^1 Ori C. The strict periodicity now established does, however, favour such a connection and makes Θ^1 Ori C the first convincing candidate of an O star oblique rotator.

Conclusion

The results presented demonstrate the considerable impact of long-term high-resolution spectroscopic monitoring programmes at small telescopes on variable star research.

The ESO 50-cm telescope, our fiber-linked echelle spectrograph and the excellent meteorological conditions of the Atacama desert – a perfect match for investigating the long-term spectroscopic behaviour of bright stars.

References

Conti, P.: 1972, *ApJ*, **170**, 325.

Mandel, H.: 1988, in IAU Symp. 132, eds. G. Cayrel de Strobel and M. Spite, p. 9–13, Kluwer.

Stahl, O., Mandel, H., Wolf, B., Gäng, Th., Kaufer, A., Kneer, R., Szeifert, Th. Zhao, F.: 1993a, *A&AS*, **99**, p. 167–177.

Stahl, O.: 1993, in New Aspects of Magellanic Cloud Research, eds. B. Baschek, G. Klare, J. Lequeux (Proc. Sec. European Meeting on the Magellanic Clouds, SFB 328), p. 263.

Stahl, O., Wolf, B., Gäng, Th., Gummersbach, C.A., Kaufer, A., Kovacs, J., Mandel, H., Szeifert, Th.: 1993b, *A&A*, **274**, L29–L32.

Sterken, C.: 1977, *A&A*, **57**, 361.

Sterken, C., Gosset, E., Jüttner, A., Stahl, O., Wolf, B., Axer, M.: 1991, *A&A*, **247**, 383.

van Genderen, A.M.: *A&A*, **208**, 135.

Wolf, B.: 1989, *A&A*, **217**, 87.

Wolf, B.: 1992, in Nonisotropic and Variable Outflows from Stars, eds. L. Drissen, C. Leitherer, A. Nota, (A.S.P. Conf. series Vol. 22), p. 327.

Probing the Kinematics in the Core of the Globular Cluster M15 with EMMI at the NTT

P. DUBATH and G. MEYLAN, ESO

D. QUELOZ and M. MAYOR, Geneva Observatory, Switzerland

1. M15: a Prototype Collapsed-Core Cluster?

There is now a global theoretical understanding of the long-term dynamical evolution of globular clusters. Different kinds of theoretical approaches predict the collapse of the cluster core, which can then be halted or even reversed by a core heating due to stellar encounters involving binary stars. A cluster could suffer a succession of collapsing and expanding phases: the so-called gravothermal oscillations (for recent reviews see the proceedings of the workshop *Structure and dynamics of globular clusters*, Djorgovski and Meylan eds. 1993).

From an observational point of view, however, the situation is much less clear (see e.g. Meylan 1993). A major difficulty in finding a signature of core collapse in a globular cluster is that the observable structural changes may occur only in a very small central area, where accurate measurements of surface brightnesses and velocity dispersions are greatly complicated by the small number of bright stars dominating the integrated light. In the case of the high-concentration globular cluster M15, considered for a long time as a prototype of the collapsed-core star clusters, the observational difficulties are particularly important.

The current determinations of the surface-brightness profile of M15 do not allow us to discriminate between pre- and post-core collapse models, nor to exclude the presence of a central massive black hole. Although the central luminosity cusp in M15 has now been clearly resolved into several bright stars (see Figures 1 and 2), even the most recent studies from HST data cannot unambiguously determine whether the surface-brightness radial profile flattens off interior to a radius of about 2″ or continues to rise at subarcsecond radii (see Lauer et al. 1991 and Yanny et al. 1993). The central velocity dispersion profile in M15 is also poorly known. Accurate central velocity dispersions are difficult to obtain from radial velocities of individual stars because of crowding and the small number of bright stars. An alternative is to use integrated-light spectra to derive velocity dispersions by measuring the line broadening that arises from the random motions of the stars. In this way, Peterson et al. (1989) obtained velocity dispersion values $8.4 \leq \sigma_p \leq 30.0$ km s^{-1} over different small ($\sim$ 1″) areas of integration in the central few arcseconds of M15. They retain as their best estimate a central velocity dispersion of 25 km s^{-1}, a value difficult to reconcile with any existing model, and possibly indicative of the presence of a central black hole. More recently, we derived a velocity dispersion of 14 km s^{-1} from an integrated light spectrum obtained over a central area of integration of 6″×6″ (Meylan et al. 1991, Dubath et al. 1993, 1994). Because of our larger sampling area, we probably would have missed any central velocity dispersion cusp over an area of $\sim$1″. However, recent numerical simulations (Zaggia et al. 1992a, b, and Dubath et al. 1993, 1994) pointed out that the velocity dispersions derived over such small central areas in M15 are affected by large statistical errors because of the dominance of too small a number of bright stars. These errors can explain the large variation of velocity-dispersion estimates obtained at different locations in the core of M15.

In order to test the existence of a central velocity dispersion cusp in the

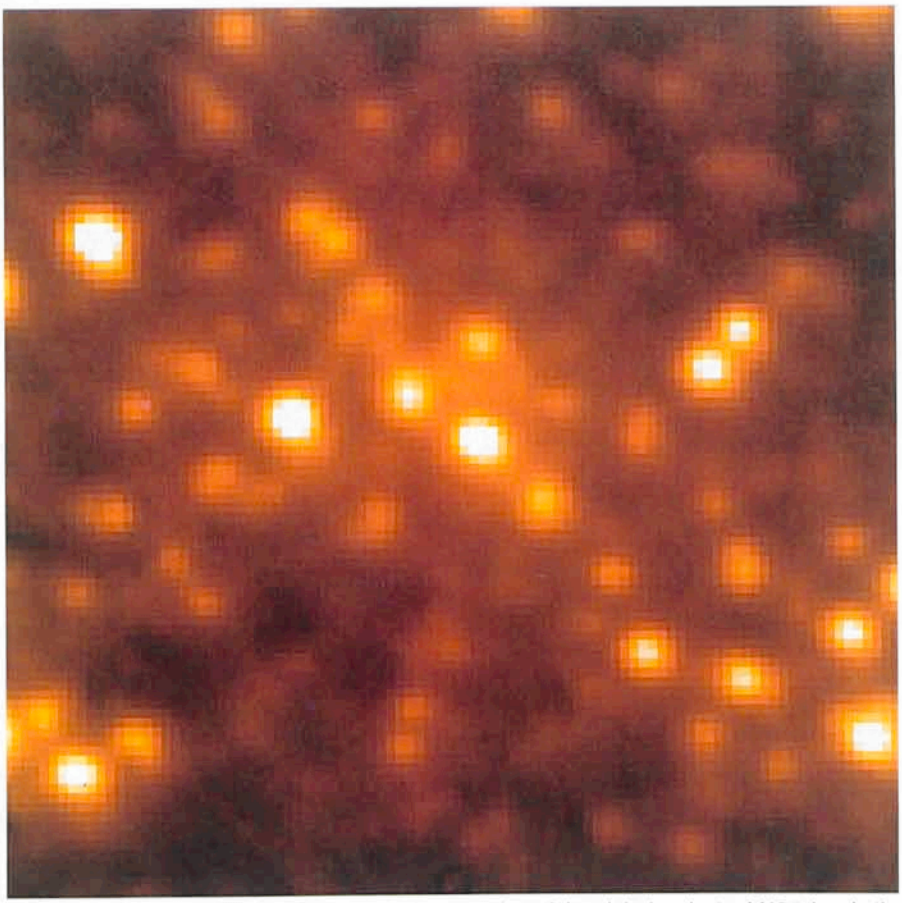

Figure 1: *CCD image of the central 10.5″ square region of the globular cluster M15 taken in the V-band with HRCam at the CFHT (from Racine & McClure 1989). The angular resolution on this image is 0.35″ FWHM. The three stars, forming an equilateral triangle at the centre of the figure, are the main contributors to the former unresolved luminosity cusp.*

2. Mapping the Core of M15 with EMMI Observations

In July 1993, we obtained five high-resolution integrated-light echelle spectra in the core of M15. We used a 1″×8″ slit, with exposures offset in 1″ steps in order to cover a total central area of 5″×8″ (see Figure 3). The exposure times were ~30 minutes for each exposure. During these observations, the seeing values (determined from EMMI CCD images) were about 0.9″. EMMI was used in echelle mode with the echelle grating #10 and the cross-dispersing grism #5 (see the EMMI operating manual). The CCD used is the ESO CCD #34. It is a LORAL CCD with 2048×2048 pixels of a size of 15 μm which correspond to 0.35″ on the sky. For our instrument setup and slit width, the typical full-width at half-maximum (FWHM) of the emission lines of the thorium-argon comparison spectra, i.e., our typical spectral resolution, is 9–10 km s^{-1}.

Before each exposure on the cluster core, we also obtained (1) an echelle spectrum of an isolated red giant member of M15, and (2) CCD images of the core of M15 in the V-band. The observations of red giant stars show that the width of stellar cross-correlation functions is perfectly constant during all the observations and small (6.5 km s^{-1})

core of M15, we carried out new high-resolution observations with the ESO Multi-Mode Instrument (EMMI) on the NTT. The best way to minimize the statistical error due to a small stellar sample is to obtain a full 2-D kinematical map of the cluster core, i.e., to derive radial velocities and velocity dispersions at many different locations. The unique imaging/spectroscopic capabilities of EMMI are very useful to carry out such observations. CCD images taken just before an echelle spectrum allow very precise *a priori/posteriori* positioning of the slit within the crowded core of M15.

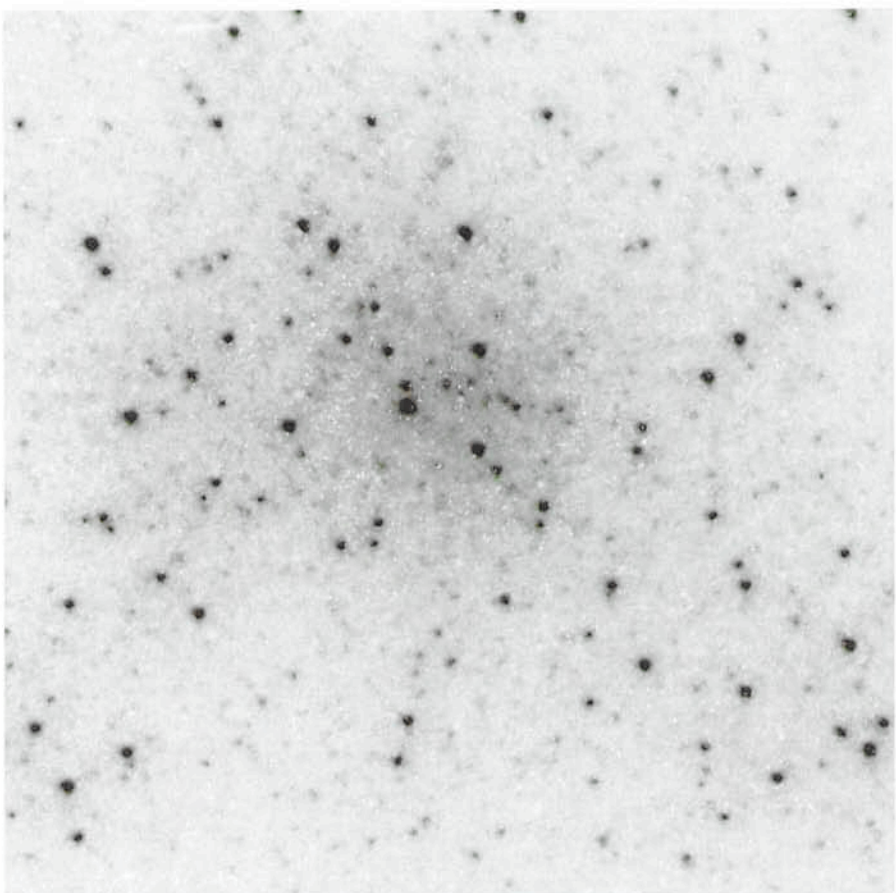

Figure 2: *The same region of M15 as in Figure 1, as seen by the Faint Object Camera (FOC) of the HST (Dubath et al. 1994). This public image was obtained in the F/96 mode with the F342 (central wavelength 3420 Å) filter. The sharp cores of the point spread functions have FWHM = 0.08″. No image restoration has been applied to this image. The three central stars are even more prominent at this wavelength than in the V-band image (Figure 1).*

in comparison with the expected central velocity dispersion (10–25 km s^{-1}) in M15. The width of the cross-correlation functions of stars depends mostly, when the intrinsic width of the stellar lines is small, on the spectral resolution of the observations.

The CCD images were first used to position the slit with the usual procedure. A bright isolated star is accurately centred on the slit in echelle mode using the slit viewer. EMMI is switched to the imaging mode, and the position on the CCD corresponding to the slit position in echelle mode is determined from an image of the star. The telescope is then shifted to move the cluster location to be observed to the same pixel coordinates as those of the bright star, and EMMI is switched back to the echelle mode to start the spectral observation. These CCD images also allow an *a posteriori* check of the slit position. The intensity profile through the slit is compared with that from the CCD image at the expected slit location. Thanks to the crowded stellar field in the core of M15, a good match between the two profiles is only obtained at one location on the CCD. Moving by one pixel in any direction degrades significantly the agreement between the two intensity profiles. In this way, we can determine the position of the slit to better than half a pixel, i.e., to better than 0.2″. The exact locations of the 1″×8″ slit during the five high-resolution spectral observations are displayed in Figure 3.

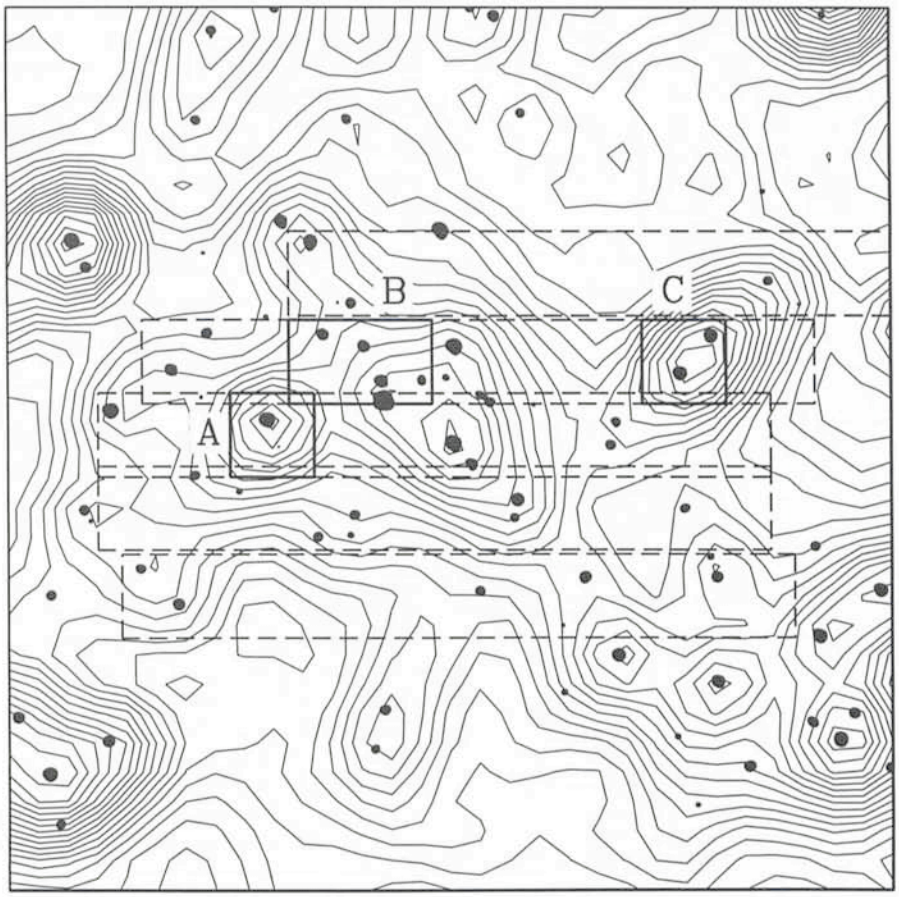

Figure 3: *In this figure, the HST image from Figure 2, displayed with a high low-cutoff so as to show only the bright stars of this image as black dots, is superposed to isomagnitude contours from one of the V-band CCD images taken with EMMI at the NTT. The isolated stars of the EMMI image have FWHM of 0.9″. The five dashed-line rectangles show the exact positions of the 1″×8″ slit during the five high-resolution spectral observations on the cluster core. The three solid-line rectangles are three particular areas of integration for which the corresponding cross-correlation functions are displayed in Figure 4.*

3. Data Reduction with INTER-TACOS

The data reduction was carried out with a new software called INTER-TACOS (INTERpreteur-Treatment, Analysis, COrrelation of Spectra) developed by L. Weber and D. Queloz at the Geneva Observatory. This programme is built and optimized for the automatic data reduction of echelle spectra from fiber-fed spectrographs but is also efficient for images from slit spectrographs. INTER-TACOS is now in operation at the Observatoire de Haute-Provence to do on-line the automatic data reduction of spectra from the ELODIE echelle spectrograph.

This software includes a cross-correlation package which works easily with very low signal-to-noise images, typically used for cross-correlation analysis. Optimal orders extraction and very efficient cosmic correction algorithms (Horne 1986) are available. Great care was taken to define a good wavelength calibration algorithm. Using about 1000 calibration lines, we measured with ELODIE at the OHP a wavelength calibration reproducibility of 2 m/s! The cross-correlation algorithms work with 2-D spectra (orders – pixels) and a wavelength solution stored in coefficients. The different orders are neither rebinned in wavelength units, nor merged together.

The five echelle spectra of the cluster core were reduced by taking advantage of the spatial resolution along the slit, as for long slit spectra. The spatial information along the slit of EMMI in echelle mode is fully conserved. We checked this by observing isolated stars positioned at different locations along the slit. In addition, with a slit of 8″ in length and the EMMI setup used, the successive orders do not overlap.

For each of the five observations in the cluster core (see Figure 3), we extracted spectra from each order in many spatial bins along the slit direction. These spectra were then reduced using INTER-TACOS, and the reduced spectra cross-correlated with a numerical mask. The properties of this mask, as well as the details of our cross-correlation technique, are described in previous studies (e.g., Dubath, Meylan and Mayor 1992). Our cross-correlation technique produces a cross-correlation function (CCF) – relative intensity as a function of the radial velocity V_r – which is nearly a perfect Gaussian (see Figure 4). The radial velocity is given by the abscissa of the minimum of the CCF, and the velocity dispersion can be derived from the broadening of the CCF in comparison with CCFs of individual stars.

4. Results

The radial velocity and the broadening of the cross-correlation function were derived for each pixel position in the area covered by the five slits displayed in Figure 3. The spatial resolution of these measurements is limited in one direction by the slit width (1″) and in the other direction – along the slit – by the seeing (~0.9″). This kinematical map fully confirms the results of our numerical simulations (Dubath et al. 1994) which predicted large statistical errors,

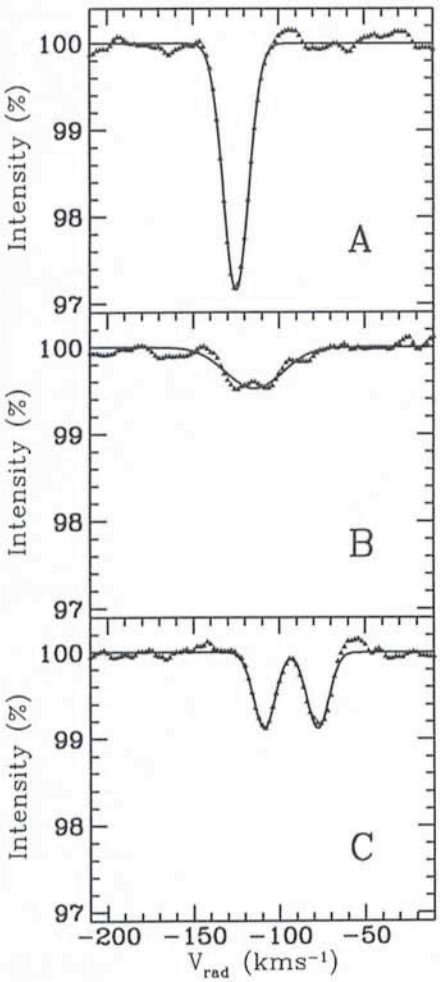

Figure 4: *Cross-correlation functions of the integrated light spectra taken over three particular areas of integration illustrated by the three solid-line rectangles in Figure 3. The CCF A has a stellar width and allows us to derive an accurate radial velocity for the star located in the rectangle A in Figure 3. The double CCF C shows that the two stars in rectangle C, barely spatially resolved, are clearly resolved in velocity by our observations. In the case B, we have integrated over a slightly larger area in order to produce a CCF as large as possible. The velocity dispersion derived from the broadening of the CCF B is 15 km s^{-1}.*

due to small samples, on the velocity dispersion measurements derived from integrated light spectra taken over small areas of integration at the centre of M15. The CCFs derived at the locations of the brightest stars are not significantly larger than the CCF of isolated stars. Around these locations, the CCFs are barely broadened, and any velocity dispersion measurement derived from these CCFs would underestimate strongly the real velocity dispersion. At other locations, the CCFs are clearly double (or triple) and sometimes two (or three) spatially unresolved stars appear to be spectroscopically resolved. In these cases, if the few dominant stars have unusually large radial velocity differences, the CCFs are artificially broadened leading to overestimates of the velocity dispersion. These different cases are illustrated in Figure 4, which shows three CCFs A, B, and C obtained respectively from the area of integration A, B, and C displayed in Figure 3. The CCF A has a stellar width and allows us to derive an accurate radial velocity for the star (AC 212, Aurière and Cordoni 1981) located in the rectangle A in Figure 3. The double CCF C shows that the two stars (AC # 214 and # 215) in rectangle C, barely resolved under the seeing conditions during the observations, are clearly resolved in velocity. Accurate radial velocities were also derived for these two stars. In the case B, we have integrated over a slightly larger area in order to produce a CCF as large as possible. The velocity dispersion derived from the broadening of the CCF B is 15 km s^{-1}, however, the statistical error on this result is large since the CCF B includes mostly the contributions of three stars. This is not obvious from Figure 4B, but appears unambiguously in CCFs obtained over smaller spatial bins.

The broadening of the cross-correlation functions is always $\leq$ 17 km s^{-1}, at any location in the 5″×8″ central area mapped. Our numerical simulations show that this value provides very probably an upper limit for the central velocity dispersion. The CCFs of integrated spectra taken at locations away from the brightest stars are less affected by statistical errors due to small samples and give velocity dispersions $10 \leq \sigma_p \leq$ 15 km s^{-1}. In order to minimize the statistical error due to a small sample, one can reduce the domination of the few brightest stars by taking the average of the *normalized* CCFs over all locations in the 5″×8″ central area. In this way, a velocity dispersion of 11.7 km s^{-1} is derived.

The radial velocities of the 14 best resolved (spatially or spectroscopically) bright stars were also determined. The velocity dispersion from these stars is 16.0 ± 3.0 km s^{-1}. This value is also likely to be an upper limit, since stars with large relative velocities are more easily spectroscopically resolved. We have radial velocities for two of the three brightest stars (AC # 214, 215, 216, the three bright stars in the centre of Figure 1 and 2) of the former unresolved cusp, the third being too blue to provide a radial velocity. Two of the brightest stars, separated by 2.5″, AC # 212 and 215, have radial velocity values differing by 48.9 km s^{-1}. A brief account of these results is published in Meylan and Dubath (1993).

5. Conclusion

We do not find any evidence for a velocity cusp in M15 from our mapping of the kinematics in the central area of 5″×8″. There is no evidence for a central velocity dispersion significantly larger than 15 km s^{-1}, and our best estimate is σ_p = 13±3 km s^{-1}. This value is consistent with predictions of several pre- or post-collapse theoretical dynamical models of M15: $\sigma_p(0)$ = 12–17 km s^{-1} from Illingworth and King (1977), $\sigma_p(0)$ = 13–15 km s^{-1} from Phinney and Sigurdsson (1991) and Phinney (1993), and $\sigma_p(0)$ = 14 km s^{-1} from Grabhorn et al. (1992). Consequently, there is no need to invoke the presence of any massive central black hole in the core of M15.

References

- Aurière, M., & Cordoni, J.-P. 1981, *A&A*, **100**, 307.
- Dubath, P., Meylan, G., & Mayor, M. 1992, *ApJ*, **400**, 510.
- Dubath, P., Mayor, M., & Meylan, G. 1993, in *Structure and Dynamics of Globular Clusters*, ASP Conference Series, Vol. 50, eds. S. Djorgovski & G. Meylan (San Francisco: ASP), p. 69.
- Dubath, P., Meylan, G., & Mayor, M. 1994, *ApJ*, in press.
- Grabhorn, R.P., Cohn, H.N., Lugger, P.M., & Murphy, B.W. 1992, *ApJ*, **392**, 86.
- Horne, K. 1986, *PASP*, **98**, 609.
- Illingworth, G., & King, I.R. 1977, *ApJ*, **218**, L109.
- Lauer, T.R., Holtzman, J.A., Faber, S.M., Baum, W.A., Currie, D.G., Ewald, S.P., Groth, E.J., Hester, J.J. Kelsall, T., Light, M., Lynds, C.R., O'Neil, E.J., Schneider, D.P., Shaya, E.J., & Westphal, J.A. 1991, *ApJ*, **369**, L45.
- Meylan, G. 1993, in *Ergodic Concepts in Stellar Dynamics*, eds. D. Pfenniger and V.G. Gurzadyan (Berlin: Springer), in press.
- Meylan, G., Dubath, P., & Mayor, M. 1991, *BAAS*, **23**, 833.
- Meylan, G., & Dubath, P. 1993, *BAAS*, **23**, in press.
- Phinney, E.S., & Sigurdsson, S. 1991, *Nat.* **349**, 220.
- Phinney, E.S. 1993, *MNRAS*, in press.
- Peterson, R.C., Seitzer, P., & Cudworth, K.M. 1989, *ApJ*, **347**, 251.
- Racine, R. & McClure, R.D. 1989, *PASP*, **101**, 731.
- Yanny, B., Guhathakurta, P., Schneider, D.P., & Bahcall, J.N. 1993, *ApJL*, in press.
- Zaggia, S., Capaccioli, M., & Piotto, G. 1992a, in *Star Clusters and Stellar Evolution*, eds. E. Brocato, F. Ferraro, & Piotto, *Mem. Soc. Astron. Ital.*, **63**, 211.
- Zaggia, S., Capaccioli, M., Piotto, G. & Stiavelli, M. 1992b, *A&A*, **258**, 302.

A New Quasar Pair: Q2126-4350 and Q2126-4346

M.R.S. HAWKINS, Royal Observatory Edinburgh, Great Britain
R.W. HUNSTEAD, School of Physics, University of Sydney, Australia
G. MEYLAN, European Southern Observatory, München, Germany
P. VÉRON, Observatoire de Haute-Provence, France
S.G. DJORGOVSKI, S.G. and J.D. SMITH, Division of Physics, Mathematics and Astronomy, Caltech, Pasadena, USA

Since the discovery in 1979 of the first gravitationally lensed quasar Q0957+561, a lot of effort has been devoted to finding more such objects. Twelve are now known, the largest separation between the various images being 6.5 arcsec.

However, neighbouring quasars having the same redshift are not necessarily images of a gravitationally lensed system. Six pairs of quasars have been found with separations in the range 3 to 10 arcsec corresponding to a few tens of kiloparsecs. These objects are believed to belong to the same group or cluster of galaxies.

Another pair of quasars, Q1146+111 B and C, at z=1.012, with a separation of 157 arcsec, attracted a lot of attention some time ago. Turner et al. (1986) have suggested that this is a single quasar gravitationally lensed by a massive cluster of galaxies. Blandford, Phinney and Narayan (1987) have shown that this assumption is very unlikely to be correct and Phinney and Blandford (1986) have suggested that Q1146+111 B and C are two distinct quasars separated by ~ 700 kpc whose proximity is attributable to clustering.

In the course of a survey for optically variable quasars (Hawkins and Véron, 1990), we have found a new pair of quasars (Q2126-4350 and Q2126-4346) with similar redshift (z~1.10) and separation (202 arcsec) to Q1146+111. These two objects have about the same magnitude (B=20.2 and 20.4 respectively on the reference UKST Schmidt plate). Both have a high amplitude of variability, AB=1.0 mag. We have determined that, in our sample, ~8 % of all UVX quasars have such a high amplitude of variability; this fact suggested to us that, in this case, we were possibly observing a large-separation gravitationally lensed system.

A 60-min exposure spectrum was obtained on August 18, 1993 with the EMMI spectrograph at the ESO NTT 3.5-m telescope (shown in Figure 2). The two objects were placed simultaneously on the slit. The stronger object (Q2126-4350) shows a broad Mg II emission line and a narrow [OII] emission line allowing to determine an accurate redshift z=1.116. The fainter object has only a broad Mg II emission line at the same redshift. The two spectra look significantly different, but if the objects are two images of a single quasar, these differences could perhaps be due to the time delay between the two light paths.

The whole 19-deg^2 field of our variable quasar search has been surveyed at 843 MHz with the Molonglo Observatory Synthesis Telescope (MOST) (Mills, 1981). One member of the new quasar pair (Q2126-4346) is a strong radio source, with a flux density of 178 mJy, whereas the other quasar (Q2126-4350) is not detected at 843 MHz, having a 3σ upper limit of 2.5 mJy. Furthermore, Q2126-4346 is not detected in the PNM survey at 4850 MHz (Gregory et al. 1993), implying that the source is weaker than 45 mJy at this frequency and therefore that it has a normal spectrum ($\alpha < -0.8$) and is unlikely to be variable. Consequently, the radio information almost certainly excludes the hypothesis that we are looking at a gravitationally lensed system and reinforces the idea that quasars cluster on a scale ~1 Mpc.

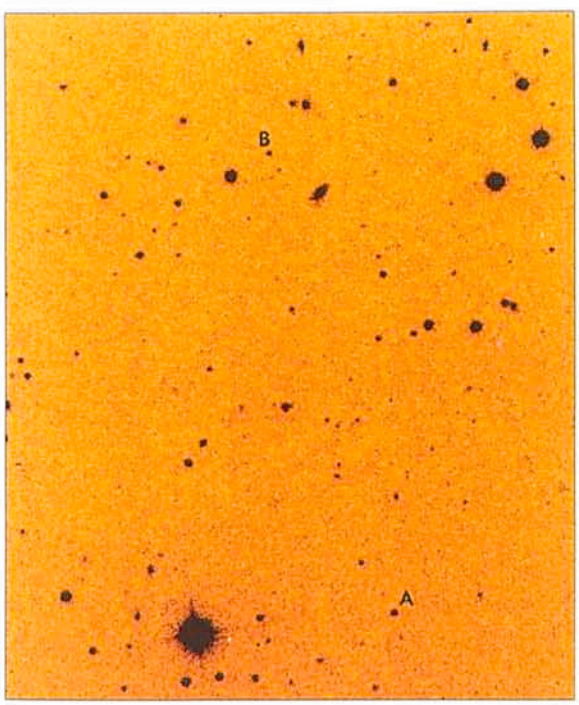

Figure 1: *Part of a 2-minute exposure frame taken on August 18, 1993 through a I filter with EMMI at the ESO NTT on La Silla. The size is 3.9 arcmin × 4.7 arcmin. North is up, east to the left. The seeing is 1.4 arcsec. The two quasars, Q2126-4350 and Q2126-4346, identified with the letters A and B, respectively, are separated by 202 arcsec.*

References

Blandford, R.D., Phinney, E.S. and Narayan, R. 1987, *ApJ* **313**, 28.
Gregory, P.C., Vavasour, J.D. and Scott, W.K. 1993, *NRAO* preprint.
Hawkins, M.R.S. and Véron, P. 1990, *The Messenger* **61**, 46.
Mills, B.Y. 1981, Proc. ASA **4**, 156.
Phinney, E.S. and Blandford, R.D. 1986, *Nature* **321**, 569.
Turner, E.L. et al. 1986, *Nature* **321**, 142.

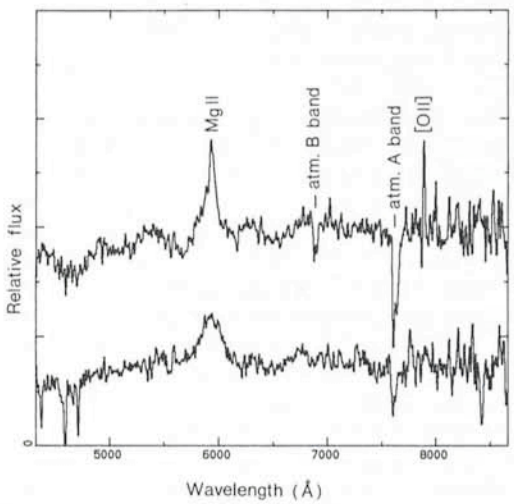

Figure 2: *Spectra of the two quasars observed with EMMI. Top: Q2126-4350, bottom: Q2126-4346.*

VLT Working Group for Scientific Priorities – Status of the Work

L. VIGROUX, Service d'Astrophysique, Saclay, France

In its May 1993 session, the ESO Scientific and Technical Committee formed a working group to propose a set of main scientific priorities to serve as guidelines for future discussions on the VLT and its instrumentation. A number of working groups on this matter existed during the early definition phase of the VLT. Their reports are included in the proceedings of the 2nd VLT Workshop, held 1986 in Venice. On that basis, ESO worked out the VLT Instrumentation Plan which was widely circulated in the community in June 1989 and discussed by ESO committees. Between the preparation of the Blue Book and the commissioning of the first unit telescope, about 12 years will elapse – even more for the other unit telescopes. Being roughly half-way between these two events, the STC thought it timely to reassess these scientific priorities for the VLT and the instrumentation plan, taking into account recent scientific and technical developments. Another goal of this exercise is to provide scientific priorities which can later be used as guidelines in prevision of future problems, technical trade-off or descoping.

After some changes during the summer, the group is now composed of STC members K. de Boer, B. Marano and L. Vigroux (chairman), ESO representatives J. Wampler, J. Walsh and S. D'Odorico and two external experts, B. Fort and R. Kudritzki.

To involve the ESO community in this activity, we circulated during the summer a questionnaire about the scientific programmes to be done with the VLT. The real work of the group started in September 1993. The main line of our reflection is organized around several steps:

- review the capabilities of other observatories in the VLT era, both on ground and in space. Scientific programmes for the VLT have to be examined in the context of what will be done at the other observatories,
- assess the uniqueness of the VLT, both as single 8-m telescope or with the four telescopes,
- define a set of scientific domains in which the VLT with an appropriate instrumentation will have the capabilities to create a unique breakthrough,
- make recommendations in several areas of the VLT: telescopes, detectors, instruments and operations.

The first part of this work is now completed. Preliminary versions of the other points have been presented and discussed during the November 1993 STC meeting. We do not yet have a detailed new instrumentation plan, but we are almost getting there. I will indicate here only the general directions to get a flavour of our work.

To define the scientific priorities, we have not tried to make an extensive survey of all the astrophysical problems which can be tackled with the VLT, but rather to focus on a few scientific domains in which we expect that the VLT will provide a significant gain over existing capabilities. For the time being, we have selected four domains, star formation and young stellar objects, starburst galaxies and active nuclei, formation and evolution of galaxies, and formation and abundances of the elements. For each of these themes, we have identified programmes which can be done with the planned instruments, and those which require new instruments. This part of the work must be followed in two directions, elaborate on these themes, and incorporate one or two additional themes.

For the telescopes and the instruments, we have agreed on two main directions: emphasize the importance of the infrared, and the need for very large detectors.

Arguments for supporting infrared work on the VLT are overwhelming. Infrared astrophysics deals with crucial areas such as star-forming regions which are generally embedded in dusty clouds and accessible only in infrared, or detection of very distant galaxies which are about 5 to 10 times brighter in the infrared than in the visible. The largest gain provided by large telescopes is for infrared wavelengths where observations are limited by the background. In this case, the sensitivity increases as D^4, D being the telescope diameter. In addition, a revolution in IR detectors is now taking place. We should expect a boost of IR observations similar to the dramatic developments of optical observations coincident with the use of 2D electronic detectors 25 years ago. New techniques of imaging at the diffraction limit with adaptive optics or interferometry are already operational in the infrared, but might not become available in the visible in the next few years. Together with the detector revolution and the increase of telescope size, they will provide an enormous gain in sensitivity for point source observations. Last but not least, the VLT will become operational after the ISO mission which is expected to create a scientific breakthrough with its sensitivity improved by a factor of 50 to 100 over IRAS. New scientific problems will be uncovered and will require new sets of infrared observations.

The present VLT instrument package is designed around CCDs that are about state-of-the-art at the present day. Recent developments in the CCD mosaic techniques and progress of the IR arrays will allow a new instrument design, with a good image sampling on a large field. The VLT has been optimized for image quality, and the pixel sampling must be optimized accordingly. However, further analysis is needed to assess these instrument concepts.

During the last STC meeting, it was decided to continue this work along the line defined in the preliminary report. ESO will strengthen its participation, both in scientific priorities definition, and in the assessment of the new instrument concepts. A final version of the report will be presented at the next STC meeting in May 1994 and discussed more widely in a workshop which will be organized by ESO before the summer.

Working Group for Scientific Priorities for La Silla Operations

J. ANDERSEN, Chairman, ESO-STC

Preparation of the Report

At its first full meeting in May, the WG emphasized the importance of receiving feedback and advice from the community. Since then, a total of three draft reports have been widely circulated, the last two through the members of the STC and Users Committee. The WG also met with the UC, on September 16. The resulting numerous comments have all been considered in the preparation of the final Report, dated October 23, which was submitted to the STC at its 34th meeting, November 4–5, 1993.

The STC supported the basic proposals of the Report and encouraged the Director General to implement them "in good spirit". With this recommendation, the WG has forwarded its report to the Director General and Council for further action.

The Report of the WG is freely available from ESO (Section Visiting Astronomers), and readers interested in the details are encouraged to consult it. The following is just a brief summary of the rationale for its recommendations, and of some lessons learned.

Background

The La Silla Observatory will, for at least another decade, remain the bread and butter of ground-based European observational astronomy in the southern hemisphere. Currently, La Silla is probably unsurpassed for the range and flexibility of its facilities. Basically, Visiting Astronomers (VAs) can expect to use front-line instrumentation covering the range from the atmospheric cutoff to millimetre wavelengths, with few other restrictions than the competition for observing time. In addition, La Silla hosts a number of more specialized experiments not directly related to the research conducted by ESO staff astronomers or VAs.

However, in recent years, new telescopes and instruments have appeared on La Silla at an accelerating rate, with no corresponding increase in the staff. Particularly after the advent of the NTT, it is proving impossible to adequately support all the facilities currently offered to visiting astronomers. Several changes and upgrades at the larger telescopes remain to be fully tested and implemented.

An overload of conflicting demands and a lack of clear priorities have prevented the staff from addressing these problems in a systematic way. As a result, the scientific productivity of La Silla's telescopes – even some of the newest and most powerful – is being compromised. Clearly, this state of affairs cannot be allowed to continue.

Yet, with the VLT project on its hands, it is difficult for ESO to boost La Silla by new recruitment or by drawing on Garching staff. Bringing the top-priority facilities up to standards worthy of a world-class observatory must happen within an essentially constant staff and budget envelope.

It follows that increased effort in some areas will draw resources from others: Quality must be enhanced at the expense of quantity. In order to thus qualitatively enhance the scientific productivity of La Silla within the existing means, a set of scientific priorities for the operation of the observatory are needed.

In order for ESO to steer through this process in a responsible and transparent manner, the Director General appointed in early 1993 a Working Group on Scientific Priorities for La Silla Operations. Its members are: J. Krautter (OPC), J. Lub (UC), M. Mayor (ex-STC), and J. Breysacher, D. Hofstadt, J. Melnick, and J. Wampler (all ESO staff), with the writer as Chairman. The proposals of the WG were to be submitted to the DG with the comments of the STC.

Defining Scientific Priorities

While never trivial, it is relatively easy to agree on priorities for exciting new opportunities. It is far more difficult to choose which facilities and freedoms may have to disappear in order for La Silla as a whole to perform optimally. Scientific priorities have not previously been formulated in a way suitable for that purpose. This is clearly reflected in the comments received from users: about 99 per cent emphasize the unique value of a particular piece of equipment as seen in isolation, but without regard for the entire picture.

As guidelines for its own discussion of priorities for instruments, services, and scheduling techniques, the WG used the following criteria. The list below is indicative, but neither complete nor in strict order of importance:

- Uniqueness, on an international scale, of the scientific opportunities offered: La Silla belongs at the frontiers of astronomical research.
- Direct relevance for the VLT project. ESO's resources, and the credibility of the ESO community, are largely tied to the timely and successful completion of the VLT. Early experience on how to control, equip, staff, and operate the VLT is crucial.
- Long-term importance for a broad segment of the user community. ESO was created to serve the scientific interests of the community and should provide optimum conditions for its top-priority research projects.
- Importance for specific interests of user communities in the member states, at a support level consistent with the importance of the research and the size of the community.

When considering a specific facility, the WG consulted the statistical information available from the OPC on the number, rating, and approval rate of the proposals received. Individual proposal ratings are, of course, confidential, but average grades and general trends were available.

Proposed Improvements

The clear top priority for increased support is the NTT: This telescope must now be brought to technical and operational standards at which its great scientific potential can be realized. Moreover, valuable experience can be gained for the VLT project by upgrading and operating the NTT according to VLT standards. ESO is already planning how to achieve these goals by concerted action from La Silla and Garching. The WG strongly welcomes this initiative.

Second priority is to bring the other major telescopes to consistently high performance, especially as regards image quality. Items include fast and reliable top-end exchanges and mirror realignment (3.6-m and 2.2-m); improved dome seeing; and a new control system at the 2.2-m for optimum IR performance. A full complement of modern CCD detectors and on-line data reduction facilities are urgently needed at all telescopes.

First among third-priority items is a permanent CAT-CES optical fibre link: The CAT M3 drive is becoming increasingly unreliable. Improved measurements of seeing and other meteorological data are also high on this list. Finally, numerous improvements of individual telescopes and instruments are proposed throughout the report.

Proposed Economy Measures

A recommendation for increased priority also implies an identification of other areas where a corresponding reduction of effort can be made. Minor, cosmetic measures will not lead to significant overall relief, nor can a single radical measure do so at a scientifically acceptable cost. Hence, the recommendations of the WG have considered a broad range of actions.

Much of the workload on the staff is due to frequent instrument changes. Hence, the WG proposes a system of block scheduling on all telescopes on which the instrument configuration cannot be frozen entirely. Service observing would be introduced as a serious option. Test and setup time can be minimized as part of the benefits.

In parallel, a balanced plan is proposed (summarized in Chapter 6 of the Report) to redistribute the instrumentation among the telescopes so that maximum specialization is achieved at each telescope while limiting the total choice as little as possible. Rare exceptions would still be allowed.

Finally, the WG recommends that a few facilities be decommissioned as no longer competitive on the basis of quality of the data, quality and quantity of recent proposals, and operational and maintenance effort. In addition to a few instruments, this category includes the Schmidt telescope (as a general user instrument), the GPO, and ESO use of the Danish 50-cm telescope.

Lessons Learned

Most reactions to these proposals have shown real understanding of the factual situation: Despite very difficult financial conditions in most of the member states, ESO is nevertheless allowed to proceed with the construction of our most coveted tool: The full-scale VLT – the world's largest telescope. Looking at the fate of some other large research projects in the world, it is not unreasonable that we contribute by trimming some of our lower-priority activities.

Other comments have taken the form of unconditional demands for continued support for this or that favourite facility, regardless of the impact on the rest of ESO. Few of us are in a position to make such demands in our home countries, and even powerful rhetoric cannot by itself make staff and money appear.

The central message of the report is that ESO is now finding itself in the real world of limited resources, and we have to respond rationally to this discovery. This includes the ability to assign priority to certain overall scientific goals in a long-term strategy, and to programme resources so as to actually achieve them. Demands for wholesale perfection beyond ESO's means are basically pointless and lead instead to general dissatisfaction.

Longer-Term Prospects

Human beings are imperfect, and conditions change. The WG therefore strongly emphasizes that the task is not finished with the present report: Reviews of operating modes and adjustment of the facilities offered must become a permanent (e.g. annual) feature of ESO's forward planning.

The compromises reached can never satisfy everybody. The inevitable dissatisfaction of some is best turned into proposals for future improvements. Its least constructive expression would be to criticize those on La Silla who are charged with the execution of these necessary policies.

A final important lesson from this work is how little even relatively major restructuring of the observing facilities on La Silla and the way they are scheduled results in measurable effects on the total workload of the T.R.S. Department, let alone on the budget of ESO/Chile as such. For the longer term, this exposes again painfully clearly how small a fraction of the total effort and budget of ESO has direct impact on the scientific productivity of the La Silla Observatory.

It follows that when further efficiency measures become necessary in 1996, mere reduction of scientific opportunities along the course explored here, leaving the organization itself untouched, is not the appropriate starting point for a rational solution.

Profound reorganization of the entire ESO infrastructure in Chile will be needed in order for La Silla and Paranal together to serve the ESO community in a scientifically competitive and cost-effective way in the VLT era.

Proposal Statistics

J. BREYSACHER, ESO, and J. ANDERSEN, Chairman ESO-STC

In the following figures, the number of observing proposals received (dotted lines) and accepted by the OPC (full lines) is plotted for each telescope/instrument combination as a function of the ESO period number. The data cover Periods 41 through 52 (1988–1993).

These statistics were prepared for the Working Group on Scientific Priorities for the La Silla Operations.

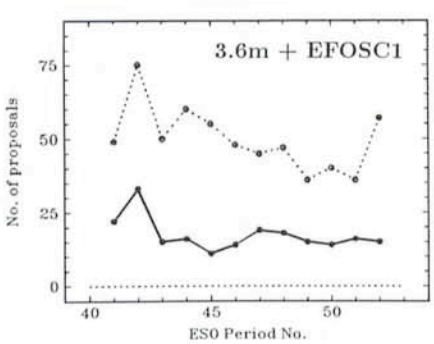

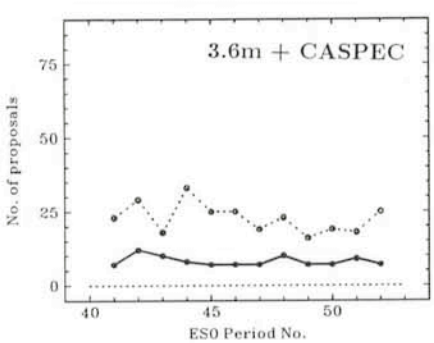

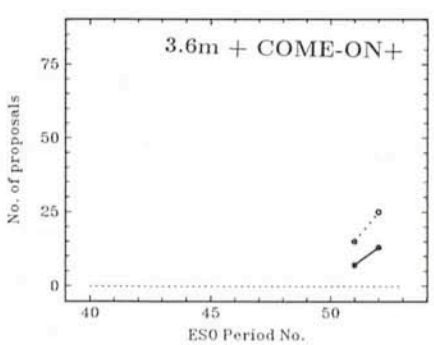

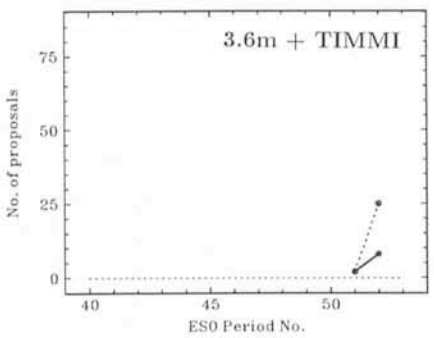
3.6m + TIMMI
No. of proposals
ESO Period No.

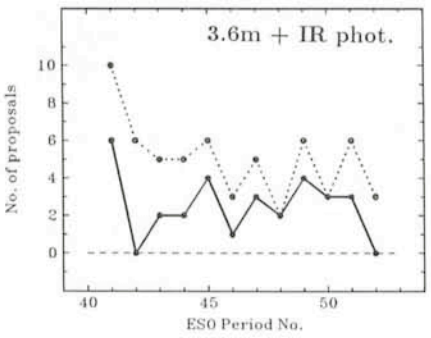
3.6m + IR phot.
No. of proposals
ESO Period No.

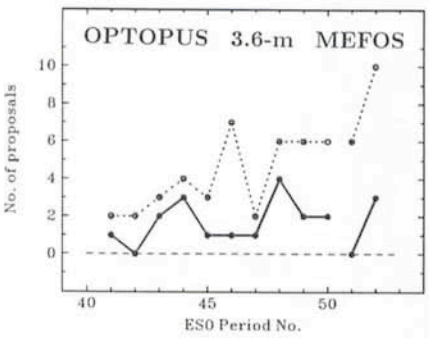
OPTOPUS 3.6-m MEFOS
No. of proposals
ESO Period No.

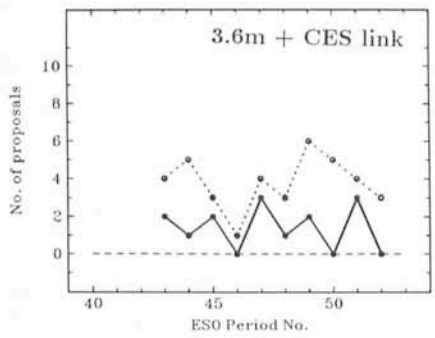
3.6m + CES link
No. of proposals
ESO Period No.

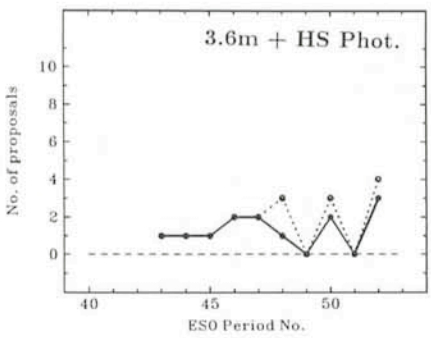
3.6m + HS Phot.
No. of proposals
ESO Period No.

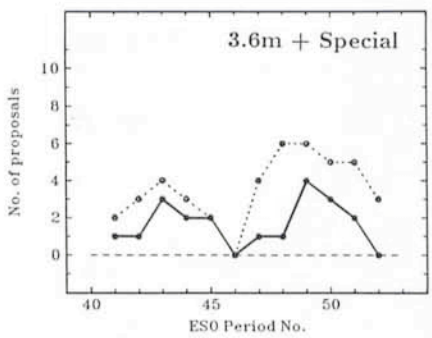
3.6m + Special
No. of proposals
ESO Period No.

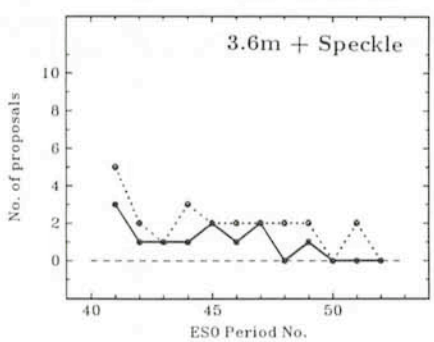
3.6m + Speckle
No. of proposals
ESO Period No.

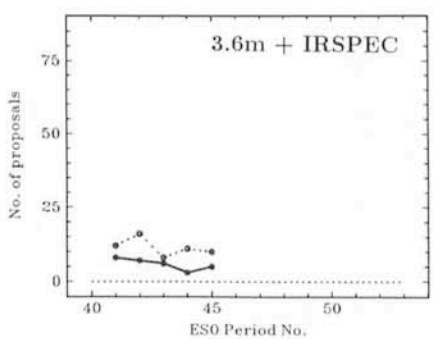
3.6m + IRSPEC
No. of proposals
ESO Period No.

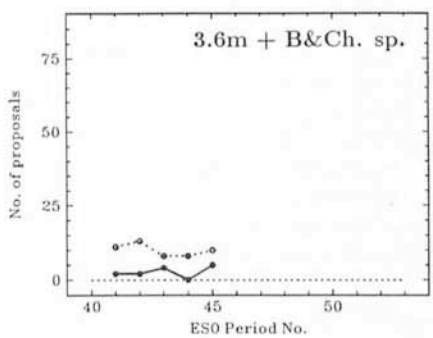
3.6m + B&Ch. sp.
No. of proposals
ESO Period No.

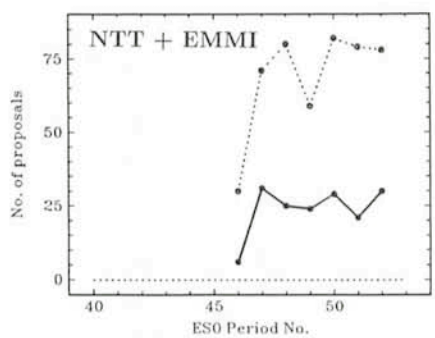
NTT + EMMI
No. of proposals
ESO Period No.

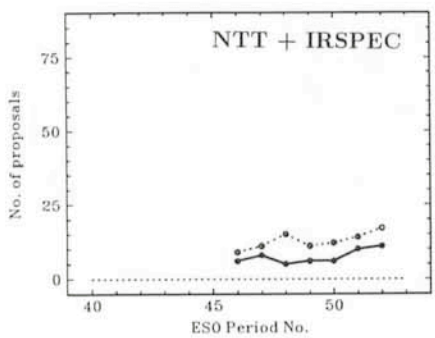
NTT + IRSPEC
No. of proposals
ESO Period No.

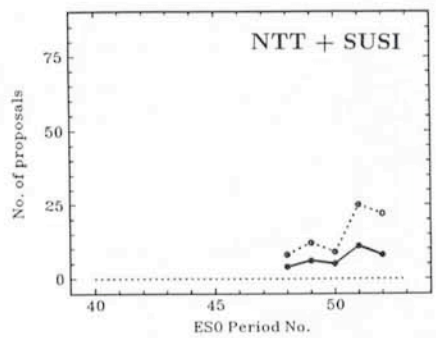
NTT + SUSI
No. of proposals
ESO Period No.

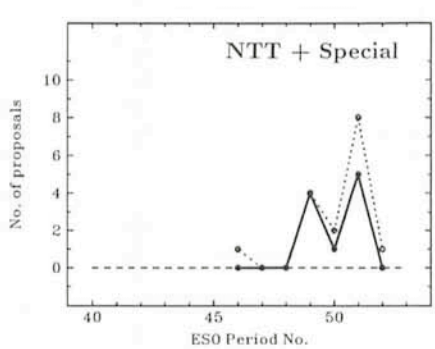
NTT + Special
No. of proposals
ESO Period No.

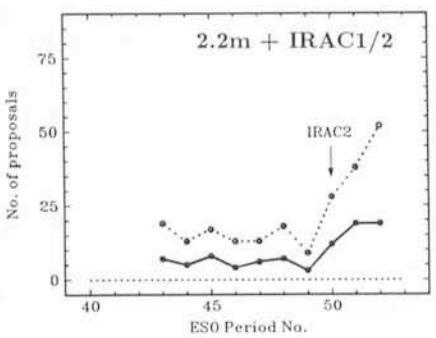
2.2m + IRAC1/2
IRAC2
No. of proposals
ESO Period No.

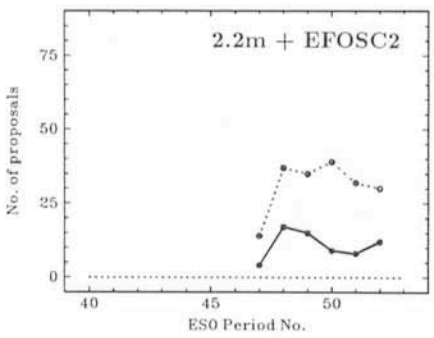
2.2m + EFOSC2
No. of proposals
ESO Period No.

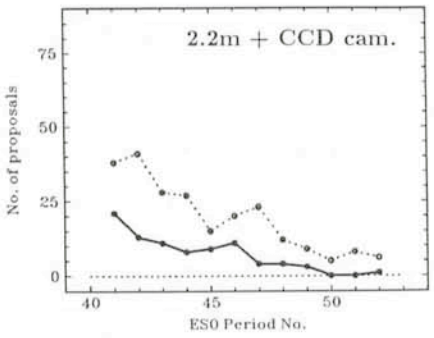
2.2m + CCD cam.
No. of proposals
ESO Period No.

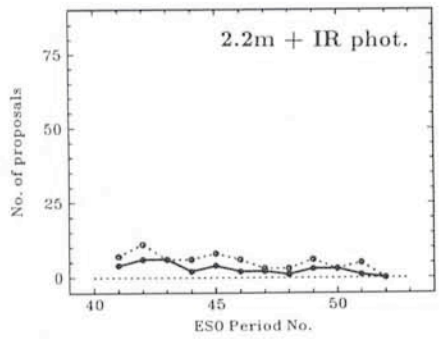
2.2m + IR phot.
No. of proposals
ESO Period No.

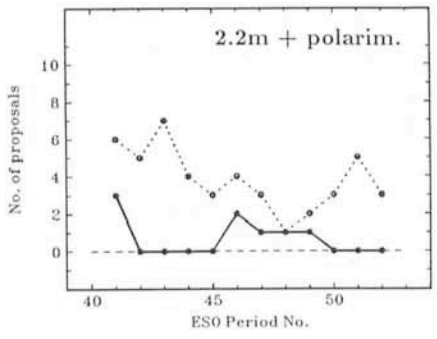
2.2m + polarim.
No. of proposals
ESO Period No.

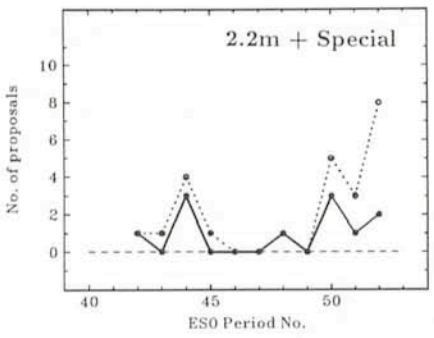
2.2m + Special
No. of proposals
ESO Period No.

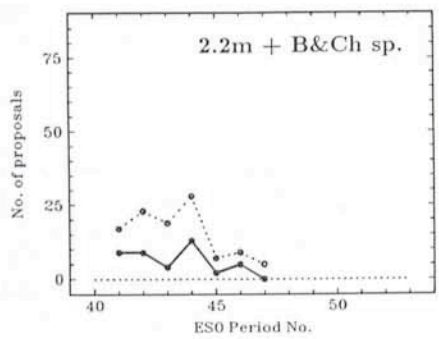
2.2m + B&Ch sp.
No. of proposals
ESO Period No.

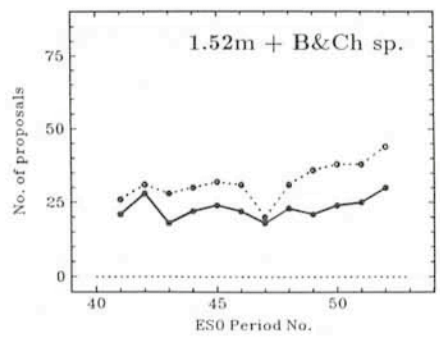
1.52m + B&Ch sp.
No. of proposals
ESO Period No.

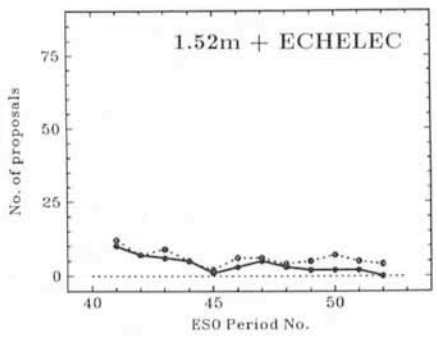
1.52m + ECHELEC
No. of proposals
ESO Period No.

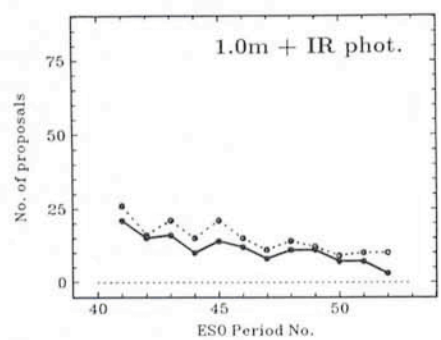
1.0m + IR phot.
No. of proposals
ESO Period No.

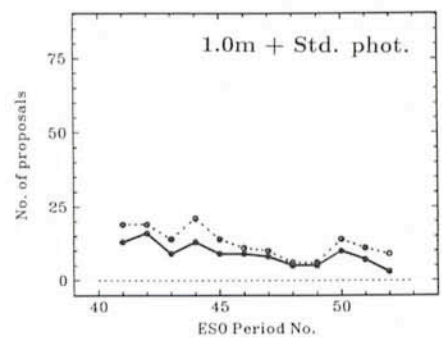
1.0m + Std. phot.
No. of proposals
ESO Period No.

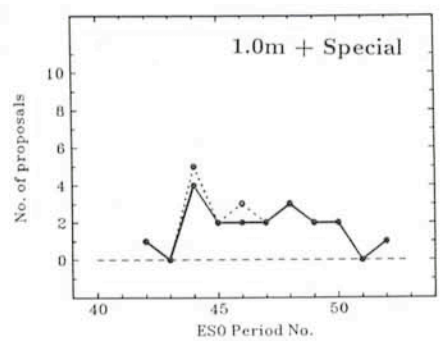
1.0m + Special
No. of proposals
ESO Period No.

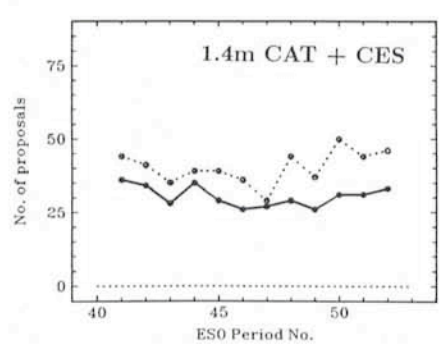
1.4m CAT + CES
No. of proposals
ESO Period No.

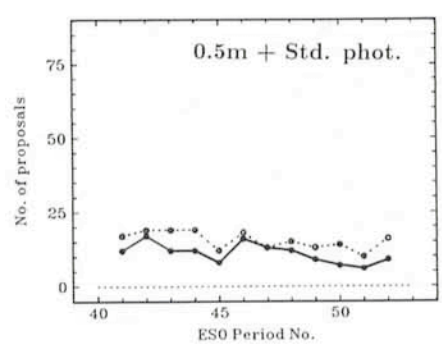
0.5m + Std. phot.
No. of proposals
ESO Period No.

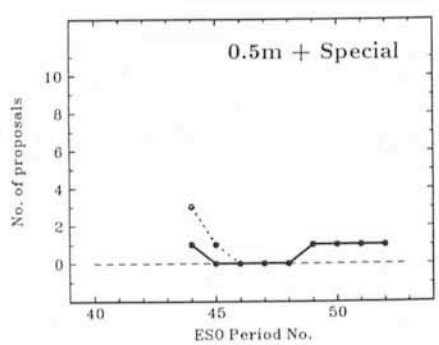
0.5m + Special
No. of proposals
ESO Period No.

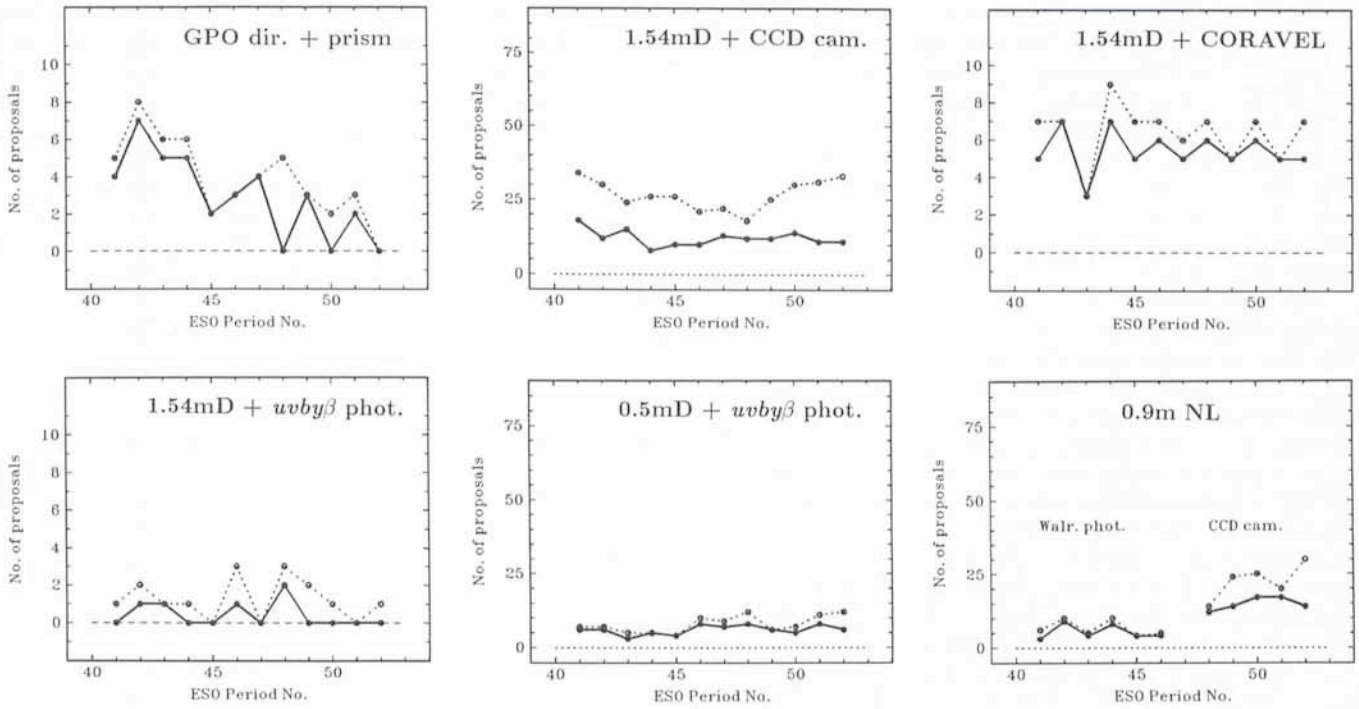

The 93NOV Release of ESO-MIDAS

ESO Image Processing Group

The new release of ESO-MIDAS contains a substantial number of improvements and new features. Among these is the implementation of a new set of Graphical User Interfaces based on OSF/Motif, which makes the usage of a number of application packages easier. In the sections below the main improvements are highlighted. For more detailed information we refer to the last issue of the ESO-MIDAS Courier (July 1993).

1. New Features and Application Packages

1.1 System

Significant modifications and enhancements have been implemented in the MIDAS Command Language, e.g. an improved debugger for MIDAS procedures, more robust error handling and direct access to all data structures from within a procedure. To improve the information transfer, the support of help text for descriptors in data files has been added. A prototype of communication protocols has been implemented to enable interaction of any stand-alone programme with MIDAS.

1.2 Data Organizer

A new application package called DO (Data Organizer) for preparation of data reduction procedures has been implemented. The Data Organizer uses as input a list of FITS files or MIDAS images as well as a list of FITS keywords or MIDAS descriptors which are considered to be relevant (e.g., exposure time, telescope setting, instrument mode) to create an Observation Summary Table.

Each entry of this table is then classified according to a set of user-defined rules: the user may for instance group the data according to the exposure type and put together all frames observed in a given instrument mode. An interface based on the Table Editor has been developed to facilitate the formulation of these rules.

The association of science frames with suitable calibration exposures is achieved by using the same rule-generating interface as referred to above even though the rules to be applied are different: One may want for instance to look for all the Flat Fields which have been taken within a certain time interval of the science exposure. The Association Process creates a MIDAS table which can be used by any reduction package. It contains one column for each type of exposure (e.g. SC, BIAS, DK, WCAL), while each row contains for the corresponding science image the set of suitable calibration frames.

The Data Organizer has been tested on the ESO Archive which contains so far 30,000 EMMI/SUSI exposures. This version of the package is still a preliminary version and the structure of the output association table may be changed in the future.

1.3 CCD Package

Since the last update of the MIDAS CCD package in 1986 a number of new instruments have been installed on the La Silla Telescopes. In addition, new CCDs became available offering large pixel areas and higher quantum efficiency. With these innovations the variety of observing modes has grown and, as an obvious consequence, the amount and the diversity of data taken have dramatically increased. It is clear that the MIDAS CCD reduction software should be able to cope with these improvements and hence requires compatibility with the hardware as it exists at present.

When designing the basic layout of the CCD software, a number of basic requirements were kept in mind: e.g. robustness, user-friendliness, easy adaption for new or non-ESO instrumentation, automatic calibration procedures to enable a quick-look facility at the telescope. In what sense these requirements can be realized depends on the data-acquisition system, archiving and, obviously, the data-reduction

system. In this respect the development of the CCD package took place at the right time. The ESO archive project has accomplished that for a number of telescopes and instruments the setup specifications are stored together with the data. In addition, the new MIDAS Data Organizer package offers a significant help in preparing the data for reduction (see above).

The new CCD package in MIDAS makes use of the output MIDAS table of the Data Organizer package that contains the science and calibration data and the relation between these two. The package provides commands to do the various bias calibration steps like combining calibration frames, subtraction of the bias level determined from the over-scan area or from a separate bias frame, correction for dark current, division by the correction for illumination, and correction for the fringe pattern. Also, tools are provided for trimming the frames of the unwanted over-scan strip, and for correcting the frame for bad pixels intensities. All operations steps that successfully finished are recorded in the descriptor of the reduced frame. This recording, which includes updating the HISTORY descriptor, avoids repetition of reduction sequences, and provides the user with the information on what has been done to the data.

By combining the basic reduction steps, a complete reduction pipeline procedure is built that enables the user to do an automatic reduction of all science frames. The pipeline procedure is controlled by a set of reduction keywords in combination with the information stored in descriptors of the data frames. Therefore, apart from commands that do the actual work, a number of commands help the user to manage keywords and descriptors.

1.4 Spectroscopy Packages

The long-slit spectroscopy package Long has been totally refurbished since the version 92NOV. It includes all functions of the previous packages Spec, Long and XSpectra as well as many additional features, such as batch reduction. The Long package now supports 1D and long-slit spectroscopy and includes a graphical user interface. A tutorial (command TUTORIAL/LONG) demonstrates the commands of the package.

A new package for spectral analysis has been developed by Juan Veliz at La Silla and is based on the graphical user interface XAlice. It provides basic functions for:

- flux integration, including continuum fitting and determination of line parameters like fwhm, equivalent width, flux and continuum level
- rebinning (logarithmic, frequency, red-shift)
- filtering by smooth or median filters
- multiple-component fitting by a set of gaussians.

2. Graphical User Interfaces

The version 93NOV includes four OSF/Motif based interfaces:

1. XHelp provides access to the on-line documentation. More functions have been implemented since the 92NOV version, including a history mechanism, strings search, files printing, context selection and feedback (problem report).
2. The new interface XDisplay implements a number of display related commands. It enables manipulation of images, LUTs, ITTs and cursor commands in an easier way.
3. The interface XLong is related to the new long-slit spectroscopy package Long. The interface allows the activation of calibration commands and provide convenient panels for arc lines identification and batch reduction.
4. The interface XAlice is related to the new spectral analysis package Alice (see Spectroscopy Packages).

All these interfaces conform to the ESO GUI Common Conventions which define the Look and Feel for all ESO interfaces in the fields of telescope and instrument control, archives and data analysis. In addition to the OSF/Motif XHelp interface, the 92NOV release included several Athena-based interfaces (XSpectra, XEchelle, XFilter, XStella). Some of them (XEchelle, XFilter, XStella) have not yet been ported to OSF/Motif and compiled versions for Sun and HP will be available through our anonymous ftp account.

3. Availability

The 93NOV release of MIDAS is scheduled for distribution in December 1993. An alpha version was frozen in July and tested internally. After this test, the beta version was shipped to more than 15 sites representing the major hardware platforms. Based on these test reports, the release will be finalized in November. The 93NOV MIDAS release will be verified on the following systems: SUN SPARC Solaris 1.x and 2.x, HP 9000, IBM PS/6000, DEC Ultrix-(MIPS), DEC VAX/VMS, DEC Open VMS (APX), Silicon Graphics and PC/Linux. DEC OSF/1 systems are not yet supported but a beta-test version is expected to be available in the spring of 1994. Sites must explicitly request the release, specifying the medium.

The MIDAS system is, at the moment, distributed free of charge to non-profit research organizations. They must sign a User Agreement with ESO in order to obtain the system. Information and requests for MIDAS should be directed to the Image Processing Group at ESO, Karl-Schwarzschild-Str. 2, D-85748 Garching, Germany, or through E-mail (Internet: midas@eso.org). A Hot-line service is also available at the same address. New releases and patches can be copied from the midas account on the Internet host 'ftphost.hq.eso.org'. Application packages and documentation are also available on our anonymous ftp account. A bulletin board can be accessed through the 'esobb' account on the Internet host 'bbhost.hq.eso.org'.

An ESO-MIDAS Implementation for PC/Linux

C. GUIRAO, ESO Image Processing Group

It may seem to be a contradiction to implement a large image processing system like ESO-MIDAS on PC type systems; however, they are becoming surprisingly powerful. Although normal reduction of data is better performed on workstations, the final analysis, which requires much more time for the interpretation of data than for actual computing, may be well suited for a PC. One of the main objectives is to provide an ESO-MIDAS implementation on a very inexpensive system that small institutes and even individual scientists can afford.

We decided to focus on Linux, a public domain Unix system, as the most suitable for the MIDAS community.

Linux not only satisfied the requirements to install MIDAS (C and Fortran compilers plus X11) but it also complies with ANSI-C and POSIX standards. In addition, it includes all the network software necessary to integrate the PC into a LAN. Linux is supported by the Free Software Foundation which also provides other public domain software (like GNU).

The popularity of Linux has increased enormously in the last months (as indicated by the "linux" newsgroup, one of the most active newsgroups on USENET), and with it the interest of the Astronomical community for having MIDAS ported to it. This became apparent during the 5th ESO/ST-ECF Data Analysis Workshop where the MIDAS Group showed the progress with PC port.

Now, the situation has improved substantially and we are glad to announce that the complete "core" of MIDAS has been successfully implemented and verified on Linux SLACKWARE 2.01. Some other MIDAS packages have also been tested by their authors (like `WAVELET`, `PEPSYS`, `ECHELLE` and `LONG`). A pre-release of the 93NOV release has already been distributed to several test-sites for a complete check-out.

The Graphic User Interface (GUI) packages for MIDAS are being ported to Linux. Two of them, XHelp and XDisplay, are already available while the rest will follow soon. The MIDAS GUIs are based on OSF/Motif which is a licence produce not included in the distribution of Linux. Thus, we can only distribute them in binary executable form as an option in the distribution tape. They will also be available under our "anonymous ftp" account.

Table 1: *Configuration of PC test system.*

Hardware	Software
i486DX/25 20 Mbytes RAM Adaptec 1542B SCSI board 1 Gbyte SCSI hard disk WD-8013 Ethernet board Local Bus S3 Video Card	Linux SLACKWARE 2.01 0.99.pl12 cc: GNU compiler 2.4.5 (included) f2c: f77 to C translator 22 (included) X11 R5 (included) Motif 2.1 (not required) MIDAS beta-release 93NOV (28 Mbytes)

The hardware and software configuration for the test system is given in Table 1 for information only. It does not mean to be the unique or minimum hardware setup. MIDAS requests only a 386 CPU, Linux release 0.99pl12 or higher, a minimum of 16 Mbytes of memory and some disk space depending on the amount of data needed. With shared libraries, the MIDAS executables and help files take around 30 Mbytes.

Table 2 gives a comparison of the performance of some MIDAS tasks on a PC and SPARCstation 2. It should be noted that on Linux there is no real Fortran compiler but a Fortran-to-C translator, and access to the disk on SPARCstation 2 is about 5 times faster than on our PC.

Both SunOS and Linux used the MIDAS shared library. The C-Whetstone benchmarks by H.J. Curnow and B.A. Wichman (1976, Computer Journal, Vol. 19, No. 1) were used to compute the "cwhetstones". The last columns with MIDAS benchmarks refer to the `filter/median` command executed on a 1000×1000 image and the Wavelet tutorial written 100 % in C code.

Besides the official distribution of MIDAS in source form, we intend to make a fully installed version for Linux available on the `midas ftp` account. It will be located in a subdirectory called "linux" and be available in two forms: one with sources (≈ 60 Mb) and another with only binaries (28 Mb), all packages included.

In order to limit our administrational overhead, we will not distribute the ESO-MIDAS PC/Linux version to individuals but only to registered sites. Thus, we will give MIDAS site managers permission to distribute PC versions of MIDAS to people associated with their institute.

Table 2: *Performance of MIDAS on a PC/Linux system.*

System	Core install	Size of core	Cwhetstones	Filter	Wavelet
PC/Linux, i486DX/25	49 min	11 Mb	10 MIPS	2435 sec	313 sec
SUN SPARCstation 2	30 min	26 Mb	10 MIPS	2045 sec	405 sec

DDS/DAT Tape Cartridges as New ESO Tape Standard

D. HOFSTADT, J. MELNICK, P. GROSBØL, ESO

The 9 track ½" tape format has during the last many years proved to be a very reliable tape standard for the exchange of data. Its main disadvantages are the relatively small data capacity per volume (approximately 200 Mbyte for a 2400-foot tape written with 6250 bpi) and very bad data density in terms of Gbyte per volume or mass. Large CCD detectors can now easily produce over a Gbyte of data per night. These facts demand that a new standard for data exchange must be adopted to facilitate easy transport of data acquired at La Silla.

Several aspects must be considered when choosing a new standard. The media must be reliable both in the sense of data security and with regard to support from multiple independent vendors. Its total storage capacity and data density are also important factors. Data transfer rates and speed of positioning on the media should be considered. Since many user sites would need to purchase devices for the chosen media, the price of both media and drives cannot be disregarded. A crude comparison of different media is given in the table, where values for the relative cost

and speed are only indicative. The "forward" speed indicates the time for a fast forward positioning on a file and depends on the size of the files being skipped. CD-ROM was included for comparison only since it is a read only medium. Drives for writing CD-ROMs are becoming available but are still rather expensive as shown in the table.

Weighing the different factors, the DDS/DAT tape cartridge seems to be the better choice. A main point is the very good operational experience with DDS/DAT tapes used during the last two years for transferring data from the NTT to the ESO archive in Garching. It has reasonable storage properties and is supported by multiple independent manufacturers. The lower price for drives and a relative fast positioning on files are also important factors.

Thus, the DDS/DAT tape format is adopted as the new standard for export of data from La Silla. Hardware compression is not used since a common standard has not been defined for this medium. It will still be possible for users to request their data on ½" tapes but by default DDS/DAT tapes are provided. The Exabyte format is also available but users who want their data on this medium must perform the copying themselves.

Media	Capacity	Density		Cost		Speed	
	Gb	Mb/g	Mb/cm^3	media	drive	rate	forward
½"	0.2	0.2	0.1	1	12	0.8	92
MO-disk	0.6	3.1	2.8	7	4	1.4	1
CD-ROM	0.6	5.7	3.3	1	(20)	0.4	1
QIC	1.0	3.7	2.7	3	1	1.0	380:
DDS/DAT	2.0	47.6	27.8	1	3	0.5	10
Exabyte	5.0	64.9	35.8	1	4	0.5	15

ESO/OHP Workshop on Dwarf Galaxies

From September 6–9, 1993, more than 90 astronomers from all over the world met at the Observatoire de Haute-Provence (OHP) for a workshop on "Dwarf Galaxies" jointly organized by ESO and OHP.

Dwarf galaxies are inconspicuous, faint and small stellar systems which, until recently, have largely been neglected. The much rarer giant spirals and ellipticals, more visible, attract more attention. This is mirrored by the fact that there have been only two meetings on this subject before, one in 1980, organized by ESO in Geneva, and one in 1985 in Paris, organized by the Institut d'Astrophysique.

Today, dwarf galaxies are recognized as prime laboratories for the study of some of the most burning issues of astronomy, such as structure formation, galaxy evolution, star formation, and dark matter. The number of workers in the field is growing very rapidly. The response to the announcement of the present workshop was accordingly large. This clearly shows the need for more meetings on this subject.

Talks and posters about every aspect of dwarf galaxies were presented. There have been a number of hot topics, such as the question of dark matter in the local dwarf spheroidals, the big holes in the HI component of dwarf irregulars, the possible discontinuity between normal and dwarf ellipticals, and star formation.

Although there was clearly an atmosphere of unanimity about the subject, it was amusing to see that there is apparently not yet a consensus as to the definition of what a dwarf galaxy is. But there is nothing wrong with this. A physical definition of the subject would imply an understanding of the physical nature of dwarf galaxies. While we are still far from this goal, the workshop has brought us a good deal closer. . . .

B. BINGGELI, G. MEYLAN, P. PRUGNIEL

ANNOUNCEMENTS

CNRS – OBSERVATOIRE DE HAUTE-PROVENCE and EUROPEAN SOUTHERN OBSERVATORY

4th ESO/OHP Summer School in Astrophysical Observations

Observatoire de Haute-Provence, France, 18–29 July 1994

The rapid advances made in the area of astronomical instrumentation had the side effect that fewer students have ready access to up-to-date observing facilities. As a contribution to reducing this imbalance in the training of young astronomers, the ESO/OHP Summer School offers the opportunity to gain practical experiences under realistic conditions.

In groups of three, each guided by an experienced observer, the participants will use the equipment of the OHP to carry out a small observing programme with telescopes of 1.2–1.9 metre aperture (direct imaging and spectroscopy, both with a CCD detector), to reduce the data with a modern image processing system (MIDAS or IHAP), to extract relevant additional information from the astronomical literature, and to describe the results in a brief summary which is to be presented to the other participants at the end of the school.

The preparation of the practical work will be supplemented by a series of 90-minute lectures which will be given by invited specialists. Foreseen subjects include: (a) Modern Telescope Layout, (b) Detectors, (c) Optical instrument design, (d) Principals of Photometry, (e) Spectrographs and spectroscopy, (f) IR Astronomy from the ground and from space, and (g) Data reduction techniques. A scientific talk on a frontier astronomical subject is also foreseen.

The working language at the summer school will be English. Applications are invited from graduate students working on an astronomical Ph.D. thesis at an institute in one of the ESO member countries. Application forms are available from the organizers and have to be returned by March 31, 1994. Additionally, a letter of recommendation by a senior scientist familiar with the applicant's work is required. Up to eighteen participants will be selected and have their travel and living expenses fully covered by ESO or OHP. (Reports on the previous ESO/OHP Summer Schools have appeared in *The Messenger:* see No. 53, p. 11, No. 61, p. 8 and No. 69, p. 17).

The Organizers:

M.P. Véron
Observatoire de Haute-Provence
F-04870 Saint-Michel-l'Observatoire
France

Internet: MIRA@OBSHPA.OBS-HP.FR
SPAN: OBSHPA::MIRA
EARN/Bitnet:

J. Wampler
European Southern Observatory
Karl-Schwarzschild-Str. 2
D-85748 Garching
Germany
JWAMPLER@ESO.ORG
ESO::JWAMPLER
JWAMPLER@DGAESO51

ESO Workshop on The Bottom of the Main Sequence – And Beyond

ESO, Garching
August 8–10, 1994

An ESO Workshop on the objects at, and below, the bottom of the stellar main sequence will be held from August 8–10, at the Headquarters of the European Southern Observatory, Garching, Germany.

This workshop aims to discuss recent observational and theoretical issues related to the lowest mass stars and brown dwarfs, both in the Galactic Disk and Halo, including the following topics:

- Searches for Low Mass Objects in the Disk and Halo
- Studies of Spectral Properties
- Progress in Parallaxes
- Searches for Li
- Progress in Models
- The T_{eff} and L Scales
- Future Directions

Scientific Organizing Committee:
Chris Tinney, R.F. Jameson, Rafael Rebolo, Francesca D'Antona, Mike Bessell, Jim Liebert, France Allard, Neill Reid.

Contact Address:

Chris Tinney
European Southern Observatory,
Karl-Schwarzschild-Str. 2
D-85748 Garching, Germany.
e-mail: ctinney@eso.org FAX: (089) 320 2362

ESO Libraries On-Line Catalogue

The ESO Libraries On-line Catalogue is now publicly available. The system allows access to the Library Catalogue for all ESO libraries, informs about new acquisitions, and enables library users to view their checkouts.

Users from within ESO reach the system via the rlogin command: rlogin -l library ac4 (for users in Garching) or rlogin -l lslib ac4 (for users in Chile). From outside ESO, use the telnet address libhost.hq.eso.org, login: library (defaults will refer to Main Library in Garching) or lslib (defaults refer to La Silla Library).

Two user guides are available: "The ESO Libraries On-line Catalogue in a Nutshell" and "The ESO User Guide to the On-line Catalogue". Both are available from the ESO Library in Garching (esolib@eso.org).

Further information about the system will be given in a forthcoming issue of the *Messenger.*

New ESO Publications

(September–November 1993)

The SEST Handbook (ESO Operating Manual No. 19 – August 1993).

Annual Report 1992.

Scientific Preprints

939. A. Renzini: Searching for Type 1a Supernova Progenitors. To appear in *Supernovae and Supernova Remnants,* IAU Coll. 154, ed. R. McCray (Cambridge University Press).

940. S. Savaglio et al.: The Metal Systems in Q0000–2619 at High Resolution. *Astronomy and Astrophysics.*
941. L. Wisotzki et al.: The New Double QSO HE 1104–1805: Gravitational Lens with Microlensing or Binary Quasar? *Astronomy and Astrophysics.*
942. H.W. Duerbeck and E.K. Grebel: Recovery of the Classical Nova AR Cir. *M.N.R.A.S.*
943. J.C. Cuillandre et al.: "Va-et-Vient" Spectroscopy: a New Mode for Faint Object CCD Spectroscopy with Very Large Telescopes. *Astronomy and Astrophysics.*
944. E. Krügel and R. Siebenmorgen: The Transfer of Radiation in Galactic Nuclei – Dusty Hot Spots in the Star Burst Galaxy M82. *Astronomy and Astrophysics.*
945. R. Siebenmorgen and R.R. Peletier: Search for the 1.67 μm PAH Emission Band: More Upper Limits. *Astronomy and Astrophysics.*
946. A. Cimatti: Stellar and Scattered Light in a Radio Galaxy at z = 2.63. *The Astrophysical Journal.*
S. di Serego Alighieri and A. Cimatti: Misdirected Quasars in Distant Radio Galaxies. Paper presented at the IAU Symp. 159 on "AGN across the electromagnetic spectrum", held in Geneva, August–September 1993.
947. A.A. Zijlstra and R. Siebenmorgen: The Past and Present Infrared Spectrum of BD+30°3639. Paper presented at the workshop "Planetary Nebula Nuclei: Models and Observations", Bachotek, 31 August–2 September 1993.
948. O. von der Lühe: Speckle Imaging of Solar Small Scale Structure. II. Study of Small Scale Structure in Active Regions. *Astronomy and Astrophysics.*
949. T.R. Bedding and A.A. Zijlstra: Angular Diameters of Compact Planetary Nebula. *Astronomy and Astrophysics.*
950. L. Pasquini and H. Lindgren: Chromospheric Activity in Pop II Binaries. *Astronomy and Astrophysics.*
951. B. Pettersson and Bo Reipurth: Young Stars Associated with the Vela Molecular Ridge: I. VMR Clouds C and D, Collinder 197 and Vela R2. *Astronomy and Astrophysics.*
952. S. Refsdal and J. Surdej: Gravitational Lenses. Accepted for publication in *Reports on Progress in Physics.*
953. S. Benetti et al.: The Late Evolution of the Type II SN 1990 E. *Astronomy and Astrophysics.*
954. L.M. Buson et al.: The Distribution of Ionized Gas in Early-Type Galaxies. *Astronomy and Astrophysics.*
955. E. Bica, D. Alloin and H.R. Schmitt: Integrated Spectral Properties of Star Clusters in the Near Ultraviolet. *Astronomy and Astrophysics.*
956. G.M. Stirpe et al.: Steps Toward Determination of the Size and Structure of the Broad-Line Region in Active Galactic Nuclei. VI. Variability of NGC 3783 from Ground-Based Data. *The Astrophysical Journal.*
957. M. Della Valle and M. Livio: On the Nova Rate in the Galaxy. *Astronomy and Astrophysics.*
958. E.K. Grebel et al.: Be Stars in Young Clusters in the Magellanic Clouds. D.J. Bomans and E.K. Grebel: Blue and Red Supergiants and the Age Structure of the NGC 330 Region. Papers accepted for publication in *Space Science Reviews.*
959. H. Van Winckel et al.: V417 Cen: A Yellow Symbiotic System in a Resolved Nebula. *Astronomy and Astrophysics.*
960. M.C. Festou, H. Rickman and R.M. West: Comets. *Astronomy & Astrophysics Reviews.*

Technical Preprints

56. A.F.M. Moorwood: IR Array Instruments for the ESO VLT. To appear in *Infrared Astronomy with Arrays: The Next Generation*, ed. I. McLean, Kluwer: Dordrecht.
57. N. Hubin, J.L. Beuzit, E. Gendron, L. Demailly: ADONIS – a User-Friendly Adaptive Optics System for the ESO 3.6-m Telescope. To be published in the Proc. ICO-16 Satellite Conf. on "Active and Adaptive Optics", Garching, August 2–5, 1993.
58. M. Cullum: Detectors. Contribution to the Commission 9 report for the IAU Transactions XX11 A.
59. G. Rousset et al.: The COME-ON-PLUS Adaptive Optics System: Results and Performance. To be published in the Proc. ICO-16 Satellite Conf. on "Active and Adaptive Optics", Garching, August 2–5, 1993.
60. J.M. Beckers: Imaging with Array Detectors Using Differential Detection. Submitted for publication to *Experimental Astronomy.*
61. G. Filippi: Software Engineering for ESO's VLT Project. Paper presented at the International Conference on Accelerator and Large Experimental Physics Control Systems (ICALEPCS '93), held in Berlin, Germany, October 18–22, 1993.

Proceedings of the 5th ESO/ST-ECF Data Analysis Workshop Available

(ESO Conference and Workshop Proceedings No. 47)

The proceedings of this workshop have now been published. The 230-p. volume, edited by P.J. Grosbøl and R.C.E. de Ruijsscher, may be obtained at a price of DM 30.– (including packing and surface mail). Payments have to be made to the ESO bank account 2102002 with Commerzbank München or by cheque, addressed to the attention of

ESO, Financial Services
Karl-Schwarzschild-Str. 2
D-85748 Garching b. München, Germany

STAFF MOVEMENTS

Arrivals

Europe

CHAVAN, Alberto (I), Engineer (Software)
FERRAND, Didier (F), Engineer/Physicist
LEIBUNDGUT, Bruno (CH), Astronomer
MINNITI, Dante (RA), Fellow

Departures

Europe

BOSSE, Nathalie (F), Secretary
CAROLLO, Marcella (I), Student
KJELDSEN, Hans (DK), Fellow
KOLB, Manfred (D), Student
WOLOHAN, Deirdre (IRL), Administrative Clerk (Personnel)
ZHU, Nenghong (RC), Associate

Chile

CAPPELLARO, Enrico (I), Associate
DELLA VALLE, Massimo (I), Fellow

MESSENGER INDEX 1992–1993 (Nos. 67–74)

SUBJECT INDEX

Solar System

Stars

Interstellar Medium

Novae, Supernovae, Supernova Remnants

Galaxies

Magellanic Clouds

Quasars, Seyfert and Radio Galaxies

X-Ray and Gamma-Ray Sources

Instrumentation, Data Processing, etc.

Seeing, Atmospheric Effects and VLT Site

Science with the VLT

Organizational Matters

Other Topics

AUTHOR INDEX

A

B

C

D

E

F

G

H

I

K

L

M

N

O

P

Q

R

S

T

U

V

W

ESO, the European Southern Observatory, was created in 1962 to . . . establish and operate an astronomical observatory in the southern hemisphere, equipped with powerful instruments, with the aim of furthering and organizing collaboration in astronomy . . . It is supported by eight countries: Belgium, Denmark, France, Germany, Italy, the Netherlands, Sweden and Switzerland. It operates the La Silla observatory in the Atacama desert, 600 km north of Santiago de Chile, at 2,400 m altitude, where fourteen optical telescopes with diameters up to 3.6 m and a 15-m submillimetre radio telescope (SEST) are now in operation. The 3.5-m New Technology Telescope (NTT) became operational in 1990, and a giant telescope (VLT=Very Large Telescope), consisting of four 8-m telescopes (equivalent aperture = 16 m) is under construction. It will be erected on Paranal, a 2,600 m high mountain in northern Chile, approximately 130 km south of the city of Antofagasta. Eight hundred scientists make proposals each year for the use of the telescopes at La Silla. The ESO Headquarters are located in Garching, near Munich, Germany. It is the scientific-technical and administrative centre of ESO where technical development programmes are carried out to provide the La Silla observatory with the most advanced instruments. There are also extensive facilities which enable the scientists to analyze their data. In Europe ESO employs about 200 international Staff members, Fellows and Associates; at La Silla about 50 and, in addition, 150 local Staff members.

The ESO MESSENGER is published four times a year: normally in March, June, September and December. ESO also publishes Conference Proceedings, Preprints, Technical Notes and other material connected to its activities. Press Releases inform the media about particular events. For further information, contact the ESO Information Service at the following address:

EUROPEAN
SOUTHERN OBSERVATORY
Karl-Schwarzschild-Str. 2
D-85748 Garching bei München
Germany
Tel. (089) 32006-0
Telex 5-28282-0 eo d
Telefax: (089) 3202362
ips@eso.org (internet)
ESOMC0::IPS (decnet)

The ESO Messenger:
Editor: Marie-Hélène Ulrich
Technical editor: Kurt Kjär

Printed by Universitäts-Druckerei
Dr. C. Wolf & Sohn
Heidemannstraße 166
80939 München 45
Germany

ISSN 0722-6691

Z

Contents

TELESCOPES AND INSTRUMENTATION

SCIENCE WITH THE VLT

REPORTS FROM OBSERVERS

OTHER ASTRONOMICAL NEWS

ANNOUNCEMENTS